

**A LONGITUDINAL STUDY TO ASSESS THE PRESENCE OF  
MANGANESE IN BLOOD AND EXHALED BREATH CONDENSATE  
FOLLOWING ACUTE INHALATION EXPOSURE TO WELDING FUMES**

by  
**Julie Diana Richman, MHS**

A dissertation submitted to Johns Hopkins University  
in conformity with the requirements for the degree of Doctor of Philosophy

Baltimore, MD  
December 2009

© Julie Diana Richman 2009  
All Rights Reserved

UMI Number: 3410044

All rights reserved

INFORMATION TO ALL USERS

The quality of this reproduction is dependent upon the quality of the copy submitted.

In the unlikely event that the author did not send a complete manuscript and there are missing pages, these will be noted. Also, if material had to be removed, a note will indicate the deletion.



UMI 3410044

Copyright 2010 by ProQuest LLC.

All rights reserved. This edition of the work is protected against unauthorized copying under Title 17, United States Code.



ProQuest LLC  
789 East Eisenhower Parkway  
P.O. Box 1346  
Ann Arbor, MI 48106-1346

## ABSTRACT

The association between exposure to airborne manganese (Mn) and neurotoxic outcomes is well-understood. However, the association between airborne Mn exposure and Mn uptake from the pulmonary system remains unclear. Toxicological research indicates that the chemical and physical form of Mn in exposures is a determinant of the time course of Mn uptake. The goal of this human exposure assessment study was to identify the time course of uptake and clearance of metals in the pulmonary system following inhalation exposure.

Welding fume was selected as the source of Mn inhalation exposure and Mn in exhaled breath condensate (EBC Mn) and blood Mn were selected as biomarkers of internal dose. Two measures of exposure were developed and characterized for incorporation in the study: primary particle count median diameter (CMD) and Mn composition by size. In addition, a method for the collection and analysis of EBC Mn was characterized and incorporated in study measures.

The following sampling strategy was applied: baseline samples of EBC and blood were collected from 17 subjects, subjects then welded in a single session and particle samples were collected, and EBC and blood samples were collected at 9 more time points within 7 days. Eight subjects repeated participation in the study as unexposed subjects by following the sampling strategy, except that they did not weld.

The average Mn concentration in welding fume was  $375 \mu\text{g}/\text{m}^3$  (range 8-1800  $\mu\text{g}/\text{m}^3$ ). The average primary particle CMD was 6.9 nm (range 3.2-14.5 nm). The

average slope of Mn composition by particle size was  $0.0008 \text{ nm}^{-1}$  (range  $-0.0009 - 0.002 \text{ nm}^{-1}$ ).

No trend in uptake of Mn due to welding was measured in blood. Nine exposed subjects had a significant EBC Mn peak concentration following welding. Among subjects with an EBC-Mn peak, the primary particle CMD and the Mn composition by particle size slope were associated with the timing and concentration level of the maximum EBC Mn peak. Our findings, consistent with evidence from animal and nanoparticle exposure studies, suggest that an understanding of the particle size and composition is important when characterizing the impact of inhalation exposure to Mn.

Advisor: Alison S. Geyh



## ACKNOWLEDGEMENTS

The research presented in this dissertation would not have been possible in its current form without the advice and labor of many individuals. First and foremost, I would like to acknowledge the guidance of my advisor, Dr. Alison Geyh who entrusted me with the freedom to create the initial vision of this project and granted me the latitude to devise my approach in each step. At the same time, this project was enormously improved by the constant reshaping and fine-tuning by Alison in every aspect—from conceptualization, to the process of adapting a theoretically ideal study to something actually possible, down to the most minute details of something like how to best assess the need for matrix-matched standards in metals analysis. Through our discussions of a wide variety of research components, Alison has shared with me a rigorous and concrete research philosophy in a way that has been continuously encouraging and that has deepened my appreciation for the field of exposure assessment. I intend to uphold this philosophy and approach to the best of my ability.

Members of my research committee, Drs. Peter Lees, E. William Spannhake, and Joseph Bressler provided direction in focusing my research. In addition, each offered individual insight with an open door. Peter's experience in environmental epidemiology greatly facilitated the logistical requirements of this research, especially in helping to navigate the requirements of the Institutional Review Board.

Bill Spannhake, who I had also had the fortune of working alongside as a teaching assistant, as well as Kristin Macri, director of the Health Effects Laboratory, provided wisdom from their knowledge of respiratory physiology and experience with human

subjects studies to help establish a protocol for EBC collection. Through discussion and trial of techniques, jointly establishing a protocol for EBC collection and analysis was a uniquely rewarding experience.

The electron microscopy portion of particle characterization grew into a much larger portion of this research than initially anticipated. This was largely due to the enthusiasm and dedication of Dr. Kenneth Livi, of the Department of Earth and Planetary Sciences of the Homewood Campus. The success of the particle characterization hinged on numerous conversations with Ken to establish the balance our desire for detailed analyses with what could be done in a repeatable way for multiple samples, as well as to Ken's time commitment in obtaining the microscopy data. This collaboration provided me with an excellent introduction to the world of microscopy.

The analysis of metals in blood and EBC required that I learn to use the brand new ICP-MS of the Geyh Laboratory. If it had not been for the expertise and patience of Jana Mihalic in teaching me about ICP-MS, offering advice in sample preparation techniques, and helping to trouble-shoot multiple challenges that arose, I think I might still be in the lab in an endless phase of method development to this day.

Once the methods were established to conduct the exposure assessment project, it was clear that more hands would be needed to assist in field work. Kris Macri kindly volunteered her time helping with the EBC collection. When I asked Christine Torrey if she might also be interested in assisting me with drawing blood in our study visits, she was quickly enlisted in a phlebotomy class and ready to go. Two years later, after successfully completing our goal of 300 participant visits, Kris and Chrissy were still

amazingly resilient and even willing assist on weekend fieldwork that often occurred at unusual hours.

Many others also stepped in to help with field work and data analysis. Priya Shashidharan and Emily Berkeley worked with me in the initial phase of becoming familiar with EBC measurement. Tim Green, Lisa Polyak, D'Ann Williams, Dr. Ana Rule, and Dr. Juan Ramos-Bonilla all helped in various moments to locate, set-up and operate the particle sampling equipment. Rohan Prabhu, April Livi, and Justin Livi all gave focus in consistently followed our time-consuming data processing protocol to analyze the collected microscopy particle data with me. I'd also like to thank Dr. Jana Kesavan, a research physicist at the US Army Edgewood Chemical and Biological Center and joint faculty of the Department of Environmental Health Sciences, for letting us borrow the ELPI.

Specialized statistical and modeling techniques were required to interpret the data from this project. After several discussions of our data collection and analytical procedures, Dr. Sorina Eftim established the appropriate statistical methods and then taught me how to apply these techniques to the data in a way that greatly increased my understanding of biostatistics. In addition, Dr. Jonathan Links helped to interpret the EBC Mn data to model the estimation of lung clearance of Mn.

There was more than one moment when I wondered how it would be possible to accomplish all of the facets entailed in this research project. Alison often assured me that field work is, by necessity, a team effort. Alison was certainly correct; this would not have been possible otherwise. Furthermore, having the opportunity to collaborate with

such a fine cast of devoted and skillful researchers enlightened my graduate research experience.

Outside of the university, many other friends and also my family that I have not mentioned specifically have been great sources of encouragement to help me stay the course and maintain a sense of determination. This personal support was invaluable in assisting my progress. Thank you!



This research was funded through several different mechanisms. In alternating years I was supported by training grants from either the National Institute of Occupational Safety and Health (NIOSH) and the National Institute of Environmental Health Sciences (NIEHS). Funding for research resources was provided through a NIOSH pilot research grant, a 3M Industrial Hygiene scholarship, a David Leslie Swift Fund scholarship, and a pilot grant from the Institute of Nanobiotechnology.

# TABLE OF CONTENTS

	PAGE
<b>Chapter 1: <i>Introduction</i></b> .....	1
1.1 Sources and Routes of Exposure to Manganese.....	2
1.2. Neurotoxic Effects of Manganese Exposure.....	4
1.3 Routes of Toxicity.....	6
1.4 Biomarkers of Manganese Exposure.....	7
A. Exhaled Breath Condensate.....	8
B. Blood.....	9
1.5 Determinants of Manganese Uptake and Clearance.....	10
A. Physiological Characteristics.....	10
B. Chemical Composition of Manganese Exposure.....	11
C. Physical Composition of Exposure.....	12
<b>Chapter 2: <i>Development of a Microscopy Method for Determination of Mn Composition in Welding Fume by Primary Particle Size</i></b> .....	17
2.1 Introduction.....	18
2.2 Methods.....	21
A. Particle Sample Collection.....	21
B. Electron Microscopy Method Selection.....	23
C. Scanning Transmission Electron Microscopy.....	24
D. Determination of Primary Particle Size Distribution.....	25
E. Determination of Manganese Composition by Particle Size .....	28
F. Measurement of Total Metal Content.....	28

## TABLE OF CONTENTS (Continued)

	PAGE
<b>Chapter 2: (Continued)</b>	
G. Size Distribution of Particles Collected by Impaction.....	29
2.3 Method Validation.....	30
2.4 Results.....	31
A. Particle Sample Collection.....	31
B. Total Metals Analysis.....	32
C. Primary Particle Size Distribution.....	32
D. Characterization of Mn Composition by Particle Size.....	33
E. Confirmation of Mn Composition.....	33
F. Size Distribution of Particles Collected by Impaction.....	35
2.5 Discussion.....	35
2.6 Conclusion.....	40
2.7 Tables and Figures.....	41
<b>Chapter 3: <i>Characterization of a Portable Method for the Collection of Exhaled Breath Condensate and Subsequent Analysis of Metal Content</i></b> .....	51
3.1 Introduction.....	52
3.2 Methods.....	58
A. EBC Collection Device.....	58
B. Subject Training.....	59
C. EBC Metal Analysis.....	60
D. EBC Sample Collection.....	63

## TABLE OF CONTENTS (Continued)

	PAGE
<b>Chapter 3: (Continued)</b>	
E. Statistical Analysis.....	64
3.3. Results.....	65
A. EBC Collection Characteristics.....	65
B. EBC Metal Analysis.....	66
C. Correlation of Collection Parameters to EBC Metal Concentrations.....	67
3.3 Discussion.....	68
3.4 Conclusion.....	73
3.5 Tables and Figures.....	75
<b>Chapter 4: <i>A Longitudinal Study to Assess the Presence of Manganese in Blood and Exhaled Breath Condensate Following Acute Inhalation Exposure to Welding Fume</i></b> .....	<b>82</b>
4.1 Introduction.....	83
4.2 Methods.....	86
A. Study Design and Subjects.....	86
B. Welding Fume Collection and Analysis.....	87
C. Biomarker Collection and Analysis.....	91
D. Statistical Analysis.....	92
4.3. Results.....	94
A. Subjects.....	94
B. Welding Fume Exposure.....	95

## TABLE OF CONTENTS (Continued)

	PAGE
<b>Chapter 4: (Continued)</b>	
C. Biomarkers of Exposure.....	98
4.4 Discussion.....	103
4.5 Conclusion.....	109
4.6 Tables and Figures.....	111
<b>Chapter 5: Conclusion.....</b>	<b>120</b>
<b>References.....</b>	<b>125</b>
<b>Appendix.....</b>	<b>142</b>
Appendix I: <i>“Total Metal Content of Welding Fume Particle Samples”</i> .....	143
A. Introduction.....	143
B. Methods.....	143
Appendix II: <i>“Quality Control Experiments for Analysis of Blood Manganese”</i> .....	147
A. Phlebotomy Supply Background Manganese.....	147
B. Blood Manganese Storage Tests.....	150
C. Blood Preparation Method for Mn Analysis.....	156
D. Capillary vs. Venous Blood.....	159
Appendix III: <i>“Estimation of Lung Clearance of Mn from EBC Mn”</i> .....	161
A. Introduction.....	161
B. Method.....	161



## TABLE OF CONTENTS (Continued)

	PAGE
Appendix III: <i>(Continued)</i>	
C. Results.....	164
D. Discussion & Conclusion.....	165
<b>Curriculum Vitae.....</b>	<b>166</b>

## TABLES

	PAGE
<b>Chapter 2: <i>Development of a Microscopy Method for Determination of Mn Composition in Welding Fume by Primary Particle Size</i></b>	
Table 2.1: Results of primary particle size distribution comparison study.....	41
Table 2.2: Results of Mn composition by size comparison study.....	41
Table 2.3: Total metal concentrations ( $\mu\text{g}/\text{m}^3$ ) in welding fume sample.....	41
Table 2.4: Primary particle size distribution of all samples.....	42
Table 2.5: Mn composition by size estimates of all samples.....	43
Table 2.6: Bulk estimation of Relative Abundance of Mn, Relative Mass of Mn + Fe, and Relative Abundance of Si.....	44
Table 2.7: Agglomerate and primary particle size distributions.....	44
<b>Chapter 3: <i>Characterization of a Portable Method for the Collection of Exhaled Breath Condensate and Subsequent Analysis of Metal Content</i></b>	
Table 3.1: Background metal concentration ( $\mu\text{g}/\text{L}$ ) of Rtubes condensing tubes cleaned with different methods.....	75
Table 3.2: EBC sample preparation for Mn analysis.....	76
Table 3.3: ICP-MS measurement conditions for EBC Mn, Cr, Ni, and Cd.....	76
Table 3.4: EBC Collection Characteristics.....	76
Table 3.5: Analytical measures of quality control for EBC metals ( $\mu\text{g}/\text{L}$ ).....	77
Table 3.6: Association of EBC volume (ml) and metal concentrations ( $\mu\text{g}/\text{L}$ ) vs. subject collection parameters.....	78
Table 3.7: Association between EBC metal concentration measured as $\mu\text{g}/\text{L}$ EBC vs. $\text{ng}/\text{L}$ respired.....	79
Table 3.8: EBC metal concentrations ( $\mu\text{g}/\text{L}$ ).....	79

## TABLES (Continued)

	PAGE
<b>Chapter 4:</b> <i>A Longitudinal Study to Assess the Presence of Manganese in Blood and Exhaled Breath Condensate Following Acute Inhalation Exposure to Welding Fume</i>	
Table 4.1: ICP-MS measurement conditions for analysis of blood Mn, EBC Mn and particle Mn.....	111
Table 4.2: Welding fume measures of exposure.....	112
Table 4.3: Subject Characteristics.....	113
Table 4.4: Mn analytical quality assessment measures.....	113
Table 4.5: Presence of peak in EBC Mn exposed data and summary measures of exposed subjects.....	114
Table 4.6: Group differences in blood Mn and EBC Mn concentrations.....	115
Table 4.7: Spearman's correlation ( $r_s$ ) of maximum EBC Mn concentration ( $\mu\text{g/L}$ ) and time of maximum EBC Mn concentration (hours after weld) with measures of exposure and subject characteristics.....	116
Table 4.8: Blood Mn analytical quality assessment measures.....	117
<b>Appendix I:</b> <i>Total Metal Content of Welding Fume Particle Samples</i>	
Table A1.1 Quality assurance measures for total metals analysis.....	144
Table A1.2 Total metals concentrations ( $\mu\text{g/m}^3$ ) of 25 mm Teflon particle samples.....	145
Table A1.3 Total metals exposures ( $\mu\text{g/m}^3$ ) from 37 mm Teflon particle samples.....	146
<b>Appendix II:</b> <i>Quality Control Experiments for Analysis of Blood Manganese</i>	
Table A2.1 Background Mn concentrations ( $\mu\text{g/L}$ ) of phlebotomy supplies....	149
Table A2.2 Blood Mn concentrations ( $\mu\text{g/L}$ ) of a fresh blood pool "pre-mimic" vs. Mn concentrations following collection into blood containers "post-mimic".....	149

## TABLES (Continued)

	PAGE
<b>Appendix II: (Continued)</b>	
Table A2.3 Blood Mn Storage Test 1 results (µg/L).....	152
Table A2.4 Blood Mn Storage Test 4 results (µg/L).....	152
Table A2.5 Blood Mn Storage Test #7 results (µg/L).....	153
Table A2.6 Blood Mn collection to processing storage test results (µg/L).....	155
Table A2.7 Blood Mn concentration (µg/L) of sample digested using 5 different methods.....	159
Table A2.8 Capillary vs. venous blood Mn concentration (µg/L).....	160
<b>Appendix III: Estimation of Lung Clearance of Mn from EBC Mn</b>	
Table A3.1 Values used to determine lung clearance from EBC Mn elimination in Participant 11.....	164
Table A3.2 First order elimination constant and half time of clearance for EBC Mn peaks that contained >2 points.....	165

# FIGURES

	PAGE
<b>Chapter 2:</b> <i>Development of a Microscopy Method for Determination of Mn Composition in Welding Fume by Primary Particle Size</i>	
Figure 2.1: STEM/EELS spectrum of a single particle with labeled O, Mn, and Fe peaks.....	45
Figure 2.2: TEM images of welding fume particles.....	45
Figure 2.3: Schematic of grid used for counting PPSD on DF image.....	46
Figure 2.4: Microscopy elemental maps.....	46
Figure 2.5: Results of primary particle size frequency distribution comparison..	47
Figure 2.6: Results of primary particle size distribution comparison.....	47
Figure 2.7: Results of Mn composition by particle size comparison.....	48
Figure 2.8: Scatterplots of Mn composition by particle size with smooth line fitting.....	49
<b>Chapter 3:</b> <i>Characterization of a Portable Method for the Collection of Exhaled Breath Condensate and Subsequent Analysis of Metal Content</i>	
Figure 3.1: Modified Rtube EBC Collection Apparatus.....	80
Figure 3.2: EBC metals storage test results.....	81
<b>Chapter 4:</b> <i>Assessment of Pulmonary Exposure to Manganese</i>	
Figure 4.1: Results of two individuals' paired exposed and unexposed EBC Mn concentrations.....	117
Figure 4.2: Scatterplot of EBC Mn concentrations in the exposed and unexposed group.....	118
Figure 4.3: Results of two individuals' paired exposed and unexposed blood Mn concentrations.....	118
Figure 4.4: Scatterplot of blood Mn concentrations in the exposed and unexposed group.....	119

## FIGURES (Continued)

### PAGE

#### **Appendix II:** *Quality Control Experiments for Analysis of Blood Manganese*

Figure A2.1 Blood Mn Storage Test #1 results.....	153
Figure A2.2 Blood Mn Storage Test #4 results.....	154
Figure A2.3 Blood Mn Storage Test #7 results.....	155
Figure A2.4 Blood Collection to Processing Mn Storage Test results.....	162

#### **Appendix III:** *Estimation of Lung Clearance of Mn from EBC Mn*

Figure A3.1 Schematic model of EBC Mn measure of lung clearance.....	163
Figure A3.2 EBC Mn concentration ( $\mu\text{g/L}$ ) following welding exposure for a single subject.....	163
Figure A3.3 Estimated lung clearance from EBC Mn concentration of a single subject.....	163

## COMMON ABBREVIATIONS

Al	aluminum
APSD	agglomerate particle size distribution
ATS/ERS	American Thoracic Society/European Respiratory Society
Avg	average
BAL	bronchoalveolar lavage
Cd	cadmium
CMD	count median diameter
Co	cobalt
Conc	concentration
COPD	chronic obstructive pulmonary disease
Cr	chromium
Cu	copper
DF	dark field
DMT1	divalent metal transporter 1
EBC	exhaled breath condensate
EDS	energy dispersive spectroscopy
EELS	electron energy loss spectroscopy
EFTEM	energy filtered transmission electron microscopy
ELPI	electrical low pressure impactor
EPA	Environmental Protection Agency
Fe <sub>3</sub> O <sub>4</sub>	magnetite
GSD	geometric standard deviation
HNO <sub>3</sub>	nitric acid
ICP-AES	inductively coupled plasma atomic emission spectroscopy
ICP-MS	inductively coupled plasma mass spectrometry
IDL	instrument detection limit
IS	induced sputum
ISTD	internal standard
K	rate constant
L	liter
M <sup>3</sup>	cubic meter
MDL	method detection limit
MIG	metal inert gas
min	minute
ml	milliliter
mm	millimeter
MMAD	mass median aerodynamic diameter
MMT	methylcyclopentadienyl manganese tricarbonyl
Mn	manganese
Mn <sub>3</sub> O <sub>4</sub>	manganese tetroxide
MnP <sub>2</sub> O <sub>7</sub>	manganese pyrophosphate,

## COMMON ABBREVIATIONS (Continued)

$\text{Mn}_5(\text{PO}_4)_2[(\text{PO}_3)(\text{OH})]_2$	manganese phosphate, hureaulite
$\text{MnCl}_2$	manganese dichloride
$\text{MnFe}_2\text{O}_4$	manganese iron oxide, jacobsite
$\text{MnO}_2$	manganese dioxide
$\text{MnSO}_4$	manganese sulfate
MREC System	modified Rtube EBC collection system
ng	nanogram
$\text{NH}_3\text{OH}$	ammonium hydroxide
Ni	nickel
NIST	National Institute of Standards and Technology
nm	nanometer
OSHA	Occupational Safety and Health Administration
O	oxygen
PMASS	personal and microenvironmental aerosol speciation sampler
PPSD	primary particle size distribution
PTFE	Polytetrafluoroethylene
Rpm	rotations per minute
$r_s$	Spearman's rho
Si	silicon
SRM	standard reference material
Std Dev, SD	standard deviation
STEM	scanning transmission electron microscopy
TEM	transmission electron microscopy
TIG	tungsten inert gas
$\text{TiO}_2$	titanium dioxide
TLC	total lung capacity
TPN	total parenteral nutrition
$\mu\text{g}$	microgram
$\mu\text{l}$	microliter
$\mu\text{m}$	micrometer
V	vanadium
VIS	visual incentive spirometer
W	tungsten
XRD	x-ray diffraction
Zn	Zinc



# 1

## Introduction

According to the US Bureau of Labor Statistics, there were approximately 400,000 “welders, cutters, solderers, and brazers” in the US in 2008 (1). This number does not include self-employed welders or people who weld frequently, but not as part of their job title, so the number of people who participate in welding is much higher. Welders are exposed to a complex mixture of chemicals and gases depending on the type of welding being performed, the materials being used, and the technique of the welder (2). In addition to chemical exposures, other hazards can include excess noise, heat, vibration, ultraviolet radiation, and potential for electric shock. Several acute and chronic health effects have been related to welding, including: acute photo kerato conjunctivitis (“arc eye”), bronchitis, metal fume fever, occupational asthma, siderosis, and possibly lung cancer (2). Among the many hazards of welding, there is emerging concern about potential neurotoxic effects that may be attributed to the presence of Mn in most welding fume (<5-20% of metal content in fume) (3).

Mn is an essential element that is necessary for maintaining good health. It is associated with many enzymatic reactions, such as the synthesis of amino acids, lipids, proteins, and carbohydrates (4). However, the toxic effects of high-level exposure to Mn from mining have, been recognized for well over a century (5). Long-term elevated Mn exposures have been linked to the development of an irreversible Parkinson-like disease known as manganism. While much is understood about the relationship between Mn

exposure and the development of this disease, many questions remain regarding the dependence of neurotoxicity on the initial form of Mn in inhalation exposures.

### **1.1 Sources and Routes of Exposure to Manganese**

Manganese is distributed widely in the environment as the 12<sup>th</sup> most abundant element and 5<sup>th</sup> most abundant metal on earth (6;7). It is found in several foods. A cup of tea can contain up to 1.3 mg of Mn while other foods, such as grains, rice and nuts have been found to contain Mn at concentrations exceeding 30 mg/kg. The main source of Mn exposure in the general public is through the diet. It is estimated that adults consume approximately 0.9 mg to 9.4 mg of Mn every day (8). Animal studies have shown Mn deficiencies can lead to a range of adverse effects from growth inhibition to defects in lipid and carbohydrate metabolism. There is, however, little information regarding deficiencies in humans, as Mn is present in a large array of foods and only trace amounts are required for maintaining a healthy status. Over-exposure to Mn due to dietary intake is also generally not a concern because only 1-5% of ingested Mn is absorbed via the gastrointestinal tract (9). One example of over-exposure to Mn through a nutritional source comes from the use of total parenteral nutrition (TPN), which often includes Mn as an additive (9). More recently, the use of the drug methcathinone (ephedrone), which can contain Mn as a bi-product resulting from the use of potassium permanganate in synthesis, has been associated with elevated Mn exposure through intravenous injection in Russia and Eastern Europe (10).<sup>1</sup>

---

<sup>1</sup> Stepens adds that in contrast, in North America, ephedrone is more commonly made with chromate oxidation and inhaled by users (10).

While the extent of absorption of Mn via inhalation pathways in humans is not known, evidence from animal studies indicates that it is much higher than ingestion. Studies of rats have shown that intratracheal instillation of  $\text{MnCl}_2$  resulted in significantly increased levels (205%) of Mn in the striatum in comparison to levels after exposure by gavage. This suggests that inhalation exposure leads to larger Mn concentrations in the brain than if the exposure is through ingestion only.

Historically, inhalation exposure to Mn has been associated with occupational activities. Exposure to airborne Mn has been linked with a variety of industries including iron and steel production, dry alkaline battery development, ferroalloy manufacturing, Mn mining, Mn oxide and salt production, and various industries that utilize welding (9). Inhalation exposures exceeding  $1000 \mu\text{g}/\text{m}^3$  have been found among manganese miners, ferroalloy production workers, and welders (9). The application of the fungicide manganese ethylene-bis-dithiocarbamate (maneb) (11;12) is currently being investigated as a relatively new source of elevated Mn exposure.

There is growing concern that the introduction of methylcyclopentadienyl manganese tricarbonyl (MMT) into gasoline could result in increased exposure to Mn for the general population. Following an attempted ban by the EPA of MMT in fuel used in the US, which was overturned by a lawsuit, MMT is currently permitted for limited use in the US. According to Joe Sopata, of the US EPA's Office of Transportation and Air Quality, "MMT's use is prohibited in reformulated gasoline in the U.S., and the state of California bans the use of MMT...MMT's use in the U.S. amounts to about 0.5% of the total U.S. gasoline pool (13)." Ambient exposures in areas where MMT is used in vehicles have been measured as  $25 \text{ ng}/\text{m}^3$  (14), which is orders of magnitude less than

typical occupational exposures; however, recent evidence suggests that these exposure levels may be associated with deficits in nervous system functions. A study of an environmentally exposed cohort conducted in Southwest Québec, where exposure levels are assumed to be relatively low, reported an association between deficits in nervous system function and elevated levels of Mn in urine after controlling for multiple factors, including diet (15).

It is estimated that the annual average amount of inhaled Mn by the general population in areas without Mn emitting industries or use of MMT is less than 2 µg per day (7). Though occupational Mn exposures are much higher than the general public's inhalation exposures, they still tend to be much less than ingestion exposure to Mn. For example, workers in ferromanganese or silicomanganese industry are estimated to inhale 10 µg of Mn per day with 24-hour peak inhalations exceeding 200 µg of Mn (7).

## **1.2 Neurotoxic Effects of Manganese Exposure**

Toxic effects associated with chronic inhalation exposure to elevated levels of Mn have been found in several organs of the body, including the liver and the respiratory, cardiovascular and reproductive systems. The central nervous system has been observed as one of the most sensitive endpoints, with elevated inhalation exposures leading to manganism (9;16).

Manganism is generally defined by three clinical phases: the prodromal period, the intermediate phase, and the established phase (5). The prodromal period is defined by subjective symptoms including fatigue, headache, muscle cramps, loss of appetite, insomnia, diminished libido, and hallucinations. Altered emotional behavior has also

been observed including apathy, compulsive or violent behavior, and emotional instability. Initial symptoms can progress to the intermediate phase in which objective symptoms have developed, such as facial grimaces, difficulty with speech, and clumsiness in movements. The established phase is characterized by development of neurophysical symptoms including progressive muscle rigidity, bradykinesia, and dystonia in the upper limbs (5;17-20). In a study of 150 Mn miners, it was reported that disease onset can occur as little as one month after the start of elevated Mn exposure; however more typically disease onset occurs within one or two years (5).

Several epidemiological studies have measured neurobehavioral performance in populations with occupational inhalation exposures to Mn. Many different neurobehavioral tests have been employed in these studies. Most studies performing multiple tests have found that by at least one measure, elevated Mn exposure was associated with poorer neurobehavioral performance, such as decreased reaction time, motor function performance, recall, visuomotor coordination, and steadiness (21-28). Only one of these studies did not detect a difference in neurobehavioral performance between exposure groups. It is notable that in that specific study, the exposure measurements were not taken from the same person who participated in the neurobehavioral tests, and Mn concentrations of the representative personal airborne particle samples were estimated from pooled dust samples (21;29)

The reversibility of neurobehavioral function deficits associated with elevated Mn exposure has not been thoroughly investigated, but research indicates that it is likely to be dependent on factors such as the duration of cessation of exposure or the progression of symptoms. Neurobehavioral performance was found to continue to be significantly

different from controls in ferroalloy workers tested both immediately after Mn exposure and 13-42 days after Mn exposure ceased (30). Another study measured the neurological condition of Mn alloy foundry workers during elevated inhalation exposure to Mn and again one to two years after the exposure stopped. The study found that the neurological condition had improved in some subjects and declined in others (31).

A controversial issue surrounding Mn exposure is whether it contributes to the development of Parkinson's disease. It has been fairly well established that Idiopathic Parkinson's Disease and chronic Mn exposure are associated with similar symptoms, but that they are distinct conditions (4;18). Determination is further confused by recent evidence suggesting that there is a second type of Parkinson's disease, Manganese-Induced Parkinsonism, which is associated with Mn exposure (32).

### **1.3 Routes of Toxicity**

Research has indicated three potential routes for Mn entry into the brain: the cerebral capillaries, blood cerebrospinal fluid through the choroid plexus, and the olfactory nerve in nasal cavity (4). The contribution of inhalation to each of these routes of Mn transport to the brain is not well understood. These last two routes appear to occur when high doses are administered in animal studies (serving as overflow routes). Evidence suggests that at more relevant levels for human exposure, Mn forms a complex with the binding protein transferrin and is actively transported across brain capillary endothelium (33). Mn is then hypothesized to be transported through axonal transport and efferent fibers to the ventral pallidum, globus pallidus, and the substantia nigra, where it is known to accumulate.

Most Mn in blood binds to  $\beta$ -globulin or albumin (80%) and a small portion of Mn binds to transferrin. While under normal conditions transferrin binds iron (Fe) to two binding sites, under iron-deficient conditions there may be less competition from Fe providing an opportunity for more Mn to bind to transferrin. Divalent metal transporter (DMT1) also appears to assist transferrin in the transport of Mn, though the mechanism has not been established (4). A second route of transport aided by DMT1 is thought to occur independently of transferrin (6). As these mechanisms indicate, Mn toxicity is involved with the regulation of Fe status (9;34;35).

#### **1.4 Biomarkers of Manganese Internal Dose**

There has been substantial effort to establish a Mn biomarker of internal dose, but the findings have varied greatly and have resulted in no clear biomarkers. According to Casarett & Doull, “true biomarkers indicate exposure to a specific chemical, as well as susceptibility to adverse effect; and/or are predictive of disease associated with chemical exposure. They must be sensitive, specific, relevant, reproducible, and measurable in the population (36).” Measurability encompasses such factors as ease of collection, risk to study subjects and cost of sample analysis.

Biomarkers of Mn from the media of feces, urine, fingernails, hair, bone, blood, and brain (by magnetic resonance imaging) have been explored and found to be problematic in terms of utility as informative biomarkers of Mn inhalation exposure. For example, Mn concentration levels in hair are affected by pigmentation, so measures in people with different hair color vary. Measures of Mn in feces, urine, hair and bone are not specific to inhalation exposure, as they are also the result of ingestion (9;37;38).



There is not enough evidence to discern if Mn in fingernails is specific to inhalation, but it is unlikely. The most commonly used biomarkers of Mn internal dose are blood and urine, with exhaled breath condensate (EBC) currently under examination. Blood and exhaled breath condensate offer potential as media for true biomarkers of Mn inhalation exposure, and these are therefore the media selected for study in the research presented here.

#### **A. Exhaled Breath Condensate**

Exhaled breath condensate (EBC) has recently been explored as a potential medium for a biomarker of exposure and dose for both occupational and non-occupational exposures to several metals (39-41). After extensive review of the literature up until 2005, the American Thoracic Society /European Respiratory Society Task Force on EBC concluded that while none of the biomarkers had been sufficiently validated for clinical use, EBC is a “useful tool for epidemiological investigation” that is “still in its infancy” (42).

EBC is a media from the respiratory tract that is collected by having subjects breathe into an apparatus that has a chilled collection area such that the exhaled vapor and analytes carried with the vapor condense. This contrasts with the more invasive methods of broncho-alveolar lavage (BAL), in which a bronchoscope is inserted into the respiratory tract, and induced sputum (IS), in which a hypertonic solution is inhaled into the respiratory system to induce the production of sputum. While BAL is known to sample the lining fluid of the lower respiratory tract (43), and it is fairly well established that IS predominantly samples the proximal airways (44), the origin of EBC in the respiratory system is not known. Some researchers have speculated that EBC originates



from the whole respiratory tract (43), others have proposed that it reflects the composition of lower respiratory lining fluid because this is where there is greater surface area from which aerosol can be generated (44).

Recent research of EBC has expanded to include several different analytes in EBC, including the measurement of metals. These studies have either looked at EBC metal concentrations in relation to occupational exposure (39;40;45) or disease status (41;46;47). Methods to collect EBC across these studies have varied greatly, and there has been minimal reporting with regard to quality assurance in either the collection or analysis of EBC measures.

## **B. Blood**

Total Mn in whole blood, plasma, and/or serum has held promise as a biomarker because it is fairly easy to collect. An advantage of using whole blood, instead of serum or plasma, is that whole blood does not appear to be sensitive to large changes in ingestion of Mn (9). Red blood cell Mn concentrations are 10- to 15-fold higher than Mn concentrations in serum or plasma (9).<sup>2</sup>

Several studies that have looked at occupational exposures to Mn have found statistically significant differences in blood Mn between an exposed and unexposed group. However, the correlation between exposures and blood Mn at an individual level has been much less conclusive and rarely has a significant correlation been established (48-53). In a review of these studies, it was noted that there were substantial differences in the form of Mn in the exposure and in the duration between the exposure and the collection of blood likely contributing the inability to establish an association. Research

---

<sup>2</sup> Aschner et al. suggest that this is a good reason to measure Mn in whole blood rather than plasma or serum, because even slight accidental hemolysis in blood samples can significantly elevate the Mn concentration in plasma or serum (9).

suggests that the half-life of Mn in blood may be influenced by a range of factors including the physiological status of the organism being exposed and the form of Mn in the exposure, as is described in further detail.

## **1.5 Determinants of Manganese Uptake and Clearance**

### **A. Physiological Characteristics**

Among physiological parameters, iron status appears to influence Mn uptake into the circulatory system. Heilig et al. report that when an  $\text{MnCl}_2$  isotope tracer was injected into normal and iron-deficient rats, Mn concentrations in blood from the normal rat group dropped rapidly in the first 30 minutes, while in the iron-deficient rat group the Mn concentrations remained 4-fold higher for at least 4 hours (34). In a study of rats deficient in iron that were fed a high Mn content diet, greater accumulation of Mn was measured in the brain of the iron deficient rats as compared to the brains of iron-replete rats fed the same diet (9).

Age and gender also appear to modify Mn uptake. Finley et al. found that following ingestion of radio-labeled  $^{54}\text{Mn}$  and measuring clearance via whole body counts, men absorbed more Mn, but the whole body half life of Mn was longer in women (54). Finley hypothesizes that this relationship was due to a difference in iron status between men and women. In an animal study, Dorman et al. exposed rats to  $\text{MnSO}_4$  and found that young male rats had higher resulting Mn concentrations in the olfactory bulb than female or senescent male rats, and senescent male rats had higher striatum and cerebellum concentrations and slower clearance times than the other groups (55). These

findings suggest that other factors such as age and gender may also play a role in the fate and transport of Mn within the central nervous system.

## **B. Chemical Composition of Manganese Exposure**

The chemical composition of Mn, or the Mn compound, involved in the exposure also appears to result in significant differences in Mn uptake. Roels et al. found that with similar exposures in rats to either  $\text{MnCl}_2$  or  $\text{MnO}_2$  via intratracheal instillation, the concentration of Mn in blood reached a maximum peak concentration much more quickly following exposure to  $\text{MnCl}_2$  versus  $\text{MnO}_2$  (peak: within 30 minutes vs. 7 days, and maximum concentration at least 3 fold higher for Mn dichloride) (56). Drown et al. similarly found that in rats intratracheally instilled with a single dose of  $\text{MnCl}_2$  or  $\text{Mn}_2\text{O}_4$  had blood Mn concentrations twice as high after 4 hours for  $\text{MnCl}_2$  (57). These studies suggest that both the time course and maximum concentration of Mn in blood is dependent on the Mn compound present in the initial exposure.

Animal studies have also suggested that the Mn compound in the initial exposure may be an important factor in the resulting fate within organs of the body. Drown et al. report that the Mn concentrations in lung tissue of rats exposed via a single intratracheal instillation of approximately 200  $\mu\text{g/kg}$  of  $\text{MnCl}_2$  had an initial clearance rate that was nearly 4 times faster than the clearance rate of  $\text{Mn}_3\text{O}_4$  (57). Vitarella et al. and Dorman et al. conducted separate experiments in which rats were exposed via inhalation to  $\text{MnSO}_4$ ,  $\text{Mn}_5(\text{PO})_4[(\text{PO}_3)(\text{OH})]_2$  (Mn phosphate) or  $\text{Mn}_3\text{O}_4$  in similar concentrations and conditions so that all three compounds can be compared across the two reports (58;59). The lowest concentrations of Mn in lung tissue resulted from  $\text{MnSO}_4$ , with higher concentrations following  $\text{Mn}_3\text{O}_4$ , and the highest concentrations following Mn

phosphate (59). Reaney et al. exposed rats to  $\text{MnCl}_2$  or  $\text{MnP}_2\text{O}_7$  over a period of 5 weeks and measured higher concentrations in brain tissue (and blood) following exposure to  $\text{MnP}_2\text{O}_7$  (60).

### **C. Physical Composition of Exposure**

In addition to chemical properties, physical properties can play a role in the resulting impact of exposure. For inhalation exposure, particle diameter is generally recognized as a determinant of the location of deposition within the upper and lower airways, which consequently influences the pathway of uptake or clearance of particles in the body. It has been shown that during light exercise with nasal breathing, inhaled particles on the order of 20 nm deposit predominantly in the alveolar region, while particles that are either slightly smaller (e.g. 2 nm) or much larger (e.g. 2000 nm) deposit mainly in the head airways and tracheobronchial region (61). Smaller particles that deposit in the head airways may either directly cross the olfactory nerve of the nasal cavity and reach the olfactory bulb or they can be carried out of the respiratory system and eliminated from the body through the digestive system via mucocilliary transport. Particles that deposit in the alveolar region are generally either engulfed in macrophages and then carried by the mucocilliary transport or they may be directly transported into the circulatory system (61). Thus, the particle size in inhalation exposures generally alters the physiological mechanism of interaction.

Both the chemical composition and physical properties of particles involving Mn within welding fume likely contribute to the impact of exposure. The Mn composition in welding fume can vary by welding type and materials used, but it has been found to contain mostly manganese iron oxides where Mn replaces iron to varying degrees in

compounds such as magnetite ( $\text{Fe}_3\text{O}_4$ ) and jacobite ( $\text{MnFe}_2\text{O}_4$ ) (62-64). Voitkevich found that Mn on the surface of welding fume particles can also be present within silica or fluorine compounds (64).

The physical composition of welding fume adds another component that may be important in the understanding of resulting clearance and toxicity. Welding fume contains ultrafine particles (particles with at least one dimension  $<100$  nm in diameter), commonly termed nanoparticles, that are present both as isolated primary particles and as agglomerates of primary particles. Previous studies have found that the agglomerates in welding fume have diameters on the order of 100-600 nm, and primary particles have diameters ranging from 10 to 100 nm (3). There is growing evidence that these nanoparticles elicit greater toxic effects than larger particles with similar composition (65). The fate of nanometer sized primary particles within agglomerates after exposure, however is less clear.

Animal studies are beginning to elucidate the fate of agglomerated particles after inhalation. Oberdörster et al. report that following a 3-month inhalation exposure to similarly sized primary particles of  $\text{TiO}_2$  (primary particle diameter  $\sim 20$  nm) and carbon black (primary particle diameter 15-50 nm), rats exposed to the  $\text{TiO}_2$  exhibited approximately twice the lung burden in the regional lymphs as compared to carbon black (5.6% vs. 2-2.7%) (66). Oberdörster hypothesized that the ability of the  $\text{TiO}_2$  to translocate from the respiratory system may be due to the fact that carbon black fuses into aggregates, while  $\text{TiO}_2$  more readily disaggregates or remains as primary particles. Pauluhn et al. exposed rats via inhalation to agglomerated aluminum oxyhydroxides with a mass median aerodynamic diameter (MMAD) of 600 nm and primary particle size of

40 nm or a MMAD of 1700 nm and primary particle size of 10 nm (67). Pauluhn concluded that while the size of the agglomerate determined the resulting toxicity, the size of the primary particle determined the rate of clearance (faster clearance for smaller primary particles). Thus, while the site of deposition and potentially the toxicity appears to be related to the agglomerate particle size, the subsequent degree to which translocation occurs or for transport and clearance may be mediated by the primary particle size. The implication of this hypothesis is that, in addition to the size of the agglomerates, an important determinant of both toxicokinetics and toxicodynamics may also be the size of the primary particles themselves.

The composition of either primary or agglomerate particles of welding fume may differ across the size distribution. Minni et al. reported differences in welding fume particle configurations indicate there is a size component to this difference (68). Yet, they did not address the question of how size impacts composition in the welding fume. Differences in composition across the size distribution in other types of particle samples have been demonstrated using single particle analysis of aerosol time of flight mass spectrometry. For example, in a study of air pollution generated by traffic, Gross et al. found that within the total particle size distribution, polycyclic aromatic hydrocarbons were present in particles 0.2-2.8  $\mu\text{m}$ , black carbon was mainly present in particles with diameters of 0.2-0.4  $\mu\text{m}$ , inorganic material was mainly present in particles  $>1\mu\text{m}$  (69). While the chemical composition of welding fume particles is much simpler than particle samples from traffic, it is possible that the distribution of the primary constituents, iron (Fe) and Mn, across the size distribution is not uniform. A better understanding of the

composition of primary particles in welding fume across the size distribution may aid in our interpretation of the relationship between exposure and toxicity.

In summary, current research suggests that the relationship between inhalation exposures to Mn and the resulting Mn in blood is influenced by several factors. Iron status, age, and sex are physiological factors that are important effect modifiers of Mn absorption that could influence the resulting measure of Mn in blood. The form of the Mn exposure in terms of both the compound present and the particle size distribution also appear to affect the resulting uptake and clearance.

The research described in this dissertation investigated the exposure and uptake of Mn from inhalation of welding fume. In order to improve the understanding of the relationship between Mn exposure and biomarkers of internal dose, the goal of this research was to investigate the time course of Mn uptake following welding fume inhalation. The research questions were: 1) What is the time course of uptake and clearance of manganese into the circulatory system following a single inhalation exposure to welding fume? 2) Do the chemical and physical properties of welding fume inform the time course?

In order to answer these questions, methods for characterization of welding fume and exhaled breath condensate were expanded upon as part of this research. Chapter 1 describes research of the characterization of microscopy techniques for measurement of the primary particle size distribution and the Mn composition throughout the primary particle size distribution of welding fume. Chapter 2 defines a design for a method for collecting EBC and describes the analysis of EBC metals. Chapter 3 presents the exposure assessment study of exposure to Mn in welding fume and biomarkers of internal

dose of Mn that incorporated the measurement methods presented in Chapters 1 and 2, in addition to analysis of blood Mn, for exploration of the time course of Mn uptake.



## 2

### **Development of a Microscopy Method for Determination of Mn Composition in Welding Fume by Primary Particle Size**

Julie D. Richman, Kenneth J.T. Livi, Alison S. Geyh

## **2.1 Introduction**

Welding fume is composed of a complex mixture of particles and gases. The composition is dependent on the type of welding being performed, the materials being welded, and the specific conditions of the welding. The basic principle of welding is that an electrode is melted and used to join two pieces of steel. In the process, the electrode is consumed and aerosol by-products are generated. It is estimated that 90% of welding is performed with mild steel, which is composed of mostly iron (Fe) and some manganese (Mn) to strengthen the steel (3). In the fume generated by metal inert gas welding (also known as MIG or gas metal arc welding) of mild steel, previous studies have reported predominately Fe and Mn (77-88% and 10-23% mole fraction, respectively) (62). Fume generated by stick welding (also known as shielded metal arc welding) of mild steel, contains higher levels of other elements such as: silicon, potassium, and calcium in addition to Fe and Mn (62). Minor to trace levels of several other metals such as chromium, nickel, copper, aluminum, cadmium, magnesium, and zinc may also be present in either MIG or stick welding of mild steel (3;62). Previous investigations of welding fume have shown that it consists of both isolated and agglomerated particles. These agglomerates, which can have diameters on the order of 100-600 nm, are made up of clusters of primary particles with diameters ranging from 10 to 100 nm (3). The distribution of elemental content across the diameter range of the primary particles is not well understood.

Among the metals present in welding fume, Mn is of particular concern because it is a known neurotoxin. Severe cases of occupational Mn inhalation exposures have resulted in the development of manganism, a neurological syndrome that elicits

symptoms that resemble idiopathic Parkinson's disease (9;16). Following inhalation, Mn can reach the brain either by transport along the olfactory nerve or through the pulmonary system into the circulatory system (4). Clearance of Mn from the pulmonary system via mucocilliary transport may reduce the toxic effect on the nervous system. The relative participation of these pathways following exposure is likely determined by particle characteristics, specifically size and chemical composition.

Welding fume particle size distributions have generally been measured by cascade impactors, which can be assumed to measure the size distribution of agglomerated particles as well as un-agglomerated single particles (a small fraction of the distribution) (70;71). The agglomerate particle size distribution (APSD) is useful in inhalation studies for estimating the site of deposition of particles in the respiratory tract. Farrants et al. found that hundreds of small primary particles (diameter not reported) tend to form agglomerates, while medium particles tend to be present in groups of less than 20 in agglomerates (70 nm) and large particles (145 nm) are present either individually or in much smaller groups in agglomerates (72). In addition to agglomerate sizes, understanding the primary particle size distribution combined with chemical properties of welding fume particles may also inform the resulting toxicity (66).

Chemical analysis of bulk samples of welding fume provides an indication of the overall content of the welding fume. In bulk fume samples from MIG welding of mild steel, Jenkins et al. measured Mn via x-ray diffraction (XRD) mostly in the form of magnetite, which is an oxide spinel phase that predominantly contains Fe but can be replaced by Mn to varying degrees ( $\text{Fe}_3\text{O}_4$ ) (62;63). By etching the particle surfaces and analyzing via x-ray photoelectron spectroscopy (XPS), Voitkevich found that in addition

to magnetite (with Mn replacement),  $\text{MnFe}_2\text{O}_4$  is also present in the nuclei of welding fume primary particle, while Mn on the surface of welding fume particles is in silica or fluorine compounds (64).

In an effort to understand the relative solubility of Mn compounds present in welding fume, Berlinger et al. utilized a sequential extraction sample preparation technique followed by inductively coupled plasma mass spectrometry (ICP-MS) and inductively coupled plasma atomic emission spectrometry (ICP-AES) analysis (73). In this study, a “soluble fraction”, a fraction of metallic Mn and  $\text{Mn}^{2+}$ , and an insoluble fraction in welding fume obtained from MIG and stick welding were analyzed. Though Berlinger questioned the ability of the method to quantifiably distinguish Mn compounds within these fractions, their data suggests the presence of Mn within multiple compounds of varying solubility.

Jenkins and Eagar write that multiple phases (compounds or crystal structures), such as differences in compounds at the surface vs. in the nucleus of a particle that have been measured in bulk fume samples, cannot exist within particles with diameters less than 1000 nm (62). They conclude that the multiple compounds and chemical structures seen in bulk analyses of welding fume are either present within larger particles of the samples (but not the smaller particles), or as different compositions among the smaller particles, where each smaller particle is composed of a single compound and chemical structure (62). Either hypothesis suggests variability of particle composition throughout the fume.

A study by Minni et al. investigating composition across different types of particle configurations, including agglomerates and single particles of different sizes,

suggests that the later possibility proposed by Jenkins and Eager is true (68). Using transmission electron microscopy (TEM) with energy dispersive spectroscopy (EDS) to investigate welding fume generated by MIG welding of mild steel, Minni reports that the relative abundance of Mn is different among the various particle configurations indicate that there is a size component to this difference (68). This provides evidence of compositional differences throughout the primary particle size distribution (PPSD) in welding fume; however, they did not address the question of how size impacts composition in the welding fume. Thus, while it is known that Mn in welding fume is predominantly present within iron oxides, other Mn compounds may also be present.

The objective of this study was to develop a method utilizing electron microscopy techniques to characterize and quantify the composition of PPSD in welding fume. To accomplish this goal we explored the use of energy filtered transmission electron microscopy (EFTEM), and scanning TEM /electron energy-loss spectroscopy/energy dispersive (x-ray) spectroscopy (STEM/EELS/EDS) for the characterization of Mn and Fe content of particles ranging in size from 10 to 100 nm. We applied this method to particles collected from two groups of welding sessions. To complement our estimate of PPSD, in a subset of welding sessions we also collected samples in an impactor in order to estimate the APSD.

## **2.2 Methods**

### **A. Particle Sample Collection**

As part of a larger study examining biomarkers of exposure to welding fume, samples of welding fume were collected by using personal particle samplers deployed

within the breathing zone of each welder during the welding session. The study was divided into two groups of exposure.

In one group welding sessions were performed in the same location using the same welding materials and equipment. All welding in this group was performed with a Milleromatic 251 Metal Inert Gas (MIG) all-in-one wire welding system. The inert cover gas was composed of 75% Ar and 25% CO<sub>2</sub>. Subjects welded with wire consisting of 0.5-2% Mn onto a cold rolled steel plate consisting of 2% Mn. Welders welded according to the 60% duty cycle of the Milleromatic. All sessions were performed indoors without outdoor ventilation. Particle samples were collected for an average of 1.5 hours in this group (range 1-2 hours).

In a second group of varied welding conditions, welding sessions were performed in different locations with different equipment and supplies. MIG welding was performed in each of these welding sessions, and in one session stick welding was additionally performed for a portion of the time. Some sessions were performed outdoors and others indoors with open outdoor ventilation. Particle samples were collected for an average of 3 hours (range 1.25-4.5 hours).

Welding fume was collected using a Personal and Microenvironmental Aerosol Speciation Sampler (PMASS, MSP Corporation, Shoreview MN), which allows for simultaneous collection of duplicate particle samples. The PMASS includes a single size selective inlet and two parallel sampling channels. The inlet is an aluminum cyclone, which has a 50% cut-size of 2.5 µm at 4 L/min. The sampler operates with one pump, which pulls flow through both channels. A 3.0 µm pore size, 25 mm Teflon filter with a PTFE support ring (Pall Life Sciences, Ann Arbor, MI) was placed in one PMASS

channel and 3.0  $\mu\text{m}$  pore size, 25 mm polycarbonate filter (Nuclepore Track-Etched Membrane, Whatman, Kent, UK) was placed in the other PMASS channel. The target total flow rate, 4 L/min, was passively split to approximately 2 L/min through each channel; membrane discs were placed under filters to help balance the flow. Total flow was measured using a flow meter (Drycal DC-Lite & DC-2, BIOS, Butler, NJ). The flow rate through each filter was determined by simultaneously measuring flow through each channel using side-by-side rotameters and then calculating the percent of the total flow through the entire system. To adjust for background contamination, at least one filter blank was obtained during each welding sampling session. After collection, all samples were stored in amber glass jars under argon gas prior to sample preparation and analysis.

## **B. Electron Microscopy Method Selection**

Two techniques were explored for obtaining Mn and Fe compositional data for particles throughout the entire size distribution: EFTEM and STEM/EELS/EDS mapping, also called spectrum imaging techniques. With EFTEM, an image containing compositional information was collected relatively quickly (within minutes) (74;75). STEM/EELS/EDS analysis required longer acquisition time, but provided greater compositional contrast and lower detection limits, especially for particles at the smaller end of the size distribution. Both methods were evaluated both for precision in determining composition and feasibility of multiple acquisitions. The STEM/EELS/EDS method was selected because the STEM/EELS compositional results had greater precision for Fe and Mn in particles and STEM/EDS enabled the analysis of the bulk composition of other elements of interest, such as silicon and aluminum. This made it possible to investigate the degree of interference from these elements in the measured estimates of Mn

composition. Utilizing the STEM also provided more information for post acquisition exploration. This allowed more flexibility to investigate a specific region or composition of a sample of interest after the sample has been analyzed, because the spectral data from the complete sample has been stored. (To incorporate further investigation from samples analyzed via EFTEM, the sample would have to be re-analyzed via TEM. Locating the region previously analyzed would be very difficult.)

### **C. Scanning Transmission Electron Microscopy**

In order to determine the size and Mn composition of primary particles, STEM was used to collect dark-field intensity (DF), EELS and EDS data using a Philips CM 300 FEG S/TEM operating at 297 kV (Figures 2.1 & 2.2). A Gatan GIF 200 was used to collect EELS spectra containing the O (oxygen) *K* and Mn and Fe *L*<sub>2,3</sub> core-loss edges. A 2 mm entrance aperture resulted in a collection angle of 15 mrad and a convergent angle of 4 mrad. EDS spectra were collected using an Oxford ultrathin window detector and an EmiSpec processor. Simultaneous collection of DF, EELS and EDS data during acquisition was accomplished using ESVision software (version 4, FEI, Hillsboro, OR). Signals from three different detectors were simultaneously collected the entire EELS and EDS spectra stored for each pixel creating a data hypercube, such that quantifiable compositional data from both EELS and EDS was available for analysis from each pixel of known location in the imaged sample.

DF images were collected at a pixel resolution of 0.3 nm (3008 x 2687 pixels). EELS and EDS maps were collected at pixel resolution of 5-10 nm/pixel with maps containing approximately 100 x 100 pixels, and in an area smaller than their corresponding DF images. Chemical maps were collected with a dwell of 1 second per



pixel and resulted in total acquisition times of around 4 hrs. Drift correction was employed during the acquisition of EELS/EDS maps. However, since the DF images were acquired before the maps and at a different pixel resolution, some drift between images was still possible. Therefore, residual drift was assessed visually after acquisition.

Although the EDS spectra were inferior in precision to EELS spectra, their acquisition was critical in determining if elements other than O, Mn and Fe were present. A summation of all EDS spectra was used to assess the validity of assuming that the particles of each sample are dominated by O, Fe and Mn.

A dispersion of 0.3 eV per channel was chosen for EELS collection so that the O *K* (~532 eV), Mn *L*<sub>2,3</sub> (~640 eV) and Fe *L*<sub>2,3</sub> (~708 eV) core-loss edges could be simultaneously collected. While Mn and Fe were the elements of interest, the O *K* edge was included as this edge contains information about individual particle crystal structures, allowing for determination of the relative quantities of the elements of interest. The EELS spectra were corrected for the background by background subtraction using a power-law function (74). The atomic proportions of O, Mn and Fe were calculated using the Gatan Digital Micrograph version 3.8.2 software package (Figure 2.1).

#### **D. Determination of Primary Particle Size Distribution**

Polycarbonate filters were selected as the particle collection substrate because the particles concentrate on top of the filter and are more easily imaged in the TEM. In preparation for microscopy, particle samples were washed with 100% ethanol, embedded in epon, and sectioned to approximately 80 nm thickness on a Leica UCT ultramicrotome

through the cross section of the filter. The sectioned filters were then placed onto a nickel grid and carbon coated at 297 kV to reduce charging.

For each sample, a DF image was collected for particle sizing. Publicly accessible imaging software (Image J, US National Institutes of Health, Bethesda, MD) designed to provide an automatic estimation of the PPSD was initially explored as a tool for quantifying the size distribution. However, for these welding fume samples the imaging resolution was inadequate to correctly account for the majority of the small particles. This was primarily due to overlapping, as well as to the low contrast between the individual small particles.

A manual method was, therefore, established using ES Vision software. A grid containing up to nine 250 x 250 nm fields was drawn on each DF image to define potential areas for particle counting (Figure 2.2). To determine the minimum number of fields required for providing a statistically representative sample of particles, a series of tests were conducted, beginning with counting all particles (approximately 2000 particles) in all 9 fields of a single DF image followed by counting different numbers of fields and particles per field. Based on the count median diameter estimate, it was determined that a statistically representative sample was achieved when approximately 1000 particles within 5 fields were counted.

To characterize the size distribution, the following sizing rules were established:

- 1) All particles within 5 fields of alternating spacing were sized (see shaded fields in Figure 2.3).
- 2) If 1000 particles were not sized after assessing 5 fields, particles in the remaining fields were sized until 1000 particles had been counted.
- 3) Once starting to

size particles within a field, all particles within that field were sized. 4) At least half of a particle had to be included in the field to be counted.

Particles were uniquely identified by overlaying a circular drawing object with the best fit to the particle circumference. Applying the concept of a Porton graticule, which is used for estimating the particle size distribution in optical microscopy, size bins for spherical particles were defined based on a  $\sqrt{2}$  geometric progression of the 2D circular diameter (76). The size bins are determined by the equation:  $d_n = d_0(2)^{n/2}$ , where “d” is the diameter of the particle, “n” is the number of the size bin with “d<sub>0</sub>” as the smallest particle diameter. Based on a review of two representative samples with sufficient magnification to visualize the largest particles, it was determined that the smallest particle diameter that could be estimated with confidence was 4 nm. To be conservative, the smallest size bin was, therefore, defined as all particles  $\leq 6$  nm in diameter. The particle size distribution was determined by counting the number of particles that fall within each size bin, and measuring the cumulative frequency of particles throughout the size distribution. In order to determine the count median diameter (CMD), the log of the mid-point diameter of each size bin was then plotted against the “z score” (the statistic from a normal distribution) corresponding to the value of the cumulative fraction of particles (Z), such that:  $CMD = \text{EXP}(m \cdot Z + b)$ , where “m” is the slope and “b” is the y intercept. Typically the particle CMD is estimated by measuring the midpoint of the logarithm of the particle diameter vs. the cumulative fraction on a log-probability scale (76). In review of these measurements, the results are equivalent and the described method allows for greater statistical interpretation.

### **E. Determination of Manganese Composition by Particle Size**

To characterize composition, the DF image processed for size distribution was overlaid onto an EELS map with corresponding composition spectrum (Figure 2.4). For quantification of Mn and Fe content from EELS spectra within each particle size bin, 10 particles were selected at random from the DF image that had previously been used for estimation of PPSD. Within each particle analyzed for Mn composition, areas free of overlap from other particles were selected as the integration area for EELS and EDS spectra. The spectra stored at every pixel within the overlap-free region of a particle were summed and processed for determination of Mn composition.

Mn composition was measured as the relative abundance of Mn, specifically:  $\text{Mn}/(\text{Mn} + \text{Fe})$  (atomic fraction). The particle diameter measured from the PPSD measurements of the DF image were reported with the Mn composition data specific to that particle. An estimate of the Mn composition across the size distribution was made by regressing the relative abundance of Mn vs. the particle diameter of the analyzed particles from each sample. The slope of the linear regression is the estimate of “Mn composition-size slope”.

### **F. Measurement of Total Metal Content**

Total Mn content was assessed using the duplicate particle sample collected on a Teflon filter. All filters were weighed with a Mettler T5 microbalance with precision of  $\pm 0.003$  mg (Mettler-Toledo, Toledo OH) after equilibrating for 24 hrs in a temperature and humidity controlled weighing environment. All mass values of samples were blank-corrected.

Prior to analysis, particle samples were prepared by removing the polyolefin ring from the Teflon filter microwave digestion (MARS XPress CEM Corp., Matthews, NC). In the first microwave digest the samples were digested in 74% HNO<sub>3</sub> (optima grade, Fisher Scientific, Columbia MD) plus ultrapure water. HF (optima grade, Fisher Scientific, Columbia MD) and more HNO<sub>3</sub> were added before the second microwave digest, resulting in a final solution of 73% HNO<sub>3</sub> and 9% HF. In both microwave digests, the temperature of the sample solution was held at 150°C for 30 minutes. Digested samples were then diluted in ultrapure water such that the final solution had a maximum of 2% HNO<sub>3</sub>.

Filters were analyzed for total Mn and Fe concentration by inductively coupled mass spectrometry (ICP-MS, Agilent 7500ce, Agilent Technologies, Newark, DE). For every ten samples, at least two standard reference material (SRM) samples were also digested and analyzed (NIST material 2709 San Joaquin soil; National Institute of Standards, Rockville, MD). All samples were run against a 4-7 point calibration curve, depending on the concentration range of the samples. Scandium was used as an internal standard. Sample metal concentrations corrected by subtracting the blank values. (For measurements of additional metals of interest from welding fume were, see Appendix I.)

#### **G. Size Distribution of Particles Collected by Impaction**

For a subset of welding sessions, a stationary Electrical Low Pressure Impactor (ELPI, Dekati Ltd., Tampere, Finland) collected welding fume simultaneously with particle samples collected by the PMASS. The ELPI reports the number of particles by directly measuring the change in current on each of 12 stages that collect particles with diameters between 30 and 10,000 nm when operated at 10 L/min. Prior to entering the

impaction portion of the ELPI, particles are charged, then separated based on the aerodynamic diameter. The measure of current is related to the number of particles on each stage. The intake of the ELPI was placed approximately 10 feet away from the source of welding fume. Greased aluminum substrates were placed on each stage in order to reduce particle bounce.

To improve the accuracy of the ELPI results, the Cunningham slip correction factor was calculated for the midpoint diameter of the size range of particles collected on each impactor stage and then applied to adjust the estimated number of particles counted (automatically performed using Dekati instrument software). The Cunningham slip factor was applied because the particles being sampled are less than 1  $\mu\text{m}$  in diameter, where the aerodynamic properties are different than for larger particles.

From the cumulative fraction of particles in each size-specific stage, the size distribution from ELPI measurements was determined by estimating the CMD in the same manner described for estimating the primary particle CMD (as described in section 2.2, section D). As the particle collection of the ELPI is based on aerodynamic properties of the particles, and within welding fume there are mostly agglomerate particles with few isolated primary particles present (70;71), it is assumed that the particles collected are separated by the size of the agglomerates. Thus, in this study the ELPI data is applied as an estimate of the APSD of welding fume samples.

### **2.3 Method Validation**

Four people were involved in the analysis of the STEM/EELS/EDS data sets. To validate reproducibility of the method, each person involved in data analysis was asked to

evaluate a common data set from a single sample, and the results were compared.

Between-person comparability in the assessment of PPSD was evaluated by comparison of the CMD estimates. Mn composition across the size distribution was evaluated by comparison of Mn composition size slope estimates.

The PPSD of the validation sample measured by 4 people had an estimated CMD of 7.6 nm (range: 7.0-8.2 nm) and average geometric standard deviation of 2.5 (range: 2.4-2.7), (Figures 2.5 & 2.6, Table 2.1). The 95% confidence intervals of the estimated CMD's overlap, and a chi-squared test indicates that the estimated CMD's are not statistically different ( $p=0.99$ ).

The average estimated Mn composition-size slope of the validation sample by the 4 counters was  $0.0021 \text{ nm}^{-1}$  (SD  $0.0006 \text{ nm}^{-1}$ ), (Figure 2.7 & Table 2.2). The 95% confidence intervals of the slopes overlap, and a chi-squared test indicates that the composition measures are not significantly different between counters ( $p=0.13$ ). Therefore, according to this assessment, there is no significant difference in measures of either PPSD or Mn composition across the size distribution between the four counters.

## **2.4 Results**

### **A. Particle Sample Collection**

A total of 10 samples were collected and characterized for size and composition. The average pump flow for samples collected on Teflon filters for total Mn concentration was 2.24 liters per minute (range: 1.89-2.68 liters per minute). The average pump flow for samples collected on the polycarbonate filter for the Mn composition across the size distribution was lower (average: 1.57 liters per minute, range: 1.43 to 1.89 liters per



minute). An imbalance of flows through the PMASS channels means that the mass loading of the Teflon and polycarbonate samples was not identical.

### **B. Total Metals Analysis**

The particle samples were analyzed in two batches for total metals concentration. Method detection limits (MDL) for each batch and each metal (3 times the standard deviation of the blank filter) are: Mn: 0.6 and 0.2  $\mu\text{g}/\text{m}^3$ , and Fe: 6 and 2  $\mu\text{g}/\text{m}^3$ . SRM recovery was within 10% of the expected values in both batches, so no correction factors were applied.

The total content of Mn relative to the total mass was  $7.3\% \pm 2.3\%$  for welding fume samples collected under similar conditions, and  $4.2\% \pm 3.4\%$  for welding fume samples collected under varying conditions. The total content of Fe relative to the total mass was  $37\% \pm 10\%$  for similar welding condition samples and  $28\% \pm 9.4\%$  for varying welding condition samples, respectively (Table 2.3).

### **C. Primary Particle Size Distribution**

Particle samples collected under similar welding conditions had an average primary particle CMD of  $5.7 \pm 2.4$  nm (range: 3.2-8.3 nm). Particle samples collected under diverse welding conditions had an average primary particle CMD of  $6.9 \pm 2.3$  nm (range of 3.3-9.8 nm). The range of geometric standard deviations (GSD's) in the samples collected from similar welding conditions is 2.2-3.0 nm, and in the varying welding condition samples is 1.9-2.8 nm, indicating that there is a similar variation in the distribution of both groups (Table 2.4). Samples collected within either similar condition or varied conditions indicate that within either group the primary particle CMD's were significantly different (chi-squared test,  $p < 0.05$ ). However, the average primary particle



CMD from samples of similar vs. varied weld conditions are not significantly different (t test,  $p=0.44$ ).

#### **D. Characterization of Mn Composition by Particle Size**

Relative abundance of Mn across the PPSD is shown for each sample in Figure 2.8. As demonstrated in the scatterplots, Mn composition was not uniform throughout the distribution nor across samples. To evaluate the relationship of Mn composition by size, a smooth fitted line (“lowess” in STATA) of the relative abundance of Mn was fit to the data. The smoothed line of the samples suggests a linear trend by size, although for the larger size bins where there are few data points, the trend fails.

Samples were subsequently tested individually for linearity. Of the 5 samples collected under similar welding conditions, 3 had a statistically significant positive linear slope (Table 2.5). A chi-squared test indicates that the Mn composition-size slopes of samples collected under similar weld conditions are significantly different ( $p<0.05$ ). Of the 5 samples collected under varying welding conditions, 2 samples had a statistically significant positive slope. Mn composition-size slopes of samples collected under varied weld conditions are also significantly different ( $p<0.05$ ). However, the average slope estimated from samples collected under similar weld conditions was not significantly different from the average slope estimated from varied conditions (t test,  $p=0.87$ ).

#### **E. Confirmation of Mn Composition**

To determine if the STEM analysis of Mn content is quantitative for the entire sample, results of the ICP-MS analysis for Mn were converted from a mass fraction to atomic fraction of relative abundance of Mn (as atomic fraction Mn/[atomic fraction Mn

+ Fe)). This allows for comparison of ICP-MS results to bulk results of STEM/EDS and STEM/EELS.

Combining all 10 samples for both welding conditions, the average percent difference of relative abundance of Mn measured by ICP-MS vs. EELS is 66% (range: 10-338% difference), with higher measures in EELS (Table 2.6). The two samples collected under varied welding conditions with the greatest percent difference between ICP-MS and EELS estimates, sample 6 and 8, also had the lowest content of Mn (5 and 4  $\mu\text{g}/\text{m}^3$  respectively), (Table 2.3). If these two samples are excluded, the average percent difference for ICP-MS vs. EELS is 26%.

The average difference between ICP-MS and EDS estimates of relative abundance of Mn for all samples collected is 33% (range: 4-94% difference), with higher measures in ICP-MS. If sample 6 and 8 are excluded, the average percent difference for ICP-MS vs. EDS is 27%.

Of the analyses presented, the fraction of Mn + Fe vs. the total particle content can only be estimated from the mass fraction metals analyzed via ICP-MS. The average relative mass of Mn + Fe of all welding fume samples is 0.39 (range: 0.23-0.56), (Table 2.6).

In viewing the EDS spectra, the presence of silicon was found to vary widely between samples. The bulk data show that the relative abundance of Si, defined as: atomic fraction of Si/(atomic fraction of Si + Mn + Fe), was 0.15 on average (range: 0.005–0.42), (Table 2.6).

In reviewing the EDS bulk analyses, there were also a few samples where the relative abundance of aluminum appeared high. The relative abundance Al (defined as:

atomic fraction Al/[atomic fraction Al + Mn + Fe]), in sample 6 is 0.24, and in sample 8 is 0.45 (data not shown).

#### **F. Size Distribution of Particles Collected by Impaction**

Agglomerate particle size distribution (APSD) was measured by the ELPI for 4 of the welding sessions conducted under similar conditions. The average CMD measured by the ELPI was 105 nm with an average geometric standard deviation (GSD) of 2.7. This is an average of 16 times the CMD of primary particles as measured by TEM (Table 2.7).

### **2.5 Discussion**

Inhalation of welding fumes has been associated with various health effects including respiratory problems (2). The chemical composition is complex, with a wide range of metals present (62). Several of the metals present in welding fume, including Mn, have been associated with different types of toxicity (2). In addition to understanding the chemical composition, the physical composition, where particles are present as both nano-scale agglomerate and primary particles, may also be important in assessing physiological interactions following inhalation (66;67). Primary particles in welding fume can range in size across 2 orders of magnitude, and it is not well understood if the content of these particles is uniform across the size distribution. Therefore, the purpose of this study was to characterize the size distribution and content of welding fume particle generated under a range of conditions. Analysis of the particle samples was carried out using well established microscopy methods. A new method to

characterize composition was developed that allowed for characterization of differences in PPSD's and relative abundance of Mn throughout the PPSD in welding fume samples.

The new method involved incorporated microscopy techniques. A measure of the PPSD, the primary particle CMD, was manually estimated from a dark field image collected via TEM. The PPSD information was then applied to STEM/EELS data collected from the same location on the welding fume sample in order to estimate the relative abundance of Mn across the primary particle size distribution. The relative abundance of Mn across the size distribution was measured as the Mn composition-size slope. Estimates of primary particle CMD's and Mn composition-size slopes were validated by comparison of results from four individuals who processed the same sample for size and composition. The result the validation study indicated statistically reproducible results, as the measures of either CMD or Mn composition-size slope of 4 people were not significantly different (chi-squared tests,  $p > 0.05$ ).

Analysis of the PPSDs of welding fume samples collected from a variety of welding conditions resulted in CMD estimates that ranged between 3.2 and 9.8 nm. The primary particle sizes measured in samples collected in this study ranged between 4 and 166 nm, and the majority of particles (85%) were <17 nm in diameter. The implications with regard to understanding the impact of exposure to welding fume are under current investigation, but animal studies indicated that physiological clearance rates are faster for smaller primary particles (67). Current methods for assessing welding fume exposure that are typically used, such as total metals concentrations estimated by ICP-MS, depend on integrated sampling methods that provide a summary estimate of exposure in units of mass concentration and provide no information about size. Estimates of welding fume

exposure that focus on size are typically measured by methods that use impaction, which provides information about the agglomerate APSD (helpful in understanding deposition characteristics), but does not provide information about the PPSD.

A limitation of incorporating the method presented here is related to the fact that the particles generated by the welding process are spherical. This enabled us to apply a basic shape tool that provided a good estimate of the particle diameter, and which would not have been possible if the particles were irregularly shaped. Our method for estimation of PPSD may, therefore, not be applicable to other sources of particle exposure.

The agglomerate size measurements, which were collected only during similar welding conditions, had an average agglomerate CMD of 105 nm. While this is 16 times larger than the average primary particle CMD, it is still nearly within the nanometer size range. This indicates that inhalation of the welding fume particles investigated would likely result in deposition within the lower respiratory tract, where there is greater likelihood uptake into the circulatory system (61).

In this study, trends in composition were assessed by simple linear regression. Trends for some samples suggest that the relationship was not linear, as indicated by an apparent decrease in composition toward the high end of the particle size distribution. However, the number of large particles within these samples was very small. The Mn composition size slope was significantly greater than zero for half of the samples analyzed in this study. The combined data of all ten samples resulted in an estimate of the Mn composition slope that was significantly positive (slope =  $0.009 \text{ nm}^{-1}$ , intercept = 0.35, 95% CI: 0.0005, 0.001). Although the estimation of trends in relative abundance of

Mn composition-size slope was much less precise than the CMD estimates these results suggest that the fractional contribution of Mn increases with increasing particle size.

A positive linear Mn composition-size slope implies that larger primary particles have a higher relative abundance of Mn. Using the slope estimated for all combined welding fume samples, the largest primary particle (166 nm) would have twice the relative abundance of Mn of the smallest primary particle (4 nm).

The wide confidence intervals of the slopes is likely to be due both to a true spread of Mn compositions by particle size and to the fact that we only selected between 60-100 particles per sample (depending on the range of diameters in the size distribution) for compositional analysis. A test sample confirmed that analyzing more particles for each sample would have improved the statistical confidence in the measure. The composition was measured with the normal number of particles and with double the number of particles; the confidence intervals obtained were nearly half as wide as those estimated with fewer particles (data not shown). As such, a limitation of estimating the Mn composition size slope is the time required to analyze each particle.

Samples 6 and 8, for which the total Mn content measured by ICP-MS was low ( $\leq 5 \mu\text{g}/\text{m}^3$ ), showed the bulk estimates of relative abundance of Mn as measured by EDS and EELS in very low agreement with estimates resulting from ICP-MS analysis (Table 2.6). In addition to having a low total Mn concentration, the Mn content out of the total concentration for these samples measured by ICP-MS was  $<1\%$  (Table 2.3). This indicates that analyses by EDS and EELS do not provide accurate results for relative quantities that are this small. If these two samples are disregarded, both the bulk EDS and EELS results demonstrate that relative abundance Mn were within 27% agreement of

the relative abundance of Mn determined by ICP-MS. This suggests that the method for estimating Mn composition-size slopes should be interpreted cautiously if Mn content in the sample is low (<1%).

In reviewing the whole dataset, welding fume samples collected under similar conditions were not found to be more similar in terms of measurements of PPSD or Mn composition across the PPSD than the samples collected under varied conditions. While there was not a clear distinction between these two groups, there were significant differences within both groups. Our interpretation of variability across different welding fume samples is limited by the fact that only ten samples were analyzed in this study. However, as these samples were collected by different people performing welding, the variability across samples implies that the technique of welders is a more significant predictor of PPSD and Mn composition across the size distribution than welding equipment or materials. The technique of each welder may lead to differences such as the distance between the electrode and the metal and the duration of the arc, which may influence the temperature of the generated welding fume.

Further research will be needed to understand the health implications based on this small range of PPSD diameter differences and Mn compositional differences within the primary particles. As an area of future research, it is an interesting finding that the relative abundance of Si measured by bulk EDS was as high as 0.2 and 0.4 in some samples. While Mn is known to be present in iron oxides in welding fume, Si is likely to also substitute into the Mn-Fe-oxide structure. If Si is present with Mn, it may alter the solubility and oxidation state of the Mn phase, which could have implications for welding fume toxicity. In addition, it would be useful to explore if differences in metals, such as

aluminum, chromium, and zinc also vary across the particle size distribution in welding fume.

## **2.6 Conclusion**

The data processing method described here provides a measure of primary particle CMD's and linear trends of composition of Mn across the PSD. In applying this method to welding fume samples, we found significant differences among samples. Our methods of particle characterization are estimated in a form that can easily be interpreted and applied to exposure assessment studies. Ultimately, these measures of physical and chemical properties will improve our understanding of the resulting toxicity of welding fume.



## 2.7 Tables and Figures

**Table 2.1** Results of primary particle size distribution comparison study.

Counter	Image Area Counted	# of Particles Sized	CMD	95% CI CMD	GSD* ( $d_{84\%}/d_{16\%}$ ) <sup>1/2</sup>
	$\mu\text{m}^2$	(#)	(nm)	(nm)	
A	0.625	1005	7.1	(5.8-8.7)	2.4
B	0.625	1072	8.0	(6.9-9.3)	2.4
C	0.375	1050	8.2	(7.3-9.2)	2.5
D	0.563	1014	7.0	(6.2-7.9)	2.7

**Table 2.2** Results of Mn composition by particle size comparison study.

Counter	# of Particles	Slope*		Intercept*	
		Estimate	95% CI	Estimate	95% CI
A	160	0.0025	[0.0018, 0.0032]	0.11	[0.08, 0.14]
B	90	0.0013	[0.0002, 0.0023]	0.17	[0.011, 0.22]
C	96	0.0020	[0.0011, 0.0029]	0.16	[0.12, 0.21]
D	99	0.0025	[0.0016, 0.0035]	0.14	[0.09, 0.18]

\*Slope and intercepts are in units of Relative Abundance Mn/Particle Diameter (nm)

**Table 2.3** Total metal concentrations ( $\mu\text{g}/\text{m}^3$ ) in welding fume samples.

Sample	Concentration		
	Total Particle	Mn	Fe
<b>Similar Weld Conditions</b>			
1	1251	126	475
2	8467	359	1981
3	18699	1619	8816
4	9110	681	4242
5	9497	576	2994
<b>Average</b>	<b>9405</b>	<b>672</b>	<b>3701</b>
<b>Std Dev</b>	<b>6202</b>	<b>570</b>	<b>3175</b>
<b>Varied Weld Conditions</b>			
6	648	5	187
7	639	30	148
8	503	4	113
9	9252	808	4111
10	534	31	119
<b>Average</b>	<b>2315</b>	<b>176</b>	<b>936</b>
<b>Std Dev</b>	<b>3878</b>	<b>354</b>	<b>1775</b>

**Table 2.4** Primary particle size distribution of all samples.

	Area Counted	# of Particles Sized	CMD	95% CI CMD	GSD
	$\mu\text{m}^2$	(#)	(nm)	(nm, nm)	(unitless)
<b>Similar Weld Conditions</b>					
1	0.313	1474	5.0	4.4, 5.6	2.3
2	0.500	1000	3.9	3.3, 4.5	3.0
3	0.313	1209	3.2	2.9, 3.4	2.8
4	0.563	1000	8.3	7.2, 9.5	2.3
5	0.375	1036	8.3	7.3, 9.5	2.2
<b>Average</b>	<b>0.413</b>	<b>1144</b>	<b>5.7</b>		<b>2.5</b>
<b>Std Dev</b>	<b>0.113</b>	<b>204</b>	<b>2.4</b>		
<b>Varied Weld Conditions</b>					
6	0.375	994	6.1	4.7, 7.9	2.1
7	0.375	1162	3.3	2.8, 3.8	2.8
8	1.250	1087	7.5	6.4, 8.8	2.5
9	0.500	1151	9.8	9.0, 10.5	2.1
10	0.688	1169	9.3	7.2, 12.0	2.1
<b>Average</b>	<b>0.638</b>	<b>1113</b>	<b>7.2</b>		<b>2.3</b>
<b>Std Dev</b>	<b>0.366</b>	<b>74</b>	<b>2.6</b>		

**Table 2.5** Mn composition by size estimates of all samples

Sample	Slope*		Intercept*	
	Estimate	95% CI	Estimate	95% CI
<b>Similar Weld Conditions</b>				
1	0.0010	[-0.0002, 0.0021]	0.020	[-0.007, 0.046]
2	0.0021	[0.0007, 0.0035]	0.014	[0.023, 0.050]
3	-0.0010	[-0.0021, 0.0001]	0.113	[0.084, 0.143]
4	0.0009	[0.0002, 0.0016]	0.024	[-0.002, 0.051]
5	0.0019	[0.0005, 0.0032]	0.076	[0.033, 0.118]
<b>Average</b>	<b>0.0010</b>		<b>0.049</b>	
<b>Std Dev</b>	<b>0.0012</b>		<b>0.043</b>	
<b>Varied Weld Conditions</b>				
6	0.0010	[0.0004, 0.0017]	-0.012	[-0.034, 0.11]
7	0.0010	[-0.00003, 0.0020]	0.021	[-0.007, 0.049]
8	-0.0001	[-0.0004, 0.0001]	0.018	[0.007, 0.029]
9	0.0016	[0.0005, 0.0026]	0.045	[-0.0004, 0.090]
10	0.0008	[-0.0015, 0.0018]	0.021	[-0.019, 0.061]
<b>Average</b>	<b>0.0009</b>		<b>0.019</b>	
<b>Std Dev</b>	<b>0.0006</b>		<b>0.020</b>	

\*Slope and intercepts are in units of Relative Abundance Mn/Particle Diameter ( $\text{nm}^{-1}$ )

**Table 2.6** Bulk estimation of Relative Abundance of Mn, Relative Mass of Mn + Fe, and Relative Abundance of Si.

Sample	Relative Abundance Mn*					Relative Mass Mn + Fe**	Relative Abundance Si***
	Atomic Fraction			% Difference		Mass Fraction	Atomic Fraction
	ICP-MS	EDS	EELS	ICP-MS vs. EDS	ICP-MS vs. EELS	ICP-MS	EDS
<b>Similar Weld Conditions</b>							
1	0.21	0.12	0.12	45	41	0.48	0.05
2	0.16	0.18	0.17	16	10	0.28	0.13
3	0.16	0.09	0.11	42	27	0.56	0.04
4	0.14	0.13	0.10	4	29	0.54	0.15
5	0.16	0.12	--	25	--	0.38	0.005
<b>Average</b>	<b>0.17</b>	<b>0.13</b>	<b>0.13</b>	<b>27</b>	<b>27</b>	<b>0.45</b>	<b>0.07</b>
<b>Std Dev</b>	<b>0.03</b>	<b>0.03</b>	<b>0.03</b>			<b>0.12</b>	<b>0.06</b>
<b>Varied Weld Conditions</b>							
6	0.026	0.031	0.044	20	71	0.30	0.12
7	0.17	0.12	0.22	30	25	0.28	0.11
8	0.036	0.0022	0.16	94	338	0.23	0.26
9	0.17	0.18	0.18	9	11	0.53	0.20
10	0.21	0.12	0.13	43	38	0.28	0.42
<b>Average</b>	<b>0.12</b>	<b>0.09</b>	<b>0.15</b>	<b>39</b>	<b>97</b>	<b>0.32</b>	<b>0.22</b>
<b>Std Dev</b>	<b>0.08</b>	<b>0.07</b>	<b>0.07</b>			<b>0.12</b>	<b>0.13</b>

\*Relative Abundance Mn: (Atomic Fraction Mn)/(Atomic Fraction Mn + Fe)

\*\*Relative Mass Mn + Fe: (Mass Mn + Mass Fe)/(Total Mass), from ICP-MS

\*\*\*Relative Abundance Si: (Atomic Fraction Si)/(Atomic Fraction Si + Mn + Fe)

**Table 2.7** Agglomerate and primary particle size distributions.

Sample*	APSD (ELPI)		PPSD (TEM)	
	CMD	GSD ( $d_{84\%}/d_{16\%})^{1/2}$	CMD	GSD ( $d_{84\%}/d_{16\%})^{1/2}$
	(nm)	(unitless)	(nm)	(unitless)
3	125	2.9	3.15	2.81
4	101	2.6	8.25	2.30
5	88	2.7	8.35	2.16
<b>Average</b>	<b>105</b>	<b>2.7</b>	<b>6.58</b>	<b>2.43</b>
<b>Standard Dev</b>	<b>19</b>	<b>0.2</b>	<b>2.97</b>	<b>0.34</b>

\*APSD and PPSD results with the same sample number were collected during the same welding session.

**Figure 2.1** STEM/EELS spectrum of a single particle with labeled O, Mn, and Fe peaks. (Obtained from the integration region within the blue square of Figure 2.2B (right image).)

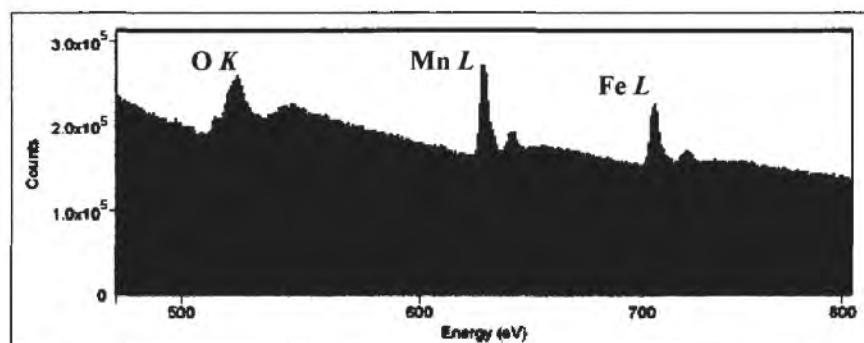


**Figure 2.2** TEM images of welding fume particles. A) Dark field image of welding fume. B) Same dark field image with overlaid circle objects for particle sizing.

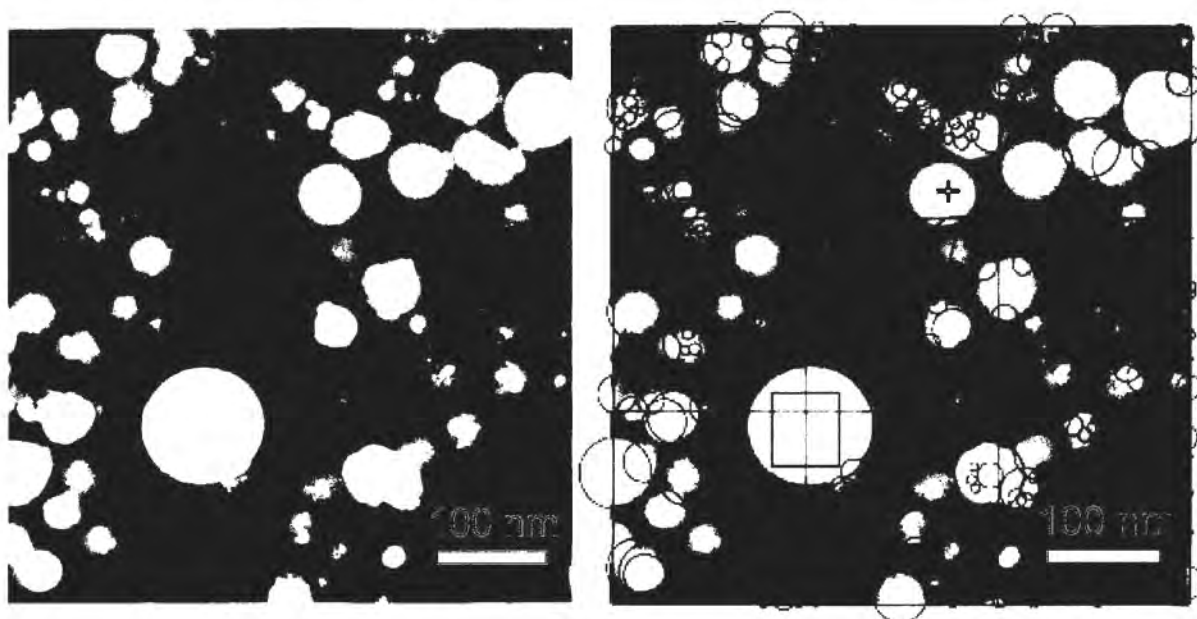


**Figure 2.3** Schematic of grid used for counting PPSD on DF image. All shaded fields were used first and unshaded fields were then used until  $\geq 1000$  particles were counted.

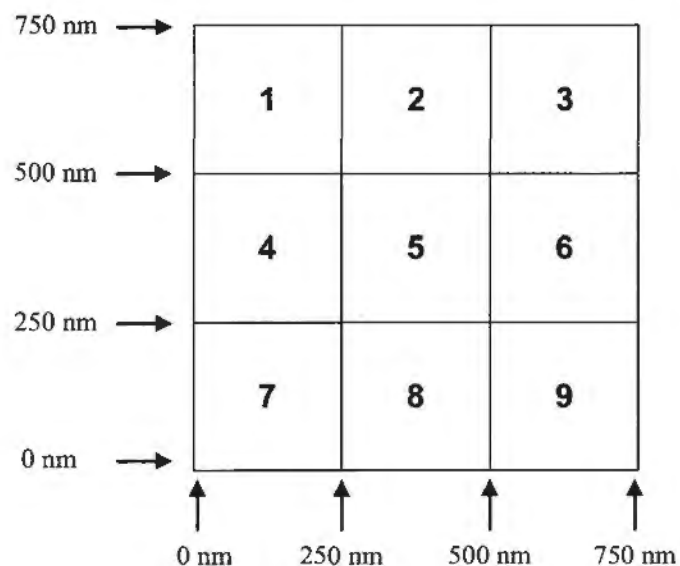


**Figure 2.4** Microscopy elemental maps. A) STEM/EELS Mn map. B) STEM/EELS Fe map. Brighter white on the maps is associated with more abundance of the element of interest for each map.

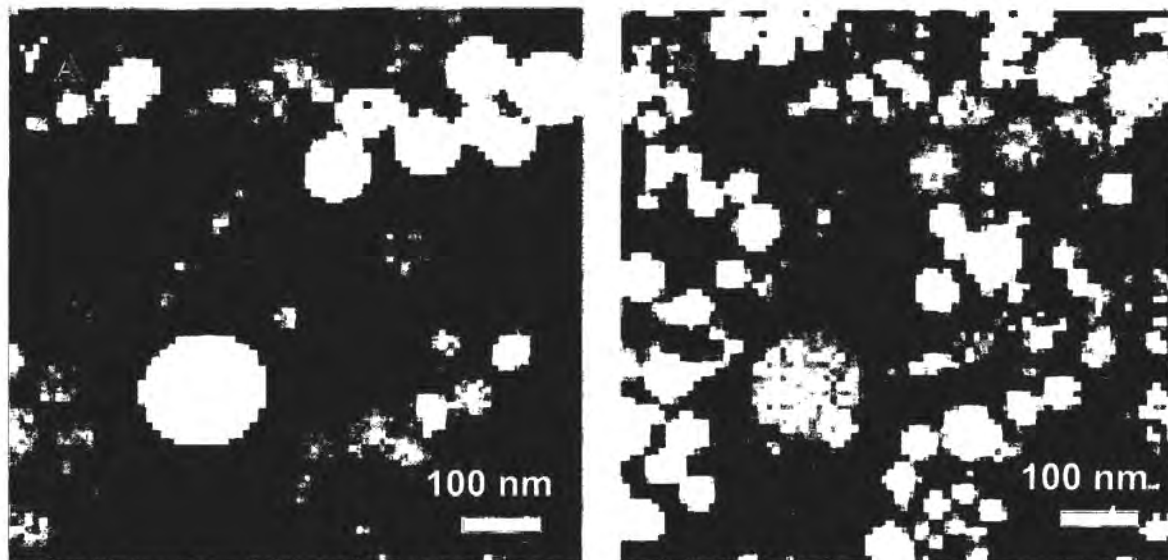


**Figure 2.5** Results of primary particle size frequency distribution comparison.

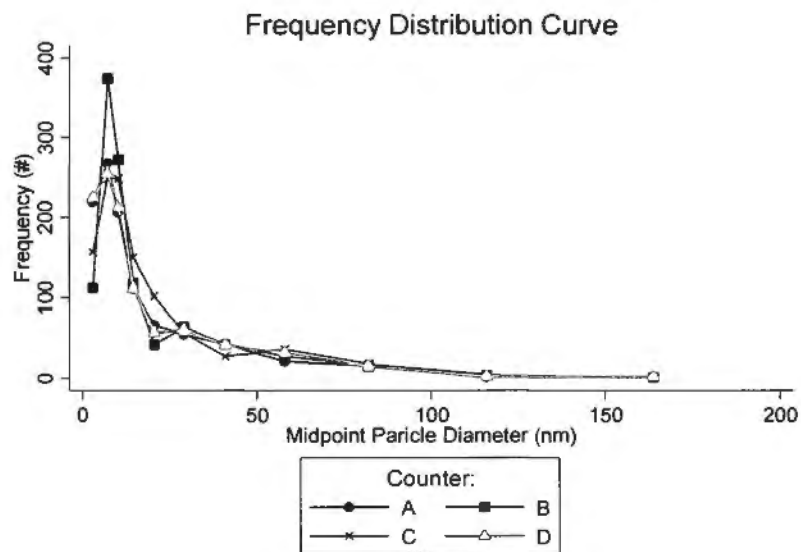


**Figure 2.6** Results of primary particle size distribution comparison.

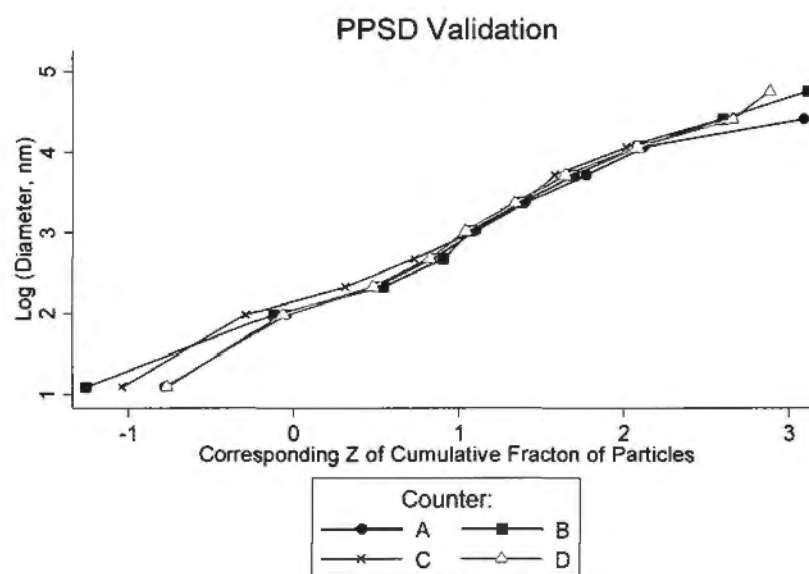


**Figure 2.7** Results of Mn composition by particle size comparison.

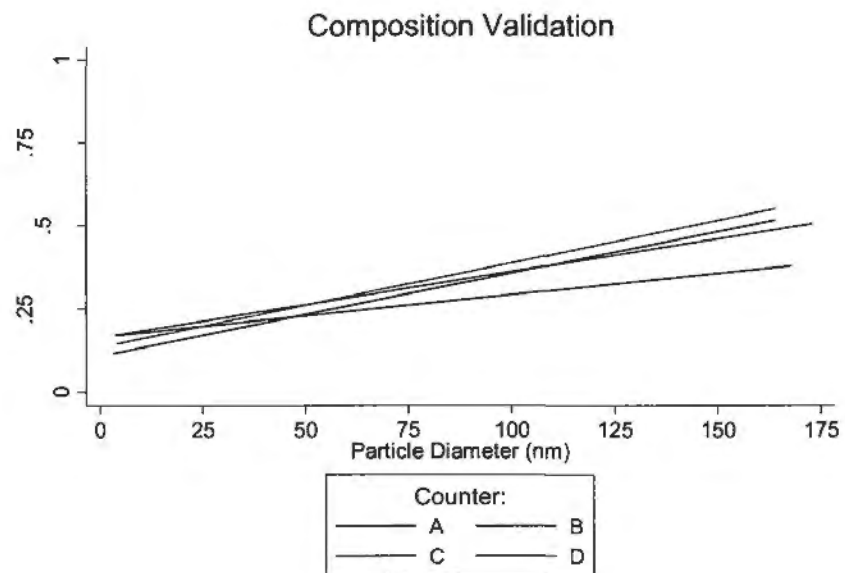




**Figure 2.8** Scatterplots of Mn composition by particle size with smooth line fitting. A) Similar welding conditions. B) Varied welding conditions.

A. Similar Welding Conditions

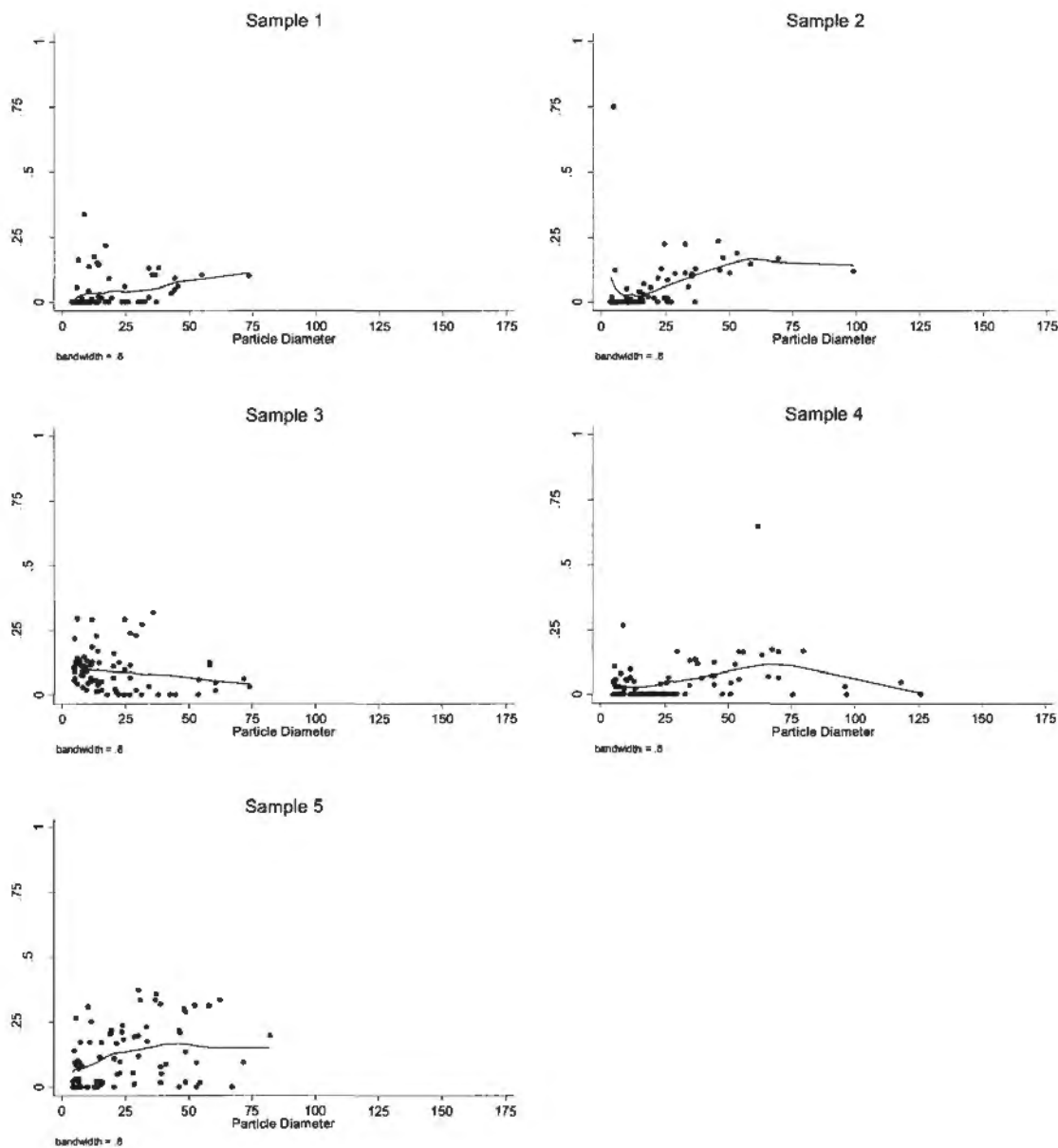
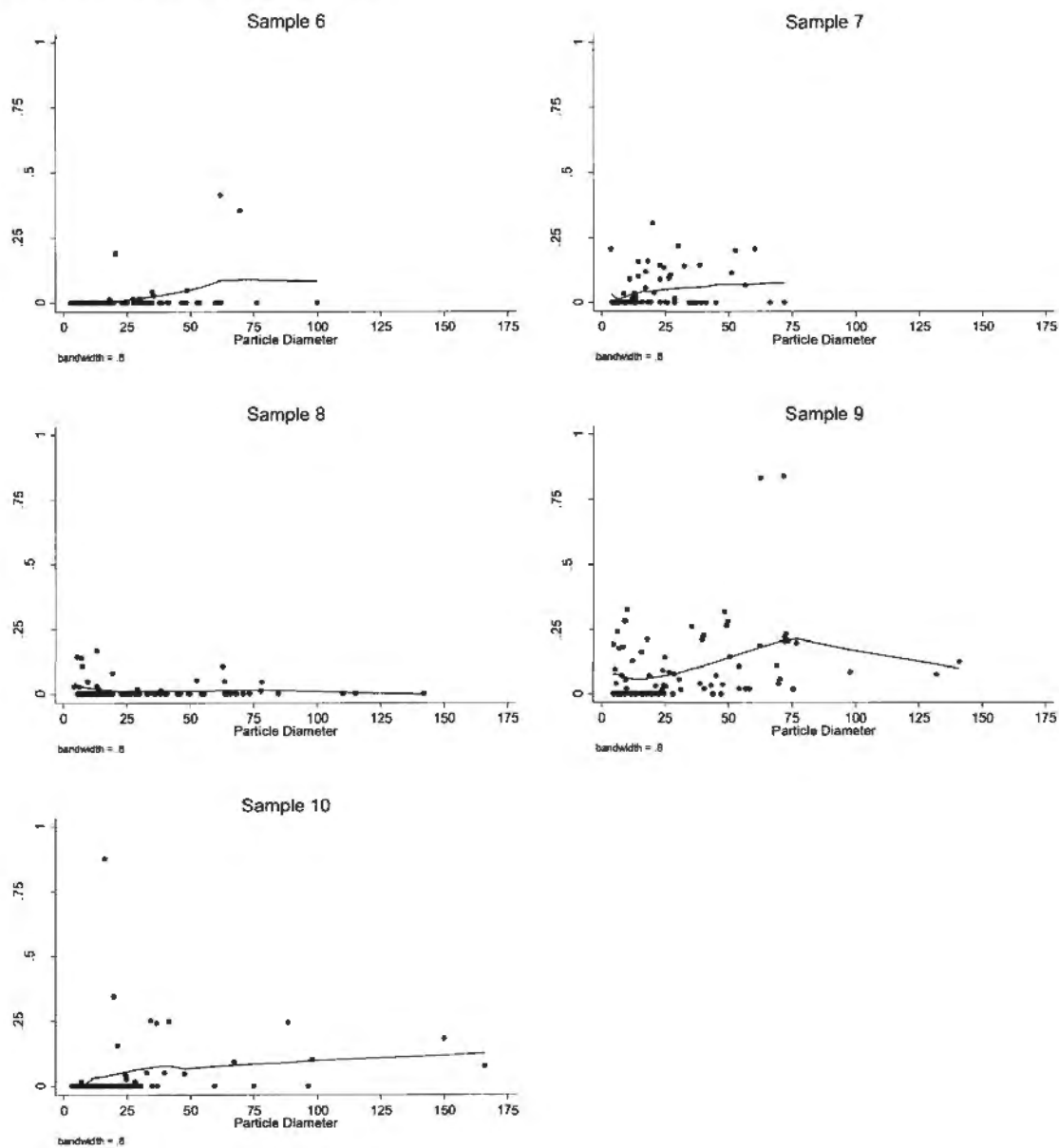


**Figure 2.8 (Continued)**

**B. Varied Welding Conditions**



# 3

## **Characterization of a Portable Method for the Collection of Exhaled Breath Condensate and Subsequent Analysis of Metal Content**

Julie D. Richman, Ernst W. Spannhake, Kristin S. Macri,  
Christine M. Torrey, Sorina E. Eftim, Alison S. Geyh

### **3.1. Introduction**

Exhaled breath condensate (EBC) is a medium from the respiratory tract which is useful for the measurement of biomarkers of internal dose and effect related to the pulmonary system. EBC is a medium collected by cooling exhaled breath (42). EBC is primarily composed water vapor (>99%), but a small fraction of EBC is derived from respiratory droplets that can contain either volatile or non-volatile components that are picked up from the respiratory tract (42). The basic method for collecting EBC samples involves a subject breathing into a chilled tube equipped with a one-way valve. Vapor exhaled from the lungs condenses onto the side walls of the tube, and collected into a container.

The collection of EBC has become an attractive alternative for sampling fluid of the respiratory tract as it is much less invasive than more traditional methods such as broncho-alveolar lavage (BAL) or the collection of induced sputum (IS). Furthermore, because of the time required to collect BAL or IS, typically hours, as well as the physiological stress associated with these methods, it can be difficult to collect repeated samples within a day or on several consecutive days. In contrast, repeat collection of EBC does not pose a significant burden to subjects and is easily collected multiple times in 15 minute intervals.

There are currently three commercially available EBC collection devices: the EcoScreen (FILT GmbH, Berlin, Germany), the EcoScreen Turbo (All Service srl, Parma, Italy), and the Rtube (Respiratory Research Inc., Austin, TX). The materials of the condensing surfaces vary between these devices. The condensing surface is Teflon (polytetrafluoroethylene) in the EcoScreen, polyethylene in the EcoScreen Turbo, and

polypropylene in the Rtube. Research groups have also designed their own devices. A benefit of the EcoScreen and the EcoScreen Turbo is that they both contain refrigeration units to cool the EBC. Temperature is not controlled during EBC collection with the Rtube, because it uses an aluminum tube that is chilled prior to use to cool the EBC. However, the EcoScreen and EcoScreen Turbo are much more expensive than the Rtube making the use of Rtubes more feasible for a small-scale study.

Despite the current interest in the collection of EBC to assess pulmonary biomarkers, a standardized protocol for EBC collection does not exist. As a result much of the literature reporting results associated with EBC assessment shows little consistency in sample collection and analysis methodology. Some effort has been made towards the standardization of the collection of EBC. Between 2001 and 2003 the American Thoracic Society and European Respiratory Society (ATS/ERS) task force convened to review the current knowledge of EBC and to provide recommendations for the collection and measurement of biomarkers in EBC (42). The general recommendations of the task force were to: 1) have subjects breath tidally during collection and wear a nose clip, 2) sample for 10 minutes, 3) use an inert material as the condenser, and 4) refrain from using a resistor or filter between the subject and condenser. They also recommended that future researchers report the temperature of collection of EBC and report the variability and reproducibility of marker measurements. The ATS/ERS task force recognized that some of these parameters may need to be altered based on the conditions of the specific experiment and the marker being analyzed. Parameters that may impact the collection and analysis of EBC can be separated into two categories: 1) physiological factors of the person providing the EBC that may affect the generation of markers in EBC, and 2)

collection and analytical factors that may affect the measurement of the generated EBC markers in the samples.

Among physiological parameters of EBC collection, subjects' ventilation patterns during sample collection have been investigated for their affect on the generation of EBC, or the total volume of EBC collected. Gessner et al. studied varied ventilation patterns during collection of EBC in both COPD patients and healthy adults and found that the total respired volume and the volume of collected EBC were highly correlated (77). No significant associations were found between the volume of collected EBC and total lung capacity (TLC), residual volume, vital capacity (VC), forced exhaled breath in 1 second ("FEV<sub>1</sub>"), airway resistance, height or body weight. Similarly, Liu et al. did not find a correlation between the collected EBC volume and TLC (or gender and age), but found that there was an association with tidal volume and minute volume (78). This evidence suggests that physiological differences between individuals do not significantly alter the amount of EBC collected.

Because ventilation volume influences the volume of EBC collected and the biomarkers of interest can be present at low concentrations within EBC, there is concern that EBC volumes change the dilution level of the marker within the water vapor and thus the measurement of the EBC biomarker may be inconsistent if ventilation patterns are altered (79). However, a study by McCafferty et al. indicated that dilution level may not be influenced by ventilation for some biomarkers in EBC (80). In this study, subjects were asked to alter minute and tidal volumes with visual and audio targets, while holding a "square wave expiratory waveform." Although tidal volume and minute volume were correlated with the EBC volume collected, there were no measureable differences in

nitrate and protein concentrations or in pH level measured. More research will be required to confirm that other biomarker concentrations are also unaffected by minute and tidal volume during collection.

Beyond subject physiological factors, there are several analytical parameters which may also influence the measure of a biomarker in EBC. One significant area of concern is chemical instability. To date, most studies of EBC have focused on markers of inflammation, such as hydrogen peroxide, leukotrienes, and 8-isoprostane, all of which are relatively unstable. Breakdown of biomarkers could occur at any point in collection through analysis, and is a major concern because it may result in losing the ability to detect the biomarker. Goldoni et al reported on the influence of temperature on biomarker stability in a study in which EBC was collected at 4 different temperatures between -10 and 5°C. Their study showed a linear decline in the measure of hydrogen peroxide and malondialdehyde with increasing temperature (81).

In chemically stable biomarkers such as metals in EBC, there is no concern that the biomarker will breakdown as they are already in elemental form; however, contamination is a major area of concern during the collection and storage of EBC. This is a particular challenge for abundant metals, such as iron (Fe) and manganese (Mn), where leaching of the metals from equipment surfaces can be a problem. Contamination generally occurs from contact with surfaces in the collection device and storage containers. An example of contamination is found in the collection of blood for analysis of Mn. Parsons et al. reports that blood lead contamination is reduced by collecting blood samples into plastic “Pb-free” microcollection tubes rather than glass micro-hematocrit tubes(82). The US EPA generally recommends that the choice of sample

container should be in the order of: polytetrafluoroethylene, plastic, and then glass depending on the sample and necessary detection levels (83). Unfortunately, the high expense of polytetrafluoroethylene products often prohibits widespread use. Within plastics there can be significant differences as well, where low density polyethylene has been found to contain lower levels of trace metal contamination than high density polyethylene (84).

The use of EBC as a medium for biomarkers of pulmonary exposure to metals, specifically Mn, has been of specific interest to our research team. Recent research involving the collection of EBC has been conducted to evaluate new biomarkers, including metals. However, many of these studies, while demonstrating the detection capability of metals in EBC, are difficult to interpret because they lack contamination controls. For example, utilizing a specially designed EBC collection device where Tygon FEP tubing was used as the condenser, Goldoni et al. measured cobalt (Co) and tungsten (W) in workers from three factories who were occupationally exposed to these metals. They reported significant difference between pre- and post- work shift measures of Co in EBC (39), but not for W. Lacking from their method section was any discussion of how they controlled for metal contamination, especially for the Tygon tubing. Due to the static properties of Tygon, it can pick up ambient dust, a potential carrier of metal contaminants. Additionally, Broding et al. used the EcoScreen to collect EBC in an investigation of occupational exposures to Co and W (45). They did not find a correlation between post-shift EBC concentration of Co or W and particle samples collected during the shift, though they did find correlation with urinary Co and W and particle samples. Again, no description was present as to how contamination was



controlled. Using a TURBO-DECCS (All Service, Parma, Italy), a commercially available device with refrigeration in which the condenser is made of polyethylene, Caglieri et al. measured levels of chromium (Cr) in EBC of chrome-plating workers (40). They found that measures of Cr in personal airborne particle samples were significantly correlated with pre- and post-work shift measures of Cr in EBC. Using the same device, Mutti et al. analyzed 33 metals in EBC samples collected from subjects with COPD, asthma, smokers, and healthy non-smokers with abnormal spirometry results (41). Controls were smokers and non-smokers with normal spirometry results. Of the 33 metals, lead, cadmium, nickel, aluminum, copper, selenium, iron, and manganese were detected in greater than 50% of COPD subjects or controls, but the percent of samples that were less than the limit of detection is not reported. No difference between groups was demonstrated. Using the EcoScreen, in separate studies Dodig et al. and Vlasic et al. measured Mg, Ca, and Fe and found measureable differences in these metals between healthy subjects and subjects with asthma (47;85).

The goals of the current study were to 1) assemble and validate an EBC collection method that incorporated several quality control features that would allow for the standardized collection of EBC samples, and 2) establish an analytical method for measuring specific metals of interest chromium (Cr), manganese (Mn), nickel (Ni) and Cadmium (Cd) in EBC under conditions rigorously controlled for contamination. This work is part of a larger longitudinal exposure assessment study of welding fume inhalation (Chapter 4). The collection and analytical methods discussed in this work were evaluated in the samples collected from unexposed subjects in the aforementioned investigation. The overall goal of this method evaluation was to assess the association of

metal concentrations in EBC with two key elements: 1) the measured respiratory parameters of subjects generating the EBC 2) parameters of EBC collection.

### **3.2. Methods**

#### **A. EBC Collection Device**

The collection of EBC was one component of a larger longitudinal study to assess the bioavailability of Mn associated with inhalation exposure to welding fume. This study was approved by the Johns Hopkins Bloomberg School of Public Health Institutional Review Board (CHR #491). A signed written consent form was obtained from each subject prior to enrollment in the study.

We selected the Rtube (Respiratory Research Inc., Austin, TX), a commercially available portable device that was economical for a small scale study, as the main instrument of collection to be adapted for our research application. The Rtube, as purchased, is fairly simple. It consists of a condensing tube made of polypropylene, a silicon one-way valve, a t-connector with a closed bottom which acts as a saliva trap, and an attached mouthpiece. An aluminum sleeve that can be cooled to the desired temperature prior to use serves as the non-electric refrigeration of the condensing tube.

Optimization of EBC collection for our study was a combination of modifications made to the collection device and the establishment of a protocol to train subjects to breathe consistently during each sample collection event. The initial modification was the addition of a spirometer designed to measure and record ventilation during tidal breathing (Ecovent, JAEGER, Höchberg Germany). In addition to the spirometer, a visual incentive spirometer (VIS) was attached at the air intake end of the breathing train

which was provided to help subjects normalize the volume of air during each inspiration. A HEPA filter was attached to the intake end of the sample train to reduce exposure to airborne particles during EBC collection. An extra t-connector and flex-tubing were used to connect the EcoVent, VIS, and HEPA filter in series with the Rtube. The modified Rtube EBC collection system (MREC system) is shown in Figure 3.1.

The aluminum condenser sleeve was stored at  $-20^{\circ}\text{C}$  until needed for sample collection. Directly before sample collection the sleeve was inserted over the polypropylene collection tube and the temperature inside the collection tube measured. Sample collection did not commence until the temperature of the tube was between  $0 - 5^{\circ}\text{C}$ .

## **B. Subject Training**

Before collecting EBC from each subject, subjects were asked to go through a training session to assist in establishing a consistent breathing pattern throughout the sample collection period. Subjects were instructed to breathe tidally through the MREC system for a few minutes by sealing their mouth on the mouth piece. They were advised that salivary build-up may occur, and that they could stop to swallow saliva as needed. Once subjects felt comfortable breathing through the MREC system, they were asked to breathe tidally through the system for 2 minutes, and the resulting tidal volume measured by the Ecovent was recorded. Each subject's tidal volume was multiplied by 1.5, which corresponded to a slightly deeper than normal breath, and this was set as the target volume for subjects to visually monitor on the VIS. Subjects were provided a nose clip and practiced breathing at a rate of 10 breaths per minute while achieving the 1.5X tidal volume with each breath. Subjects were informed that if they needed to make

adjustments to the rate or the 1.5X tidal volume, their main focus should be on consistency. EBC collection occurred over a 5-minute period with a nose clip. (Five minutes of EBC collection was selected instead of 10 minutes, as recommended by the ATS/ERS, because this was found to be less burdensome in our study requiring repeat measurements in a relatively short time scale.) The MREC system measures the volume of inhalation though EBC is generated by exhalation. If a subject had initiated an inhalation at the end of the 5 min sample collection period, they were instructed not to stop and to complete the exhalation.

The temperature inside the condensing tube was measured before and after EBC collection. Rtube condensing sleeves were kept on ice, but EBC collection did not begin until the temperature of the condensing tube was  $\geq 0^{\circ}\text{C}$ . The room temperature and relative humidity were recorded.

### **C. EBC Metal Analysis**

#### *Sample Preparation Protocol Development & Quality Control*

To evaluate the potential for surface contamination that is not related to EBC, background measures of metals in the condensing components of the MREC (the condensing tube, one-way valve, and silicon ring) were collected. Background measures were collected in a manner that mimicked the presence of EBC within the condensing tube to establish metal levels in EBC samples resulting from surface contamination that is not due to metals present in the EBC from the subject.

Condensing tube background samples were collected by rinsing the sides of the condensing tube with the one-way valve in place with 1 ml of ultra-pure water. After 5

minutes, the sample water was removed, and 300  $\mu$ l of the sample was digested in 1.5% nitric acid at a 1:4 dilution level prior to analysis.

Background concentrations of Mn were not significantly different in new vs. used Rtube condensing components when the later were soaked in  $\text{HNO}_3$  for 18 hours after use (t-test,  $p>0.05$ ), (Table 3.1). Mn background levels in condensing tubes were not improved by soaking in optima grade  $\text{HNO}_3$  (Fisher Scientific, Columbia MD) vs. ACS grade  $\text{HNO}_3$  (Acros Organics, Geel, Belgium), ( $p>0.05$ ). Soaking in 10%  $\text{NH}_3\text{OH}$  (ACS grade, JT Baker, Phillipsburg, NJ) vs. 10%  $\text{HNO}_3$  (ACS grade) significantly reduced Mn background levels. For Cr, Ni, or Cd the mean background concentrations were lower in  $\text{NH}_3\text{OH}$  vs.  $\text{HNO}_3$ , though the difference was not statistically significant. Based on these measurements, the components of the Rtube were first bleached for disinfection, and then washed in between uses by soaking in 10%  $\text{NH}_3\text{OH}$  (ACS grade) for a minimum of 5 days prior to reuse.

Additional mouth pieces and t-connectors equivalent to those within the Rtube were purchased separately and bleached prior to use (Instrumentation Industries, Bethel Park, PA). To avoid potential for infection in subjects, the mouth pieces and t-connectors were not reused.

#### *Controlling for Background*

Field blanks were collected periodically during the course of the sample collection of both groups of subjects, such that at least 10% blanks were collected per group of subjects and for each subject's sample set ( $n=10$ ) there were 3 field blank samples. (Group 1 included 5 subjects totaling  $n=50$  EBC samples; Group 2 included 3 subjects totaling  $n= 29$  samples.) Field blanks were prepared by placing an Rtube

condensing tube inside a chilled Rtube aluminum sleeve in open air during EBC collection in the same room. The field blank tube was transported in the same manner as tubes containing collected EBC and then processed in the same way as background check samples with purified water. In all cases, the Rtube condensing tube of the field blank was cleaned following the same procedure as the Rtube condensing tubes of the EBC samples it represented.

### *Sample Storage*

A storage test was conducted by measuring metal concentrations over time of multiple aliquots from a pooled EBC sample (Figure 3.2). Storage aliquots were prepared at the same time from the EBC pool and stored at -20°C until the specified analysis time. Three aliquots were analyzed in each time point. For Cr, no statically significant increase was detected at 11 days of storage. A significant increase was detected at 11 days for Mn, Ni and Cd. The change in Mn at 11 days was considered negligible because the average magnitude of this change in concentration was low (8% increase). However, for Ni the mean increase was 16%, and for Cd it was 77%. All four metals demonstrated significant increases after 29 days ( $p < 0.05$ ). Based on these results, all samples were analyzed as quickly as possible, which was always within 9 days of collection. This allowed for adequate analysis of Cr and Mn, but may have been problematic for Ni and Cd.

### *Sample Preparation for Analysis*

To determine the optimal acid solution for the digestion of EBC samples for analysis of metals, a pooled EBC sample was collected. From the EBC pool, aliquots were digested at a 1:4 dilution level in one of four solutions that resulted in the following

final acid solutions: 1% nitric acid, 1% nitric acid with 0.01% triton x100, 2% nitric acid, and 2% nitric acid with 0.01% triton x100 (electrophoresis grade, Fisher Scientific, Fairlawn, NJ). Samples were analyzed for Mn only, and the resulting concentrations were not significantly different when prepared in the four different solutions (Table 3.2). Based on the Mn concentrations, a method was established to digest EBC samples in 1.5% HNO<sub>3</sub> (without triton x100).

Samples were analyzed for metal content via ICP-MS (Agilent 7500ce, Agilent Technologies, Newark, DE). All samples were run against a 4-7 point calibration curve, depending on the concentration range of the samples. Calibration blanks and standards were analyzed every ten samples to check for drift. Analyte concentrations were adjusted with internal standard (ISTD) concentrations (Table 3.3).

The analytical program of the ICP-MS required a sample volume of 1.5 ml for the analysis of EBC metals. As a minimum of 300 µl was generated during EBC collection, samples were diluted at a 1:5 dilution level in the digest solution.

Since no standard reference material (SRM) for metals in EBC is currently available and EBC consists of >99% water (42), a NIST standard for metals in water was used to establish metal recoveries in each analytical batch ("Trace Elements in Water", 1643e). For each SRM measurement, 300 µl of SRM was added directly to a polystyrene tube and then processed by digesting in the same digest solution and at the same dilution level as EBC samples.

#### **D. EBC Sample Collection**

For this study, each subject provided 10 EBC samples during a total of 10 visits within a 5 day period, such that between 1 and 3 samples were collected on each day of



the participation. Following EBC collection, the condensing tubes were stored on ice or in a refrigerator (4°C) until required for processing. The collected volume of EBC was measured using a calibrated pipette. For each EBC measurement, 300 µl of EBC was diluted 1:5 in 1.5% Optima Grade nitric acid (Fisher Scientific, Columbia, MD) containing an internal standard mixture (Agilent, Santa Clara, CA) within an acid-washed polystyrene container (red caps, Sarstedt, Nümbrecht, Germany). More measurement preparations for a sample were prepared if there was sufficient EBC available. The samples were processed on the same day as collection and then stored at -20°C until analysis.

#### **E. Statistical Analysis**

Data preprocessing, including determination of blank subtraction factors, method detection limits (MDL), and SRM correction factors, was performed in Excel (Microsoft Office, 2003). All other statistical analysis was performed in STATA (Intercooled STATA 8, College Station TX).

##### *Measures of Association*

The association of the EBC volume collected or EBC metal concentration vs. collection parameters and physiological characteristics was estimated using a function that accounts for repeat measures, but not censored data (“xtreg” in STATA). Therefore the measured statistic is a regression coefficient with an associated p-value indicating level of statistical significance, rather than typical measures of association such as Spearman’s rho or Kendall’s tau. The same statistical function (xtreg) was used for measurement of the association between EBC metals concentrations measured as µg/L EBC vs. ng/L respired. However, in using this function for EBC metals concentrations,



only metal concentrations that were above the MDL were included in the analysis, and samples with measures below the MDL were dropped from these analyses. The measured EBC metal concentration from the first visit of subjects was found to be lognormally distributed for all four metals, so the logarithms of the concentrations were applied in the regression of each metal concentration. For all EBC metal concentrations presented, the regressions were performed with log transformed data.

#### *Measures of Means and Variability*

When determining the mean concentration of each EBC metal, concentrations that were below the MDL (left censored data) were replaced with half of the MDL. To estimate the variability of the metals concentrations in subjects, a function which accounts for both the autocorrelation present in repeat measures as well as left-censored data by applying a likelihood function was used (“xtintreg” in STATA). As such, the left-censored data were not dropped from the analysis of the estimates of variability of EBC metals concentrations. In addition, to determine the variability the EBC metals concentration, the observed concentration was used rather than the log of EBC metals concentration.

### **3.3 Results**

#### **A. EBC Collection Characteristics**

A total of 79 EBC samples (n) from 8 subjects (N) were collected and available for this assessment. Summary statistics related to sample collection are given in Table 3.4. The mean room temperature and relative humidity during EBC collection were 23°C and 36%, respectively. The mean start temperature of the Rtube condensing tube was

4°C. The average tidal volume established by subjects during the training session was 0.81 L (SD 0.35 L), which corresponded to an average target volume (1.50 \* tidal volume) of 1.22 L. The average total volume respired throughout the 5 minute period of collection was 53 L (overall SD 11 L). The average EBC volume collected was 0.540 mL (overall SD 0.099 mL) (Table 3.4).

## **B. EBC Metal Analysis**

### *Quality Control*

The EBC samples were analyzed in two batches (samples from multiple subjects were analyzed in each batch). Both analytical batches had a unique set of field blanks that were collected at the same time as the subject samples. The average of the field blank concentrations from each batch was subtracted from samples that were analyzed in the same batch (Table 3.5). The MDL was determined as 3 times the standard deviation of the field blank samples collected with the corresponding EBC samples. The MDL's of the two batches were: Mn: 0.47 and 0.92 µg/L, Cr: 0.12 and 1.27 µg/L, Ni: 0.54 and 1.97 µg/L, and Cd: 0.28 and 0.063 µg/L. Applying the batch-specific MDL's resulted in a total of 46% of Mn concentrations, 62% of Cr, 59% of Ni, and 61% of Cd <MDL. For EBC samples with multiple measurements (39% of samples), the precision of the sample estimate is measured as the difference between measurements divided by the average measurement. The average precision of EBC metals concentrations are: 0.42 µg/L for Mn, 3.37 µg/L for Cr, 1.03 µg/L for Ni, and 1.04 µg/L for Cd.

The SRM recoveries were 108% and 105% for Mn, 109% and 105% for Cr, 105% and 100% for Ni, and 105% and 106% for Cd. Since all of the SRM recoveries were within 10% of the expected value, no correction factors were applied to the EBC samples.

### **C. Correlation of Collection Parameters to EBC Metal Concentrations**

The association of EBC metal concentrations with the collection parameters and subject characteristics are presented as estimated coefficient and p-value of the regressions in Table 3.6. In summary, an increase in EBC volume was found to be significantly associated ( $p < 0.05$ ) with a decrease in relative humidity during collection, a decrease in the condensation tube temperature before and after EBC collection, an increase in volume respired during collection, and gender (higher EBC volume were collected from males). However, there was no significant association between EBC volume collected and age or the room temperature during collection.

For the EBC metal concentrations, an increase in room temperature and relative humidity were significantly associated Mn, Cr, Ni, and Cd in EBC ( $p < 0.05$ ). The condensation tube temperature before and after EBC collection was not significantly associated with any of the EBC metal concentrations. The volume respired during collection was significantly associated with an increase of EBC concentration of Mn and Cd, and marginally associated with Cr ( $p = 0.06$ ) and Ni ( $p = 0.07$ ).

The EBC volume collected was significantly associated with EBC concentration of Mn but not Cr, Ni, or Cd. Age of subjects not associated with the concentrations of the EBC metals. However, gender was significantly associated with EBC concentrations of all four metals, with females breathing significantly higher EBC metals concentrations than males.

The EBC metal concentration can be reported either as  $\mu\text{g/L}$  of EBC collected (as reported throughout this paper) or, by incorporating the EBC volume collected and volume respired, it can be reported as  $\text{ng/L}$  respired. In comparing these two measures of

EBC metal concentrations, the coefficient of the EBC metal concentration for the four metals ranges from 18.8 to 21.3 ( $\mu\text{g/L EBC}$ ) per ( $\text{ng/L respired}$ ) (Table 3.7).

### **3.4 Discussion**

Measurement of metals in EBC is still a relatively new area of research being investigated by a few research groups in the past five years. As investigators apply different techniques for collection of EBC and analysis of metals in EBC, reports have lacked information about storage and assessment of the limit of detection that would facilitate interpretation of results. For example, Broding et al. report that their method for measurement of EBC W and Co “provided sufficient sensitivity and low detection limits” without further description (45). Dodig et al. report a detection limit of  $10 \mu\text{mole/L}$  for EBC Mg and Ca, which corresponds to  $243 \mu\text{g/L}$  for Mg and  $40 \mu\text{g/L}$  for Ca, but there is no description of how this was determined (47). Goldoni writes that the detection limit for EBC W and Co is  $0.003 \mu\text{g/L}$ , based on 3 times the standard deviation of the background level, and in subsequent paper the detection limit is  $0.05 \mu\text{g/L}$  for Cr, but it is not clear that a field blank was used in either investigation (39;46). Mutti et al. report a detection limit of  $0.005 \mu\text{g/L}$  for several metals (including Mn, Ni, and Cd), except Al and Se ( of  $0.01 \mu\text{g/L}$ ) that was determined as 3 times the standard deviation of the blank (41). However, Mutti also writes that the “concentration of residual elements on the condenser walls were below the limit of detection”, implying that the condenser tube was not used as the blank (41).

In this study we implemented a series of quality control measures that would allow for the robust characterization of metal content in samples of exhaled breath

condensate. These measures included training subject to breathe consistently during sample collection, additions to the Rtube assembling to allow for the quantitative assessment of volume of air respired by each subject, and an evaluation of all sources of contamination related to the components of the Rtube.

The MDLs estimated in this investigation for the metals we targeted were at least an order of magnitude greater than those reported by other investigators (Table 3.5). Based on our MDLs, 46-62% of samples (depending on the metal) were left-censored. Differences in materials used in the condenser, sample preparation, storage, and analysis could quite possibly result in significant differences in measurement sensitivity among research groups. However, without a clear indication of the way the limit of detection was assessed, it is not possible to make a comparison.

To illustrate the importance of including a definition of the detection limit, for one of the two analytical batches of samples presented in this study the detection limits ( $\mu\text{g/L}$ ) are estimated in three ways, as follows:

- Method Detection Limit (MDL):  $3 * \text{SD of the field blank}$
- Instrument Detection Limit 1 (IDL1):  $3 * \text{SD of lowest analytical calibration standard}$
- Instrument Detection Limit 2 (IDL2):  $3 * \text{SD of calibration check standard (1ppb) analyzed throughout the sequence}$

<b>Metal</b>	<b>MDL</b>	<b>IDL1</b>	<b>IDL2</b>
Manganese	0.47	0.033	0.072
Chromium	0.12	0.028	0.070
Nickel	0.54	0.076	0.14
Cadmium	0.28	0.085	0.0078

As demonstrated, the detection limit can vary by as much as an order of magnitude depending on how it is estimated. Of these three ways of estimating and reporting the

detection limit and sensitivity of a method, the MDL is generally the most conservative measure.

A storage test of pooled EBC demonstrated negligible increases in concentration of Mn and Cr if analyzed within 11 days and stored as samples diluted in 1.5% HNO<sup>3</sup> at -20°C. However, during the same time period, Ni and Cd concentrations increased significantly. After 29 days, all four metals in EBC showed significant increases. While we were using the sample tubes recommended by Agilent, this indicates that leaching of metals occurs over a relatively short period in EBC samples.

In the present study, several parameters that were found to influence EBC metal concentrations. An increase in room temperature, relative humidity, and liters respired during EBC collection are either significantly or marginally associated with EBC concentrations of all four metals. Physiological characteristics were also important determinants of EBC metal concentrations. In contrast to the results reported of EBC volume by Liu et al. (78), in the present study an association between gender and EBC volume collected was found, where males generated more EBC than females. This is consistent with the observation that males respired greater volumes during EBC collection than females in this study (female average total volume during 5 minutes: 48.3 L, male average total volume: 64.1 L). A gender difference was also measured in the EBC metals concentrations, where higher concentrations of all four metals were found in females. Also in contrast to findings by Liu et al., an association between age and EBC volume was found in the present study. At the same time, EBC metals concentrations were not associated with age. It is not clear why there is disagreement in results of EBC volume of the present study vs. those of Liu et al., but it is possible that it can be

attributed to differences in collection and breathing patterns (subjects breathed tidally in the study by Liu et al.). However, in terms of EBC metals measurements, these findings suggest that it is important to recognize the influence of room temperature, relative humidity, liters respired, and gender.

From measurements in this study, the relationship between volume respired during sample collection vs. the volume of EBC sample collected is 106 L respired /1 mL of EBC collected (95% CI: 97, 114). Using the EcoScreen, Gessner et al. obtained similar results of 105 and 98 L/ml EBC in healthy volunteers and COPD patients (77). This repeated finding that liters respired and EBC volume collected are highly correlated suggests that a conversion factor can be applied to EBC metals concentrations to reported units as either  $\mu\text{g/L}$  of EBC or  $\text{ng/L}$  respired (Table 3.7). Measuring EBC concentration as  $\mu\text{g/L}$  is much easier, as reporting EBC concentrations as  $\text{ng/L}$  respired requires measurement of both the total volume of EBC and the total liters respired. Reporting concentrations as  $\mu\text{g/L}$  of EBC does not require either measurement.

Measurements of unexposed healthy adults presented in this study can be compared with measurements of healthy adults in a few other studies. In the present study, mean concentrations were:  $0.76 \mu\text{g/L}$  for Mn,  $0.51 \mu\text{g/L}$  for Cr,  $2.10 \mu\text{g/L}$  for Ni, and  $0.24 \mu\text{g/L}$  for Cd. For all for metals the standard deviation was greater than the mean estimate, and the majority of the variability was attributed to fluctuation within people (intra-person) rather than between people (inter-person) (Table 3.8). This suggests a high degree of typical fluctuation of EBC metal concentration in healthy adults. Mutti et al. presents scatterplots of EBC control measurements that indicate median values of approximately  $0.2 \mu\text{g/L}$  for Mn,  $1 \mu\text{g/L}$  for Ni, and  $<0.01 \mu\text{g/L}$  for Cd (visually



estimated) (41), which are all much lower than the values we obtained. Goldoni et al. also measured a lower mean control concentration for EBC Cr of 0.18  $\mu\text{g/L}$  (range <0.05-0.43). One potential source of difference for higher concentrations measured in this current study may be that both Mutti and Goldoni used the TURBO-DECCS at  $-5^{\circ}\text{C}$  to collect EBC while the temperature of collection was higher in this study (and an increase of temperature is associated with an increase in EBC metals concentrations). However, it is unlikely that this completely explains the difference in findings, and it is likely due to other collection parameter differences.

Our results indicate that several factors influence the measured concentration of EBC Mn, Cr, and Ni. This suggests that reporting these characteristics and maintaining consistency where possible is particularly important in obtaining reproducible results.

Research is continuing to demonstrate that exposures to metals are associated with numerous toxic health effects. For example, exposure to Mn is associated with neurobehavioral deficits (9); Cd exposure is associated with the development of COPD and emphysema; and Ni and Cr (VI) exposures are associated with the development of lung cancer (86). Metals are naturally present in the environment and often in foods. There is growing evidence that even relatively low-level inhalation exposures of some metals, such as Mn, may have toxic effects over a short duration (53). Having a biomarker of internal dose that is sensitive to low-level exposures, could assist our understanding of the relationship between exposure and resulting toxicity. In addition, if a tight correlation between EBC metals and exposures could be established, it may be possible to use EBC metals estimates as a replacement for ambient measures in some settings. This would be beneficial, because collecting EBC is generally much easier than



personal particle sampling. Measurement of EBC metals could prove to be such a marker, however, in this interim phase of standardizing EBC metals collection and analysis it is critical that researchers document detailed procedures and quality control estimates in order to facilitate comparison.

### **3.5 Conclusion**

The MREC system is highly portable, economical, and can be practical for small scale exposure studies. The specific focus of our study was metal concentrations in the EBC. Our assessment of the EBC metals results indicated that there can be multiple sources of metal contamination that are difficult to completely remove and this resulted in a high percentage of samples that were below the method limit of detection. While it is possible that high backgrounds of the metals of interest in this study are unique to the Rtube, it is likely that contamination is also an issue with other methods. It is also clear that when using the Rtube for EBC sample collection and subsequent metals analysis, it is critical to account for all sources of contamination. The variability of the field blank measures may be reduced with the use of other materials for the condensing tube that may be more suitable for the collection of EBC to be analyzed for metals. To our knowledge, this is the first research presenting typical concentrations and variability obtained from repeat measures of EBC Mn, Cd, Ni, and Cr in an unexposed population. Research of EBC metals is still in its early stages, and it is clear that disparate data are obtained from small changes in methods. Until further research has enabled the standardization of EBC metals analysis, we recommend that future groups continue to

measure and report associations of EBC metals concentrations with sample collection and subject parameters.

**Table 3.1** Background metal concentration ( $\mu\text{g/L}$ ) of R tubes condensing tubes cleaned with different methods.

Solution	Soln Purity	Soak Time	R tubes	N	Mn		Cr		Ni		Cd	
					Avg	Std Dev	Avg	Std Dev	Avg	Std Dev	Avg	Std Dev
10% $\text{HNO}_3$	Optima	18 hr	New	5	0.95	0.39	--	--	--	--	--	--
10% $\text{HNO}_3$	Optima	18 hr	Used	4	0.76	0.37	--	--	--	--	--	--
10% $\text{HNO}_3$	ACS	18 hr	New	5	0.50	0.18	--	--	--	--	--	--
10% $\text{HNO}_3$	ACS	5 day	New	5	1.04	0.46	0.266	0.051	4.43	7.10	0.053	0.047
10% $\text{NH}_3\text{OH}$	Optima	5 day	New	4	0.30	0.10	0.030	0.014	0.17	0.13	-0.132	0.002
10% $\text{NH}_3\text{OH}$	ACS	5 day	New	10	0.21	0.17	0.225	0.259	0.74	1.24	-0.012	0.170

**Table 3.2** EBC sample preparation for Mn analysis.

Sample Preparation	Avg Mn Conc	Std Dev Mn Conc
	( $\mu\text{g/L}$ )	( $\mu\text{g/L}$ )
1% $\text{HNO}_3$	2.33	0.33
1% $\text{HNO}_3$ + 0.01% Triton X100	2.22	0.19
2% $\text{HNO}_3$	2.29	0.17
2% $\text{HNO}_3$ + 0.01% Triton X100	2.29	0.14

**Table 3.3** ICP-MS measurement conditions for EBC Mn, Cr, Ni, and Cd.

Instrument	Agilent 7500ce, quadrupole
Torch ID	2.5 mm
Nebulizer	Micromist
Plasma Power	700-1600 W
Auxillary Gas	Mn, Cr, Ni: Helium Cd: None
Sample Uptake Rate During Analysis	0.3 ml/min (0.1 rps)
Peristaltic Pump Program	Uptake: 45 s, 0.3 rps Stabilization: 25 s, 0.1 rps Rinse: 90 s, 0.3 rps
Peak Integration	3 pts/peak, 3 reps
ISTD	Mn, Cr, Ni: Sc-45 Cd: In-115

**Table 3.4** EBC Collection Characteristics. (N=8, n=79)

Parameter	Mean	Min	Max	$\Sigma^{2*}$	$\sigma^2$ Between	$\sigma^2$ Within
Room Temp ( $^{\circ}\text{C}$ )	23	19	26	1.7	1.5	0.9
Relative Humidity (%)	36	14	51	10	9	5
Start Collect Temp ( $^{\circ}\text{C}$ )	4.0	0	10	2.8	1.0	2.6
Diff Collect Temp ( $^{\circ}\text{C}$ )	12.0	7	17	2.0	0.8	1.8
EBC Volume ( $\mu\text{l}$ )	0.540	0.300	0.750	0.099	0.091	0.049
Respired Volume (L)	53.0	33	72	10.6	10.1	4.5

\* $\sigma^2$ : Standard Deviation

**Table 3.5** Analytical measures of quality control for EBC metal concentrations (µg/L).

Metal	Batch 1 (N=50)					Batch 2 (N=29)				
	Field Blank	MDL*			SRM**	Field Blank	MDL*			SRM**
	Avg	Estimate	# <MDL	% <MDL	% Recovery	Avg	Estimate	# <MDL	% <MDL	% Recovery
Mn	0.27	0.47	22	44	108	0.42	0.92	14	48	105
Cr	0.02	0.12	27	54	109	0.78	1.27	22	76	105
Ni	0.35	0.54	31	62	105	1.05	1.97	16	55	100
Cd	0.021	0.277	32	64	105	0.032	0.063	16	55	106

\*MDL: Method Detection Limit.

\*\*SRM: Standard Reference Material

**Table 3.6** Association of EBC volume (ml) and metal concentrations ( $\mu\text{g/L}$ ) vs. subject and collection parameters. Bolded estimates are statistically significant ( $p < 0.05$ ). (N=8)

Parameter	EBC Volume (n=79)		EBC Mn (n=43)		EBC Cr (n=28)		EBC Ni (n=32)		EBC Cd (n=31)	
	$\beta^*$	p-value	$\beta$	p-value	B	p-value	$\beta$	p-value	$\beta$	p-value
<b>Collection Parameters</b>										
Room Temp ( $^{\circ}\text{C}$ )	-0.008	0.212	<b>0.68</b>	<b>&lt;0.001</b>	<b>0.33</b>	<b>&lt;0.001</b>	<b>0.37</b>	<b>&lt;0.001</b>	<b>2.5</b>	<b>&lt;0.001</b>
Relative Humidity (%)	<b>-0.004</b>	<b>&lt;0.001</b>	<b>0.92</b>	<b>&lt;0.001</b>	<b>0.84</b>	<b>0.002</b>	<b>0.86</b>	<b>&lt;0.001</b>	<b>1.1</b>	<b>&lt;0.001</b>
Condense Start Temp ( $^{\circ}\text{C}$ )	<b>-0.011</b>	<b>&lt;0.001</b>	0.91	0.183	1.00	0.980	1.06	0.666	1.0	0.827
Condense End Temp ( $^{\circ}\text{C}$ )	<b>-0.010</b>	<b>0.001</b>	0.88	0.212	1.06	0.700	1.13	0.627	1.3	0.159
Diff Condense Temp ( $^{\circ}\text{C}$ )	<b>0.014</b>	<b>&lt;0.001</b>	1.04	0.698	1.03	0.849	0.96	0.83	1.1	0.429
Volume Respired (L)	<b>0.006</b>	<b>&lt;0.001</b>	<b>1.05</b>	<b>0.002</b>	1.10	0.060	1.10	0.066	<b>0.9</b>	<b>0.011</b>
EBC Volume (ml)	--	--	<b>955</b>	<b>0.003</b>	384	0.265	29	0.526	0.005	0.192
<b>Subject Characteristics</b>										
Age (year)	0.002	0.515	0.96	0.284	1.00	0.972	0.95	0.668	1.0	0.837
Gender (1=female)	<b>-0.107</b>	<b>0.049</b>	<b>0.28</b>	<b>&lt;0.001</b>	<b>0.01</b>	<b>&lt;0.001</b>	<b>0.04</b>	<b>&lt;0.001</b>	<b>13.8</b>	<b>0.001</b>

\* $\beta$ : mixed model regression coefficient.

**Table 3.7** Association between EBC metal concentration measured as ug/L EBC vs. ng/L respired.

<b>Metal</b>	<b><math>\beta^*</math></b>	<b>95% CI</b>	<b>p-value</b>
Mn	18.8	[17.9, 19.7]	<0.001
Cr	19.9	[19.3, 20.6]	<0.001
Ni	21.3	[20.3, 22.4]	<0.001
Cd	20.0	[18.4, 21.7]	<0.001

\* $\beta$ : [avg metal concentration ( $\mu\text{g/L}$ )] / [avg metal concentration (ng/L respired)]

**Table 3.8** EBC metal concentrations ( $\mu\text{g/L}$ ). (N=8, n=79)

<b>Metal</b>	<b>Mean</b>	<b><math>\sigma^2_{\text{Between}}</math></b>	<b><math>\Sigma^2_{\text{Within}}</math></b>
Mn	0.76	0.19	0.89
Cr	0.51	$1.76 \cdot 10^{-16}$	1.36
Ni	2.10	1.87	6.64
Cd	0.24	0.09	0.48

**Figure 3.1** Modified Rtube EBC Collection Apparatus. Left (A): Rtube components: 1) insulator, 2) aluminum sleeve, 3) condensing tube, 4) one-way valve, 5) t-connector, 6) mouth piece and 7) saliva trap. Right (B): MREC System.

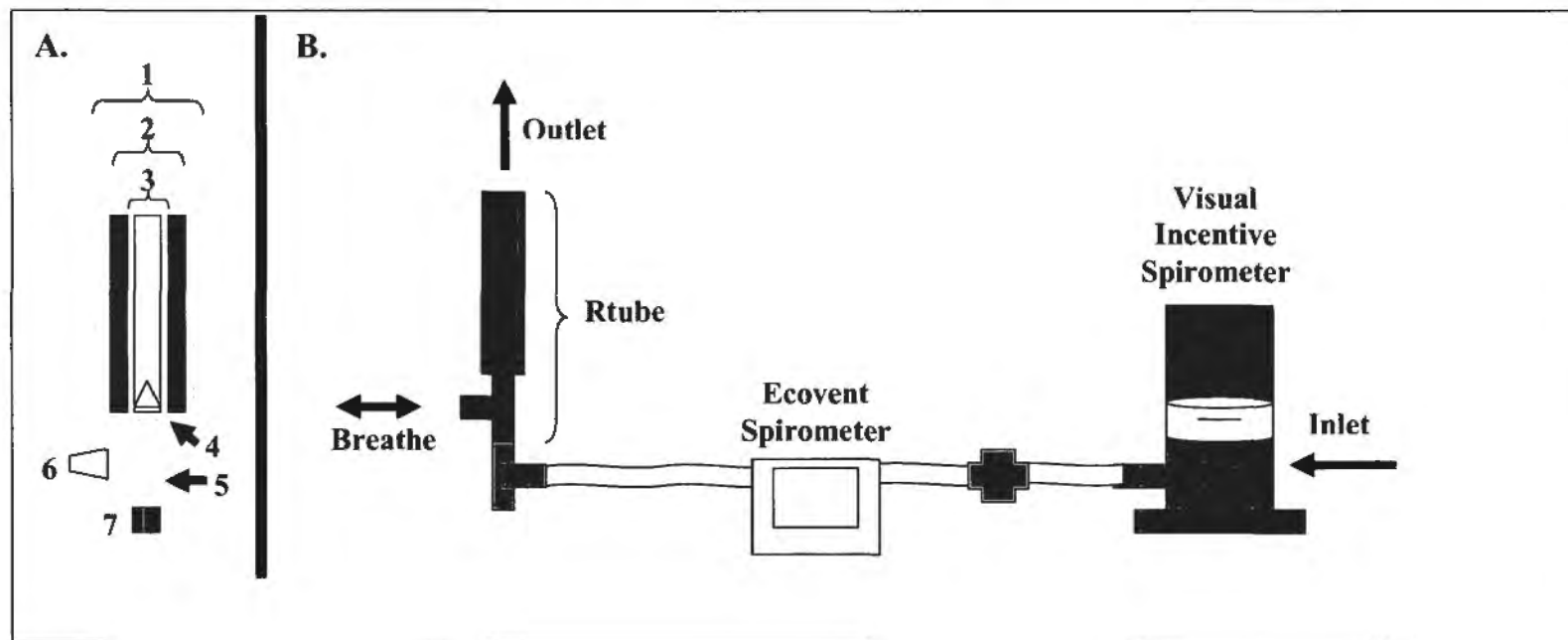
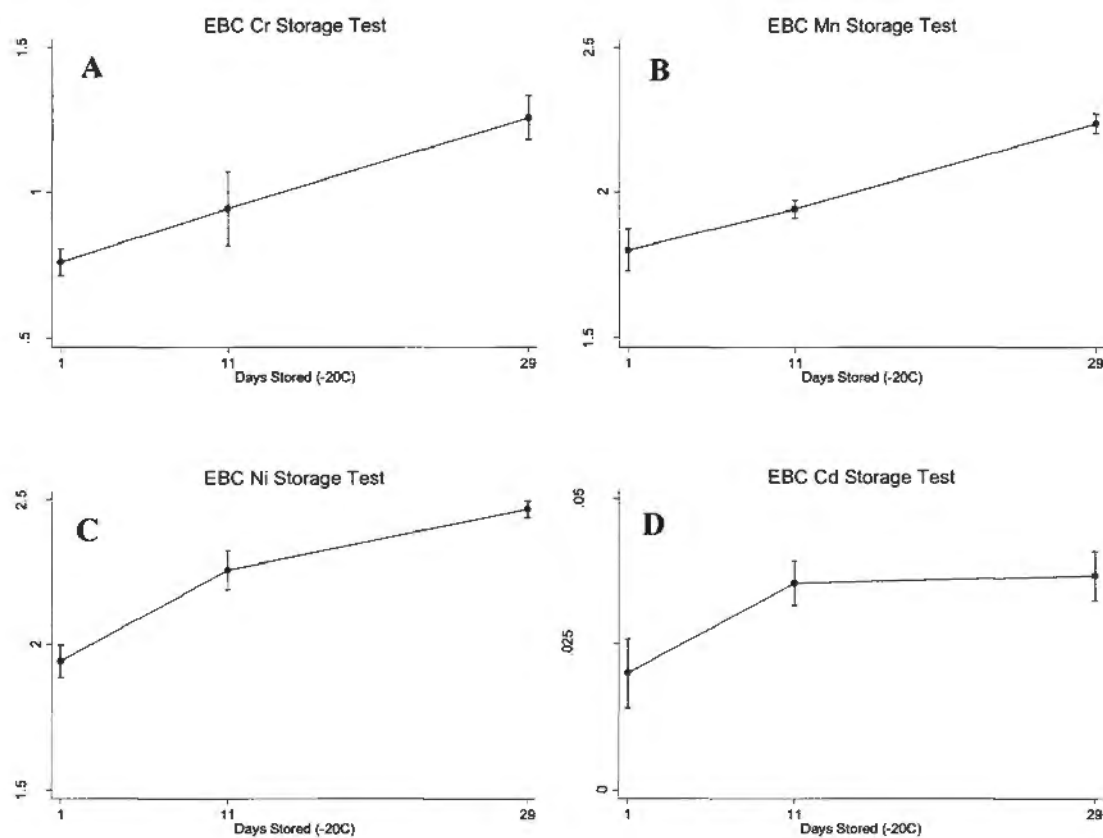




**Figure 3.2** EBC metals storage test results. A) EBC Cr Storage Test; B) EBC Mn Storage Test; C) EBC Ni Storage Test; D) EBC Cd Storage Test.\*



\* At each time point n=3, error bars = std dev.

# 4

## **A Longitudinal Study to Assess the Presence of Manganese in Blood and Exhaled Breath Condensate Following Acute Inhalation Exposure to Welding Fume**

Julie D. Richman, Kenneth J.T. Livi, Ernst W. Spannhake, Sorina E. Eftim,  
Kristin S. Macri, Christine M. Torrey, Alison S. Geyh

#### **4.1 Introduction**

Manganese (Mn) is an essential element; however, over-exposure to Mn can result in neurotoxicity. Subclinical neuropsychological changes associated with Mn exposure can range from deficits in cognitive function, recall, and upper limb motor skills (15;23;26;53;87). In the general public, diet is main source of Mn exposure, and adults consume approximately 0.9 mg to 9.4 mg of Mn every day (8). However, overexposure due to Mn from the diet is rarely a concern because only 1-5% of ingested Mn is absorbed via the gastrointestinal tract (9). While over-exposure to Mn via inhalation is uncommon in the general public, high level inhalation exposures on the order 1000  $\mu\text{g}/\text{m}^3$  have been found to occur in populations employed in manganese mining, ferroalloy production welding, and battery production (9). Animal studies indicate that the toxic effects are greater for similar doses that are inhaled rather than ingested (56). Severe Mn exposures through inhalation can result in the development of manganism, a disease with symptoms that initially resemble schizophrenia and with continued exposure progress to resemble Parkinson's disease (9).

Epidemiological studies of populations occupationally and environmentally exposed to airborne Mn have reported a relationship between exposure and neurotoxic outcomes (56). However, the relationship between airborne Mn exposure and Mn uptake from the pulmonary system remains unclear. Several studies have used biomarkers of Mn exposure to assess the relationship between Mn inhalation exposure and biological impact (25;29;48-53;87-91). Results reported from these studies have been inconsistent, especially for blood and urine. Urinary Mn is problematic for assessing the uptake by inhalation because it is not specific to inhalation. It also reflects

uptake of Mn by ingestion. Mn in blood is thought to be more reflective of inhalation exposure, results from studies attempting to show differences in individual blood Mn concentrations and Mn exposure levels have been inconclusive (48-53).

Differences in the source of Mn and the timing of biomarker collection have likely contributed to discrepancies between studies examining the association between Mn exposure and biomarkers of Mn exposure. The form of Mn varies by source and the form to which various populations are exposed varies by exposure scenario.

Toxicological research has indicated that the form of Mn in the exposure affects both the degree of bioaccumulation and the time course, or change in concentration over time, of Mn throughout the body including in the target organ, the brain (57-59;92). For example, in companion studies by Dorman and Vitarella, the bioaccumulation of Mn measured in lung tissue of rats following Mn inhalation exposure was found to be dependent on the form of Mn. In these studies, the lowest concentrations of Mn in lung tissue resulted from  $\text{MnSO}_4$ , with higher concentrations following  $\text{Mn}_3\text{O}_4$  exposure, and the highest concentrations following  $\text{Mn}_5(\text{PO}_4)_2\text{PO}_3(\text{OH})_2$  (Mn phosphate) exposure (58;59). Research by Roels et al. demonstrates that peak Mn blood concentrations in rats following exposure through both intratracheal instillation and oral gavage ranged from hours to several days depending on the form of Mn they were exposed to (56). These findings may partly explain inconsistencies in the epidemiological literature, as epidemiological studies have included several occupational groups, such as ferroalloy production workers, Mn miners, Mn chemical manufacturer and welders, among whom the sources of Mn exposure and therefore the form of Mn they are exposed to likely vary. Also, since, as Roels et al. demonstrated, Mn half-life is form-specific, inconsistency in

the findings of epidemiology studies may be explained by differences in the durations between the exposure of study subjects and the collection and measurement of Mn in biomarkers; some were immediate and others were more than 10 hours post exposure.

Beyond chemical differences influencing toxicity, the physical property of particle size is also known to be related to the interaction within the body. Following inhalation of particles, the site of deposition in the respiratory system is dependent on the particle diameter (61). Within different regions of the respiratory system, the mechanisms for clearance and transport vary. The issue may be further complicated by the fact that the initial inhalation exposure may be to particles which are present as agglomerates composed of smaller primary particles. In this case, the site of deposition may be determined by the size of the agglomerate, but the resulting interaction (clearance or toxic effect) may depend on the primary particles. In an animal study of exposure to nanometer sized particles, Oberdörster found that greater translocation from the respiratory system to lymph occurred with exposure to TiO<sub>2</sub> particles (primary particle diameter ~20 nm) compared with exposure to carbon black particles of a similar size, demonstrating that TiO<sub>2</sub> had a different physiological interaction (66). Oberdörster hypothesized that the difference in translocation may have been due to the fact that TiO<sub>2</sub> more readily disaggregates. This suggests that characterizing the primary particles in an exposure may be important to understanding the resulting interaction in the body.

In this study, we focus on exposure to welding fume, which is known to contain Mn mainly as Mn oxides, often in compounds that also contain iron within particle agglomerates (2;62;63). The goal of this study was to explore the relationship between the initial form of Mn inhalation exposure and the time course of uptake and clearance in

the circulatory and pulmonary systems as measured by Mn in blood and exhaled breath condensate (EBC). Welding fume was selected as a model of inhalation exposure to Mn because it contains intermediate levels of Mn and is representative of true occupational exposure. The target population for recruitment was beginner and recreational welders who weld intermittently to allow for the specific characterization of uptake and clearance of Mn after a unique exposure. A method developed for characterization of primary particles of welding fume that could be important in explaining uptake and clearance in both biomarkers was applied to this exposure assessment (Chapter 2).

## **4.2 Methods**

### **A. Study Design and Subjects**

Subjects were recruited through postings of flyers and word of mouth. The main criteria for inclusion were: recreational or beginning welders who had not welded within 2 weeks prior to enrollment in the study (i.e. *not* occupational welders). Using a questionnaire for screening, they also were also confirmed to be healthy adults without respiratory health problems or liver conditions, who were not pregnant, and who had no current or past history of occupational exposure to Mn. Questions about respiratory health were: “Do you currently have a respiratory health problem?”, and “Do you currently have symptoms of a head or chest cold?” To assess liver conditions we asked: “Have you ever been told by a doctor or other health professional that you had any kind of liver condition?” Examples of occupational settings associated with elevated Mn exposure were listed (“steel foundry, ferroalloy production plants, battery processing plants, subway or light rail systems, power plants, and Mn chemical manufacturing

factories”). Smoking status was assessed by asking questions about both past and present first and second hand smoking.

The study design for individuals who participated as welders was to collect baseline samples of EBC and blood, to have subjects weld for one session for a few hours, and then to collect 9 more EBC and blood samples following welding through 5-7 days after enrollment. As such, welding occurred between visits 1 and 2 of participation. The general visit schedule and mean time from welding for exposed subjects was:

Day of Study:	1			2		3			4	5-7
Visit Number:	1	2	3	4	5	6	7	8	9	10
Hours After Welding:	-6	0.5	3	18	26	42	45	50	65	94

When individuals repeated the study as unexposed subjects, the study protocol and visit schedule was the same except that subjects did not weld during the week of participation and no particle samples were collected during unexposed participation.

This study was approved by the Johns Hopkins Bloomberg School of Public Health Institutional Review Board (CHR #491). A signed written consent form was obtained from each subject prior to enrollment in the study. Subjects were compensated for their time with a \$200 Visa or MasterCard gift card.

## **B. Welding Fume Collection & Analysis**

Exposure to welding fume particles was accomplished using two sets of particle samples deployed within the breathing zone of each welder during the welding session: a total dust sample collected within a closed face total dust cassette (37 mm styrene acrylonitrile cassette, Pall Life Sciences, Port Washington, NY), and “PMASS samples” collected with a Personal and Microenvironmental Aerosol Speciation Sampler (PMASS,

MSP Corporation, Shoreview MN) which allows for simultaneous collection of two equivalent particle samples.

The total dust sample was collected onto a 2.0  $\mu\text{m}$  pore size, 37 mm Teflon filter with a PTFE support ring (Pall Life Sciences, Ann Arbor, MI) within a closed face total dust cassette with a target flow rate of 2 L/min. The PMASS includes a single size selective inlet (cut-size 2.5  $\mu\text{m}$  at 4 L/min) and two parallel sampling channels, and operates with one pump. A 3.0  $\mu\text{m}$  pore size, 25 mm Teflon filter with a PTFE support ring (Pall Life Sciences, Ann Arbor, MI) was placed in one PMASS channel and a 3.0  $\mu\text{m}$  pore size, 25 mm polycarbonate filter (Nuclepore Track-Etched Membrane, Whatman, Kent, UK) was placed in the other PMASS channel. The target total flow rate was 4 L/min passively split to 2L/min through each channel. Total flow was measured using a flow meter (Drycal DC-Lite & DC-2, BIOS, Butler, NJ). Side-by-side rotameters were used to determine the proportional flow through each filter.

Both Teflon filters were analyzed for total mass and total Mn concentration. Particle mass was measured using gravimetric analysis. Filters were weighed in a temperature and humidity controlled weighing room after equilibrating for  $\geq 24$  hours using a Mettler T5 microbalance with precision of  $\pm 0.003$  mg (Mettler-Toledo, Toledo OH).

To prepare particle samples for measurement of Mn concentration, the Teflon filters were microwave-digested in optima grade  $\text{HNO}_3$  and optima grade HF (Fisher Scientific, Columbia MD). For the analysis of total metals, for every ten samples, at least two standard reference material (SRM) samples were digested and analyzed (NIST material 2709 “San Joaquin soil” or NIST material 1648a “Urban Particulate Matter”;



National Institute of Standards, Rockville, MD). Particle samples were then analyzed for Mn-55 and Fe-56 via ICP-MS (7500ce Agilent Technologies, Newark DE), which includes collision cell technology to minimize polyatomic interferences. Collision gases include both helium and hydrogen, one of which is applied depending on the interference of concern. The applied gas for Mn was helium and for Fe was hydrogen. Sc-45 was added to each sample as an internal standard (Table 4.1).

The polycarbonate filter was designated for characterization of the primary particle size distribution (PPSD) and the Mn composition by primary particle size using microscopy techniques described in Chapter 2. In summary, the sample was prepared for microscopy by washing the filter with ethanol, embedding in epon, and sectioning to 80 nm thickness on a Leica UCT ultramicrotome through the cross section of the filter. The sectioned filters were then placed onto a nickel grid and carbon coated. The primary particle size distribution was determined from a dark field image collected with a transmission electron microscope (TEM, Philips CM 300 FEG S/TEM). The diameters of at least 1000 primary particles were visually estimated by applying image processing software (ES Vision). Particles were then divided into size bins based to estimate the count median diameter (CMD).

The Mn composition through the PPSD was determined by using the estimated particle diameters from the dark field image, and selecting 10 particles within each established size bin for determination of composition via scanning transmission electron microscope/electron energy loss spectroscopy (STEM/EELS). Mn composition across the size distribution, or Mn composition slope, was measured as the slope of the relative abundance of Mn vs. particle diameter.

### *Representativeness of a Single Measure of CMD or Mn Composition-Size Slope*

Two sets of particle samples obtained from personal samples collected from subjects who welded during the same session with shared equipment were analyzed to assess the representativeness of a single sample for a group exposure measured as PPSD or Mn composition across the size distribution (Table 4.2).

For both sets, the duplicate CMD's estimated within a single welding session were significantly different (chi-squared  $p < 0.05$ ). This suggests that a single CMD estimate obtained from a personal exposure measurement may not accurately reflect the CMD in the exposure of the whole group. However, there was suggestion of proximity of the measures. As a less restricted measurement, the range of CMD's measured was divided into two categories that split the distribution of CMD's evenly (CMD  $< 6.9$  nm, or  $> 6.9$  nm). For both duplicate sets, the measures of CMD were within the same category. Accordingly, a general category of having a small ( $< 6.9$  nm) or large ( $> 6.9$  nm) CMD size obtained from one subject in a welding session was applied to all subjects in the welding session.

The Mn composition by particle size were not significantly different (chi-squared  $p > 0.05$ ) for either set of duplicates, indicating that a single Mn composition measurement could be used to represent the Mn composition in the exposure of the group. As such, the slope estimate of Mn composition by particle was assigned for all subjects within a welding session. For the two sessions with two measures of slope, the average of the slope was applied as the estimated measure to other subjects in the session. Additionally, a categorical value of Mn composition-size slope was assigned for each subject exposure,

where the slope was either significantly positive, or the slope was not significantly positive.

### **C. Biomarker Collection and Analysis**

EBC was collected and analyzed using the method described in Chapter 3. In brief, subjects were asked to breathe into a modified Rtube collection system for 5 minutes using a visual incentive spirometer as a cue to breathe at 1.5 times their previously established tidal volume. The respired volume was measured on a spirometer designed for tidal breathing (“Ecovent”, Viasys GmbH, Höchberg, Germany).

The EBC volume was determined with a pipette. EBC samples were prepared by diluting 1:5 in 2% HNO<sub>3</sub> (optima grade), and adding 50 µg/L internal standard (ISTD) in an acid-washed polystyrene tube.

EBC field blanks were collected by placing an Rtube condensing tube with a sleeve and insulator covering it in the room of collection during collection, and then prepared in the laboratory by “drizzling” one ml of ultrapure water down the sides of the condensing tube, and the water remained in the tube for 5 minutes. Subsequently, EBC field blank samples were prepared in the same way as EBC samples.

Blood was collected into K2-EDTA lavender top whole blood containers (2 ml, BD vacutainer) using a butterfly (21 or 23 G, “Safety-Lok” or “Push Button Collection Set”, BD vacutainers). Blood samples were processed by diluting 1:50 in 0.5% HNO<sub>3</sub> (optima grade), 0.05% Triton X100 (electrophoresis grade, Fisher Chemical, Fairlawn, NJ), and 50 µg/L ISTD in an acid-washed polystyrene tube on the same day as collection. This method was selected based on previous quality control experiments for analysis of Mn in blood (Appendix II).

Serum samples were collected into gold top serum separation tubes (5 ml, BD vacutainers). At least 30 minutes after collection into serum separation tubes, samples were centrifuged for 10 minutes at 3,150 rpm. Separated serum was decanted into sterile polystyrene culture tubes. Serum was analyzed for iron at the Johns Hopkins Medical Laboratories.

EBC, blood and serum samples were transported to the laboratory on ice within hours of collection and were stored at -4°C prior to sample processing, which occurred on the same day as collection. All samples were then stored at -20°C prior to analysis. EBC and whole blood samples were analyzed for Mn within 9 days of collection via ICP-MS (Table 4.1). EBC and whole blood were analyzed with a 5-7 point calibration curve. For analysis of Mn in EBC, Sc-45 was selected as the internal standard. For analysis of Mn in blood, Ge-72 was selected as the internal standard. For EBC samples, a NIST standard for metals in water was used as the SRM to establish metal recoveries in each analytical batch ("Trace Elements in Water", 1643e). For blood samples, Seronorm Trace Elements Whole Blood L-1 was used as the SRM in each analytical batch (freeze-dried human blood, Billingstad, Norway). Correction factors were applied to EBC metal and blood metal concentrations if the batch-specific SRM recoveries differed from the expected concentration by >10%. Based on preliminary data for analysis of Mn in blood, we found that using matrix matched standards did not improve the SRM recoveries, so non-matrix matched standards were used in the calibration curve (data not shown).

#### **D. Statistical Analysis**

Data preprocessing, including determination of blank subtraction factors, method detection limits (MDL), and SRM correction factors, was performed in Excel (Microsoft

Office, 2003). All other statistical analysis was performed in STATA (Intercooled STATA 8, College Station TX).

#### *Sample Size Estimate*

The sample size was based on a power calculation of differences found in blood Mn in groups exposed to Mn concentrations ranging from 138–1330  $\mu\text{g}/\text{m}^3$ . The range of corresponding variability (SD) of Mn in blood reported is 3.8–6.4 (48;51;90;91). The assumption was made that variability of blood Mn in the present study would be 4  $\mu\text{g}/\text{L}$ . The range of variability (SD) of Mn in blood of unexposed groups in previous literature is between 1.7–2.7  $\mu\text{g}/\text{L}$  (48;51;89), and an estimate of 2  $\mu\text{g}/\text{L}$  was selected for this study. An expected difference of 4  $\mu\text{g}/\text{L}$  in blood Mn of exposed vs. unexposed subjects was selected because this was the average difference found between Mn in blood of exposed and unexposed groups in the three studies with the Mn exposure levels closest to the one expected in welding fume exposure of this research (51;90;91). Applying these measures with a significance level of 0.05 ( $z_{\alpha/2} = 1.96$ ) and power level of 80% ( $z_{\beta} = 1.84$ ) resulted in a sample size of 18 participants in the exposed and unexposed group. In order to account for 10% losses to follow-up in the exposed group, we planned for 20 participants. Because of the decreased variability in the unexposed group and the use of longitudinal data in this study, we planned for a reduced number of 10 participants in the unexposed group.

#### *EBC-Mn and Blood-Mn Concentration*

To assess the difference between exposed and unexposed group mean EBC-Mn and the between and within variability of both groups, a statistical function that accounts for autocorrelation and censored data (STATA: “xtintreg”) was applied. The estimates of

mean group EBC-Mn concentrations were determined using data where values that were less than the MDL were replaced with half the MDL, because an estimate of the mean is not provided in regression results of “xtinreg”.

#### *EBC-Mn Association with Measures of Exposure and Subject Characteristics*

Spearman’s rho ( $r_s$ ) was used to estimate the correlation between EBC-Mn and measures of exposure and subject characteristics. The association measure, therefore, does not assume a strictly linear relationship. The measures of both variables are placed in rank order for Spearman’s rho estimates.

### **4.3 Results**

#### **A. Subjects**

Subjects were divided into two groups: a group that participated as welders (exposed) and then waited the required period of time after welding to participate a second time as unexposed. The second group only participated as exposed. There were nearly twice as many exposed subjects as unexposed subjects.

Eighteen individuals participated in the study in the exposed group, though only results of 17 subjects are included for analytical reasons described below (Table 4.3). Of these subjects, 9 repeated as unexposed subjects, though results of only 8 of these individuals are included for analytical reasons. In addition, one individual repeated participation in the exposed group. Nearly half (53%) of the subjects were female. Approximately half (47%) of the subjects were either current smokers ( $n=6$ ) or former smokers ( $n=2$ ). The average age of subjects was 30 years (range: 22-44 years). The

majority of subjects were beginner welders (71%), with fewer experienced or trained recreational welders.

There were no missed visits by subjects in the study, for a total of 250 visits. However, collection or analytical errors during either the visit or afterwards, resulted in missing information for each measured parameter (note reported “n” for parameters that follow).

## **B. Welding Fume Exposure**

### *Particle Collection*

There were a total of 10 welding sessions in which subjects welded in groups of 1 to 3. Within a welding session, subjects welded during the same sampling time and shared welding equipment. Depending on the exposure level during each welding session, the particle sampling equipment for each subject was exchanged 1 – 2 times in order to reduce particle sample over-load.

There were significant challenges with overloading during the samples collected with the PMASS. This often resulted in pump failure, such that the complete exposure time of subjects was not captured by the PMASS. Due to both the lack of a complete data-set of PMASS samples and the time required for TEM analysis, a single PMASS particle sample was selected from each welding session for estimation of PPSD and Mn composition by primary particle size. These estimates were used as representative measures of all subjects throughout the welding session. Of the PMASS samples selected for analysis, the average pump flow through the polycarbonate filter was: 1.50 L/min (range: 1.12-1.89 L/min).

Sample over-load was not an issue with the total dust cassette Teflon filters. As such, analysis of total dust cassette particle filters was used for total particle and total metals exposure. If multiple total dust particle samples were collected for a subject, the reported result is the time weighted average of the welding exposure. The average pump flow through the total dust Teflon filters 2.05 L/min (range: 1.70-2.56 L/min). For welding fume collected in either the 37 mm closed-face cassettes or the PMASS, it is unlikely that any particles were selectively omitted because welding fume agglomerates have been measured with diameters on the order of 0.6  $\mu\text{m}$ , much less than either effective cut-size (3).

#### *Total Particle, Mn & Fe Mass Concentration*

The average total particle concentration was 5,300  $\mu\text{g}/\text{m}^3$  (range: 965-26,000  $\mu\text{g}/\text{m}^3$ ). Total particle samples were analyzed for total Mn and Fe content via ICP-MS against a 6-8 point calibration curve, depending on the concentration range of the samples. The ICP-MS method is shown in Table 4.2. Particles were analyzed for total metal content in 2 batches. SRM recoveries for Mn ranged from 100-111%, and recoveries for Fe ranged from 95-101%. A correction factor was applied to the corresponding samples within an analytical batch if the recovery of the SRM varied >10% from the expected value.

At least one particle blank was obtained during each welding session and analyzed for total particle content and total metal content, except for in the first welding session. Total Mn and total particle results were blank-corrected using the blank sample representative of the welding session, except for samples from the first weld session, which was blank-corrected with the mean value of all blank filters. The batch-specific



method detection limit (MDL, 3 times the standard deviation of the field blank) was 0.15 and 0.27  $\mu\text{g}/\text{m}^3$  for Mn and 3.5 and 16.8  $\mu\text{g}/\text{m}^3$  for Fe. No sample measurements for total Mn or Fe were below the MDL. Replicate personal particle samples were not collected, as the burden to a subject of wearing a duplicate set of particle sampling equipment was not reasonable. However, within the 5 welding sessions where more than one subject welded in the same environment, total Mn content was found to be within 5-40% agreement, indicating that individual exposure concentrations were sometimes quite similar within a group, and other times quite different.

The average Mn exposure measured among welding subjects was 598  $\mu\text{g}/\text{m}^3$  (range: 8-1805  $\mu\text{g}/\text{m}^3$ ). The average Fe exposure measured among welding subjects was approximately four times greater at 2490  $\mu\text{g}/\text{m}^3$ , ranging from 335-14,000  $\mu\text{g}/\text{m}^3$ . On average, 11% of the welding fume mass was due to Mn, and 47% to Fe (Table 4.2).

In order to incorporate the varying durations of exposure as an indication of the dose associated with each subject's exposure, the metric "Mn exposure-time" was estimated as the concentration multiplied by the time of welding. The average Mn exposure-time was 885  $\mu\text{g}\cdot\text{hr}/\text{m}^3$ . The rank order of Mn exposure-time for subjects is not the same as ranking by Mn exposure. (In Table 4.3, subjects are listed in order of increasing Mn exposure).

#### *PPSD and Mn Composition in Size Distribution*

The CMD and slope estimates of Mn composition by particle size were determined by four counters. In order to validate the applied methods, each counter estimated the PPSD and Mn composition by particle size of a single sample. Estimates of the CMD for the PPSD by the four counters had 95% confidence intervals that

overlapped and a chi-squared test indicated that the results were not significantly different ( $p>0.05$ ). The Mn composition by particle size slope was also found not to be significantly different among counters by a chi-squared test ( $p>0.05$ ), (Chapter 2).

The average CMD of the 12 samples analyzed was 6.9 nm (range of 3.2-14.5 nm), (Table 4.2). The average slope estimate of Mn composition by particle size was  $0.0008 \text{ nm}^{-1}$  (range of  $-0.00096$  to  $0.0021 \text{ nm}^{-1}$ ) with half of the slopes significantly positive. For the 6 subjects who did not have personal measures analyzed, a categorical estimate of CMD and a measure of Mn composition-size slope was assigned as the exposure measure from measures in the same welding session.

### **C. Biomarkers of Exposure**

#### *EBC Mn*

A total of 308 EBC samples were analyzed for Mn from 18 exposed participants and 9 unexposed participants. However, because of poor SRM recovery and a high MDL, one batch of samples (4 subjects: 3 exposed (2 as repeat exposed subjects) and 1 unexposed) was dropped, resulting in a total of 268 EBC samples. Of the remaining samples, 42% of samples allowed for duplicate analysis, and 2% for triplicate analysis. A review of the distribution of replicate measures indicated large differences between replicate measures for a small number of pairs suggesting that the mean of the two measures would not be representative the sample Mn concentration. To account for this problem the difference between all duplicate measures was calculated and the differences ranked. If the difference between duplicate measurements was greater than the 95<sup>th</sup> percentile ( $2.99 \text{ } \mu\text{g/L}$ ), the higher measurement was dropped. Following this process, 6 measurements were dropped from the duplicate dataset leaving a single to represent these

samples. The precision of EBC-Mn concentrations, measured as the difference between measures of a sample divided by the average of the measures, was 0.74  $\mu\text{g/L}$ .

At least 10% EBC field blanks were collected for each group of subjects. The average EBC Mn MDL, estimated from the field blanks, was 0.85  $\mu\text{g/L}$ , and ranged from 0.14-1.96  $\mu\text{g/L}$ . SRM recoveries ranged from 100-113%, and a correction factor was applied to measures of samples in batches with recoveries >10% of the expected value. Approximately half (51%) of all EBC Mn concentrations were less than the batch specific MDL (Table 4.4).

#### *Characterization of Mn Uptake in EBC Following Exposure to Welding Fume*

An initial visual assessment of the paired data where the same individual participated as both exposed and unexposed, indicated differences in trends across repeat measures of Mn concentration in EBC. For example, as shown in Figure 4.1, as compared to repeat measures of unexposed EBC-Mn, an elevation in EBC-Mn concentration is indicated after exposure. Interestingly, the timing of the elevation varied by subject. However, sometimes the baseline measure of the EBC Mn was either much higher or much lower than any of the unexposed measures. This indicates that from week to week individuals have varying levels of EBC Mn, or a systemic shift, but this was not the difference of interest. To assess differences between exposed and unexposed EBC-Mn concentrations other than systemic shifts over time, the exposed data was baseline-adjusted. This was done by applying the difference between the baseline measure of exposed data (i.e. the pre-exposure measurement) and the mean of unexposed data to the post-baseline exposed concentrations.

Criteria was established to define the presence of an EBC Mn peak that would enable exploration of differences in both timing and concentration of the elevated levels that were above the expected unexposed concentration ranges that accounted for week-to-week differences in Mn. Using the baseline-adjusted (or “normalized”) maximum concentration, an EBC-Mn peak in the exposed data was defined as a maximum concentration that was above the maximum concentration found in unexposed data. For individuals that participated in the study as both unexposed and exposed (n=8), their individual paired data was applied. If an individual only participated in the exposed group (n=9), an unexposed data set was established for comparison of the absolute maximum concentration of all unexposed data matched by gender (Table 4.5).

Results of this analysis indicated that 9 of 17 subjects after exposure had a maximum EBC-Mn concentration that was identified as a peak. Of the 9 results with a significant peak, the maximum EBC-Mn concentration ranged from 2.41 to 25.16 µg/L. The maximum concentration occurred between 0.2 and 89 hours after welding (Table 4.5).

The mean EBC-Mn concentration was 1.36µg/L in the exposed group, and 0.76 µg/L in the unexposed group. The group difference was not found to be statistically significant (p=0.382). A t-test indicates that there was also no significant difference in the between-subject variability (p=0.537), though the between variability estimate was higher in the exposed group. The within-subject variability was significantly higher in the exposed group (p<0.001), (Figure 4.2 & Table 4.6).

*Association of EBC-Mn Concentration with Measures of Exposure or Subject Characteristics*

The presence of a significant peak was not associated with any of the measures of exposure. Of the subject characteristics, the presence of a peak was associated with a decreased post-exposure serum Fe level ( $r_s$ : -0.52,  $p=0.03$ ).

Within results where a significant EBC-Mn peak was found, the association between peak EBC-Mn and the timing of maximum concentration and various measures of exposure and subject characteristics was assessed (Table 4.7). The maximum concentration of EBC Mn and the time of the maximum concentration of EBC Mn were not significantly associated with the basic measures of exposure: Mn, Fe, and total particle concentration ( $p>0.05$ ). The duration of welding and the duration multiplied by Mn exposure were also not significantly associated. Primary particle CMD > 6.9 nm (the average estimate) was associated with an earlier time of maximum EBC Mn concentration ( $r_s$ : -0.82,  $p=0.007$ ). The Mn composition size slope was not associated with either the maximum concentration or the timing of maximum concentration, however, the interaction of CMD\*Mn composition size slope was significantly associated with both the maximum concentration ( $r_s$ : 0.71,  $p=0.03$ ) and time of maximum concentration ( $r_s$ : -0.69,  $p=0.04$ ).

Among the subject characteristics, gender, age, and smoking status were not found to be significantly associated with either the maximum EBC Mn concentration or the time of the maximum concentration. Pre-exposure and post-exposure levels of serum Fe were also not associated with either the maximum concentration or time of maximum concentration.

### *Blood Mn*

A total of 311 samples were analyzed for blood Mn in 13 analytical batches. One batch was dropped because the corresponding batch of EBC samples had been dropped from analysis (data of 4 subjects), and an additional batch was dropped due to poor SRM recoveries). This resulted in a total of 260 samples for analysis. Blood samples were analyzed in triplicate. The COV of all triplicate samples was calculated and ranked. If the COV was greater than the 90<sup>th</sup> percentile (0.45), the measurement that was the most different from the other two measurements was dropped. This resulted in 30 dropped measurements. The precision for blood-Mn measurements, estimated as the coefficient of variation of triplicate measure, was 0.11.

The MDL was established as the 3 times the standard deviation of triplicate blood concentrations (after removing outliers) within each batch. The MDL of blood Mn ranged from 0.85 to 4.01 µg/L; 1% of samples fell below the MDL. SRM recoveries for blood Mn ranged from 91-140%. A correction factor was applied to samples with a recovery that differed by >10% from the expected concentration (Table 4.8). Blood Mn concentrations were adjusted based on the duration between collection and analysis for each sample. The adjustment was accomplished by the application of the linear equation established from a storage study conducted over a 9-day period where the decline in blood Mn concentration was measured as a decrease of 0.35 µg/L per day (Appendix II ).

In reviewing the paired data of individuals who participated in both the exposed and unexposed group, there did not appear to be a trend of peaks of increased blood Mn concentrations in the exposed group as there was in the EBC Mn data. However, in applying the same definition for a peak in blood Mn concentrations as used in the EBC

Mn data, 5 of 16 exposed individuals had a significant peak (Figure 4.3). However, no association was measured between having a peak in EBC Mn concentration and a peak in blood Mn concentration ( $r_s = 0.05$ ,  $p = 0.851$ ). In addition, there was no association between the maximum concentration in EBC Mn and blood Mn ( $r_s = 0.08$ ,  $p = 0.778$ ) or between the timing of maximum concentration in EBC Mn and blood Mn ( $r_s = 0.48$ ,  $p = 0.191$ ).

No significant difference in mean concentration between the two groups was measured ( $p < 0.001$ ). A t-test of the variability in the exposed vs. unexposed group blood Mn concentrations suggests that the between-subject variability is higher in the exposed group ( $p < 0.001$ ) but there is no significant difference in the within-subject variability ( $p = 0.133$ ), (Figure 4.4 & Table 4.5).

#### **4.4 Discussion**

This study was conducted to explore the relationship between inhalation exposure to Mn in welding fume and biomarkers of exposure (Mn in EBC and blood) in healthy participants. To accomplish this, we measured Mn in blood and EBC for 5-7 days following a single welding fume exposure.

Across the exposed group Mn concentrations ranged from 8-1810  $\mu\text{g}/\text{m}^3$ . More than half of the exposures were greater than 200  $\mu\text{g}/\text{m}^3$  and similar in magnitude to those measured in several occupational studies of exposure to airborne Mn (50;51;90;91). We found evidence of transitory increases in Mn concentration in the pulmonary system that presented hours to days post exposure. An early EBC Mn peak was significantly associated with primary particle CMD > 6.9 nm. In addition, the interaction between



CMD\*Mn composition by particle size was significantly associated with both the maximum concentration ( $r_s$ : 0.71,  $p=0.03$ ) and time of maximum concentration ( $r_s$ : -0.69,  $p=0.04$ ). Similar relationships with exposure and Mn concentration in blood were not found.

A recent analysis by Park et al. of Mn exposure and blood Mn concentrations of welders exposed to between 24 and 449  $\mu\text{g Mn/m}^3$  for up to two years estimated a significant individual correlation if the exposure was measured either as a cumulative exposure index (two-tailed F statistic,  $p=0.010$ ,  $R^2=0.31$ ) or as exposure burden assuming a half life of 150 days (two-tailed F statistic,  $p=0.004$ ,  $R^2=0.35$ ) (53). Park et al. estimate that blood Mn concentrations increase by 1  $\mu\text{g/L}$  for each increase of 1000  $\mu\text{g/m}^3$  exposure\*month of exposure. This suggests that blood Mn reflects chronic exposure, and is likely the reason that any increase in blood Mn in welders that may have occurred in the present study was below the MDL, as exposures occurred for a relatively short time.

Cowan et al. recently investigated the relationship between personal exposures of ferroalloy smelting workers (exposures 3-180  $\mu\text{g Mn/m}^3$ ) and several different measures of Mn in blood, urine, hair and saliva (93). The highest correlation was measured between Mn exposure and the ratio of Mn to Fe in serum (linear regression,  $p<0.01$ ,  $r=0.77$ ). There was no measured association between Mn to Fe and years of employment, which ranged from 0.5-12 years, indicating that levels do not significantly bioaccumulate over years of exposure. However, from this study it is not clear what minimum duration of exposure would be necessary to observe an increase in the serum Mn to Fe ratio.



In contrast to blood Mn, results of this study indicate that EBC-Mn may serve as a marker of acute inhalation exposure. The presence of a peak in EBC-mn in 9 of 17 subjects after exposure suggests an impact on the pulmonary system that is transitory. In the simplest analysis, we found no relationship between total Mn exposure and peak concentration ( $r_s$ : 0.13,  $p=0.619$ ). In fact, 3 of 5 subjects who did not have a significant peak were in the top 25% of Mn exposure.

We explored other measures of exposure to investigate potential factors that influence either the maximum concentration in EBC-Mn or the timing of the maximum concentration and found that primary particle CMD above or below the average size of 6.9 nm was significantly associated with the time of maximum concentration ( $p=0.007$ ). In this analysis an earlier peak and higher maximum concentration were associated with a CMD >6.9 nm suggesting that larger primary particles are associated with a more rapid and elevated level of clearance from the respiratory system following exposure, while smaller particles, while eventually cleared reside in the pulmonary system longer. This finding of a distinction in primary particle size behavior in EBC Mn is somewhat surprising given the relatively small range in primary particle CMD's within this sample set (3.3 to 14.5 nm), where all measured CMD's were among the smallest particles measured in exposure studies. While the sample size is small, these finding suggest that in future studies assessing the impact of exposure to Mn in welding fume should take into account particle size, which may be a more important predictor of outcome than total Mn concentration.

The exposure measure of Mn composition across the size distribution was also a significant predictor of both the maximum EBC Mn concentration and the timing of

maximum concentration when it was measured as an interaction with the measure of the primary particle size distribution (Mn composition-size slope \* CMD). A higher slope of Mn composition-size is a measure of an increase in the relative abundance of Mn as the primary particle size increases (i.e. larger primary particles within the sample have more relative quantities of Mn). The significant association with EBC of the interaction of these exposure terms can thus be interpreted as: exposure to welding fume that contains more larger primary particles that are more heavily loaded with Mn (compared to smaller primary particles) results in a higher concentration of EBC Mn that occurs more quickly. These results support the importance of an assessment of exposure that is based on measures of both chemical composition and size, and the association between these two measures in the exposure.

We also explored the possible relationship between maximum EBC-Mn concentration or the time of the maximum concentration and subject characteristics. Results show that age, smoking status, and gender were not significantly associated with these measures of EBC Mn. In contrast, Finley et al. measured a significant difference in counts of Mn following ingestion of radio-labeled  $^{54}\text{Mn}$ , where women absorbed more Mn and cleared it more quickly than men (54), potentially highlighting differences in management of Mn when inhaled versus ingested. The lack of association for age contrasts with findings by Dorman et al., who report that following inhalation of  $\text{MnSO}_4$ , older male rats had higher brain Mn concentrations and slower clearance times than younger male rats (55). Few studies have looked at Mn concentration and smoking status, but Mutti et al. also did not find a difference between EBC Mn concentrations in

healthy smokers vs. healthy non-smokers (41), though in that study there was no comparison of uptake of Mn following exposure.

Among the subject characteristics measured, only having a lower concentration of post-welding serum Fe (compared to subjects with higher post-welding serum Fe) was associated with the presence of an EBC-Mn peak ( $r_s$ : -0.52,  $p=0.03$ ), though pre-welding serum Fe was not associated ( $r_s$ : 0.38,  $p=0.13$ ). In previous studies, decreased levels of markers of iron status have been associated with increased Mn uptake and Mn neurotoxicity (17;34;94). For example, Heilig et al. report that when an  $MnCl_2$  isotope tracer was injected into normal and iron-deficient rats, Mn concentrations in blood from the normal rat group dropped rapidly in the first 30 minutes, while in the iron-deficient rat group the Mn concentrations remained 4-fold higher for at least 4 hours (34). The relationship of Mn uptake with Fe status is thought to be due to the fact that Mn is carried by transporters that also typically carry Fe in the body, though the degree of transport by each carrier remains unclear (9;95).

It is worth noting that our assessment of subjects' health status from questions about respiratory and liver health is not generally as rigorous of an assessment as obtaining measurements to reflect health status. A future study might improve on this study element by taking measurements of respiratory and liver function, both known to be associated with the toxicokinetics of Mn, in subjects to assess health status.

A major limitation of this study was a small sample size. With the number of samples analyzed, there was not sufficient statistical power to investigate multiple factors simultaneously. Had we been able to adjust for multiple factors, it is possible that a significant association with some of the parameters that were found to be associated with

EBC Mn in the unexposed group data in Chapter 2 (room temperature, relative humidity, volume respired, EBC volume, and gender) that were not found to be associated in the exposed group results of presences, concentration and timing of EBC Mn peak. In addition, having a small sample size may have reduced our ability to observe a wide range of welding fume exposures, which are known to be quite diverse. It is likely that we would have measured a wider range in the exposure characteristics with a larger sample size.

This is the first research we are aware of to investigate the timing of respiratory clearance via repeat measures of EBC Mn following an acute inhalation exposure to Mn. An exploratory assessment of the rate of clearance was performed on a subset of the EBC Mn results. While this was not a toxicokinetic study, which would have required consistency in the exposure, dose estimates, and subject characteristics, as well as more biological sampling points that continued for a longer period, it is possible to make estimates of a range of toxicokinetic parameters in order to introduce a preliminary understanding of the clearance Mn from the respiratory system as measured by EBC Mn. From the data of three subjects where there were sufficient data to estimate the initial lung concentration of Mn (a whole EBC peak measured) that included more than 3 data points, the estimated half life of Mn clearance from lungs was approximately 300 hours. (For further details of this analysis, refer to Appendix III.) This is much higher than an estimate made by making a calculation of lung clearance from data presented by Drown et al. of 50 hours, where lung tissue levels of Mn were measured over time following intratracheal instillation of MnO<sub>2</sub> in rats (57). Our results suggest a longer half life measured in EBC Mn than Drown measured in lung tissue. While this could be due to a

difference in physiological response between humans and animals, it also indicates that other routes of clearance, such as uptake into circulatory system or mucociliary clearance, from the lung are potentially faster than clearance through EBC.

#### **4.5 Conclusion**

In this study, the most basic measure of Mn exposure, total Mn concentration, following exposure to welding fume was not associated with an increase of measures of EBC-Mn or blood-Mn. However, measures of the primary particle size distribution and the Mn composition across the size distribution were associated with the timing and level of EBC Mn concentrations. This supports findings in animal studies conducted by Oberdorster and Pauluhn that the primary particles may be important determinants that pulmonary clearance is affected by the size of primary particles (66;67), and that the relationship between composition and primary particle size may also be important. Our findings also suggest that physiological characteristics may be greater determinants of whether higher levels of Mn are cleared from the respiratory system in EBC while the amount of clearance and timing of clearance may be more dependent on the physical and chemical form of the exposure. Thus, more refined measures of exposure that incorporate measures of the physical composition in addition to chemical composition may help to improve our understanding of the physiological interaction resulting from varied exposures. While EBC Mn appears to reflect acute Mn exposures, we found that the timing of EBC collection in relation to the exposure varied greatly, and is therefore a critical aspect that must be addressed for correct interpretation. Future studies will be needed to learn if differences in people's ability to eliminate Mn via EBC are associated

with other physiological differences, and additionally to learn if exposure differences that result in different EBC Mn characteristics alter the Mn toxicity.

In the continued effort to assess the relationship between individual exposure and blood Mn, our results also indicate that following short-term elevated exposures the pulmonary system is able to effectively manage the clearance of Mn, as no uptake in blood was measured. As such, blood may not be an appropriate media for biomarkers of recent Mn exposure.

#### 4.6 Tables & Figures

**Table 4.1** ICP-MS measurement conditions for analysis of blood Mn, EBC Mn and particle Mn.

Instrument	Agilent 7500ce, quadropole
Torch ID	2.5 mm
Nebulizer	Micromist
Plasma Power	700-1600 W
Auxillary Gas	Helium
Sample Uptake Rate During Analysis	0.3 ml/min (0.1 rps)
Peristaltic Pump Program	<u>Blood &amp; EBC:</u> Uptake: 45 s, 0.3 rps Stabilization: 25 s, 0.1 rps Rinse: 90 s, 0.3 rps  <u>Particle:</u> Uptake: 60 s, 0.3 rps Stabilization: 15 s, 0.3 rps
Peak Integration	3 pts/peak, 3 reps
ISTD	Blood: Ge-72 Particle & EBC: Sc-45 (added individually to each sample)

**Table 4.2** Welding fume measures of exposure. Mn composition size slope estimates that are statistically significant are in bold.

Sample	Weld Session	Weld Type	Duration (min)	MnConc* Time ( $\mu\text{g}/\text{m}^3$ )*min	Mn Conc ( $\mu\text{g}/\text{m}^3$ )	Fe Conc ( $\mu\text{g}/\text{m}^3$ )	Total Particle Conc ( $\mu\text{g}/\text{m}^3$ )	CMD (GSD)  Nm	Mn Comp Size Slope [95% CI]  ( $\text{nm}^{-1}$ )*
1	4	TIG	346	2890	8	766	1540	5.5 (1.9)	<b>0.00061</b> [0.00008, 0.0011]
2	5	MIG	180	2630	15	634	1920	7.5 (2.5)	-0.00014 [-0.00041, 0.00012]
3	3	MIG	267	5420	20	354	1330	3.3 (2.8)	0.001 [-0.000028, 0.002]
4*	7	MIG/Stick	164	4950	30	335	965	--	--
5	2	MIG	171	6350	37	2120	5100	6.1 (2.1)	<b>0.00104</b> [0.00035, 0.0017]
6*	7	MIG/Stick	150	5830	39	374	1080	14.5 (1.9)	0.00072 [-0.00041, 0.0019]
7*	7	MIG/Stick	166	9320	56	540	1400	9.3 (2.1)	0.00083 [-0.0015, 0.0018]
8B***	8	MIG	146	16900	116	711	1470	3.9 (3.0)	<b>0.0021</b> [0.00071, 0.0035]
9	8	MIG	143	24500	172	1050	2210	6.4 (2.4)	<b>0.00094</b> [0.000039, 0.0018]
10	8	MIG	119	30800	258	1440	3200	--	--
11	1	MIG	117	30900	264	1550	3050	5.0 (2.3)	0.00096 [-0.00016, 0.0021]
12*	1	MIG	120	33800	282	1570	3170	--	--
13*	9	MIG	77	30700	398	2430	5210	--	--
14	9	MIG	77	48000	623	3850	8500	3.2 (2.8)	-0.00096 [-0.0021, 0.00014]
15*	10	MIG	189	151000	799	4180	9330	--	--
16	10	MIG	190	156000	823	4410	9940	8.3 (2.3)	<b>0.00089</b> [0.00022, 0.0016]
17*	10	MIG	188	189000	1000	4500	10500	--	--
8A***	6	MIG	114	206000	1810	14000	25600	9.8 (2.1)	<b>0.0016</b> [0.00052, 0.0026]
Average			<b>162</b>	<b>53100</b>	<b>375</b>	<b>2490</b>	<b>5300</b>	<b>6.9</b>	<b>0.00080</b>
Std Dev			<b>64</b>	<b>69500</b>	<b>477</b>	<b>3220</b>	<b>6030</b>	<b>3.3</b>	<b>0.00077</b>

\*Subjects who repeated participation in the unexposed group; \*\* Subject repeated welding participation (in welding group twice)



**Table 4.3** Subject Characteristics

Experience Welding	5 Experience/Trained 12 Beginner
Gender	9 Male 8 Female
Smoking Status	6 Current 2 Former 9 Never
Age (years)	Avg: 30 Range: 22 – 44
Repeated as Unexposed (n)	8

**Table 4.4** EBC Mn analytical quality assessment measures.

Subject Group	Batches	Samples	Field Blank	MDL				SRM Recovery	
	#	#	µg/L	Avg MDL µg/L	Range MDL µg/L	<MDL #	<MDL %	Avg %	Range %
Exposed	11	179	0.643	0.848	(0.126-1.959)	95	53	107	(100-113)
Unexposed	2	79	0.344	0.696	(0.471-0.921)	36	46	106	(105-108)

**Table 4.5** Presence of peak in EBC Mn exposed data and summary measures of exposed subjects.

ID	EBC Mn Outcome					Exposure				Subject Characteristics				
	Time of Max Exp Conc (hr)	Max Exp Conc (µg/L)	Norm Max Exp Conc (µg/L)	Max Unexp Con (µg/L)	Exposed Mn Peak Present?	Mn Conc *Time (µg/m <sup>3</sup> * hr)	Mn Conc (µg/m <sup>3</sup> )	CMD (>6.9nm)	Mn Comp Slope (signif?)	Gender *	Age (yrs)	Smoke Status **	Pre-Serum Fe (µg/dl)	Post-Serum Fe (µg/dl)
<b>Matched by Same Individual</b>														
4	1.0	25.16	26.16	2.04	Yes	83	30	Yes	No	M	28	N	57	50
6	0.2	6.08	6.76	1.35	Yes	97	39	Yes	No	F	28	F	24	50
7	0.7	5.28	5.94	2.23	Yes	155	56	Yes	No	F	34	N	41	40
8A***	0.3	6.69	7.41	2.21	Yes	3433	1805	Yes	Yes	M	42	C	55	59
8B***	2.8	22.72	23.33	2.21	Yes	282	116	No	Yes	M	42	F	83	67
11	52.5	5.28	3.76	0.79	Yes	515	264	No	No	F	44	N	81	87
12	27.9	****	-3.78	2.2	No	563	282	No	No	F	31	N	142	133
15	0.5	1.87	1.6	4.18	No	2517	799	Yes	Yes	M	27	N	71	67
17	0.4	2.41	2.23	1.64	Yes	3150	1006	Yes	Yes	M	24	N	65	107
<b>Matched by Same Gender</b>														
1	86.6	2.82	3.42	4.18	No	48	8	No	Yes	M	23	C	54	67
2	0.3	0.82	-0.11	4.18	No	44	15	Yes	No	M	26	N	38	106
3	41.7	5.86	6.12	2.22	Yes	90	20	No	No	F	22	C	53	32
5	16.8	****	0.84	4.18	No	106	37	No	Yes	M	32	C	79	107
9	2.6	1.78	1.92	2.22	No	408	172	No	Yes	F	29	C	118	95
10	89.1	1.55	1.09	2.22	No	513	258	No	Yes	F	32	C	100	122
13	3.2	0.95	1.27	2.22	No	512	398	No	No	F	39	F	136	60
14	2.8	2.9	2.62	2.22	Yes	800	623	No	No	F	24	N	85	80
16	0.2	5.88	5.88	4.18	Yes	2600	823	Yes	Yes	M	32	N	84	70

\*Gender: M = male, F = female; \*\*Smoking status: N = never, F = former, C = current; \*\*\*Same individual participated in the exposed group two times;

\*\*\*\*Baseline visit had the maximum concentration

**Table 4.6** Group differences in blood Mn and EBC Mn concentrations ( $\mu\text{g/L}$ ).

Estimate (Std Dev) 95% CI
------------------------------

	Blood Mn			EBC Mn		
	Exposed (n=16)	Unexposed (n=8)	p-value	Exposed (n=17)	Unexposed (n=8)	p-value
<b>Mean</b>	7.01	7.74		1.36	0.76	
<b><math>\beta^*</math></b>	-0.88 (2.59) -1.21 -0.55	Ref	<0.001	0.44 (7.97) -0.55 1.43	Ref	0.382
<b><math>\sigma^2</math> Between**</b>	1.47 (0.79) 1.35 1.60	0.98 (0.72) 0.82 1.13	<0.001	0.99 (5.80) 0.11 1.87	0.57 (1.58) 0.22 0.93	0.537
<b><math>\sigma^2</math> Within**</b>	1.00 (0.73) 0.89 1.11	0.86 (0.64) 0.72 1.00	0.133	3.47 (3.90) 2.88 4.06	0.869 (0.969) 0.65 1.09	<0.001

\* $\beta$ : coefficient of Mn concentration in exposed group vs. Mn concentration in unexposed group for either blood or EBC.

\*\* $\sigma^2$ : standard deviation

**Table 4.7** Spearman's correlation ( $r_s$ ) of maximum EBC Mn concentration ( $\mu\text{g/L}$ ) and time of maximum EBC Mn concentration (hours after weld) with measures of exposure and subject characteristics for subject results with a significant peak ( $n=9$ ). Values in bold are statistically significant ( $p<0.05$ ).

	Maximum EBC Mn Conc		Time of Maximum EBC Mn Conc	
	$r_s$	p-value	$r_s$	p-value
<b>Measures of Exposure</b>				
Mn Exposure ( $\mu\text{g/m}^3$ )	-0.27	0.488	-0.37	0.332
Mn Exposure Category (0: $\leq 200 \mu\text{g/m}^3$ , 1: $>200 \mu\text{g/m}^3$ )	-0.43	0.244	0.00	1.00
Fe Exposure ( $\mu\text{g/m}^3$ )	-0.33	0.381	-0.33	0.381
Total Particle Exposure ( $\mu\text{g/m}^3$ )	-0.37	0.332	-0.22	0.576
Weld Duration (hr)	-0.02	0.966	-0.08	0.831
Mn exposure*time [ $(\mu\text{g/m}^3)*\text{hr}$ ]	-0.33	0.381	-0.33	0.381
CMD (0: $<6.9 \text{ nm}$ , 1: $>6.9$ )	0.46	0.217	<b>-0.82</b>	<b>0.007</b>
Mn Comp Size slope ( $\text{nm}^{-1}$ )	0.09	0.814	0.15	0.699
Mn Comp Slope Signif? (0: No, 1: Yes)	-0.17	0.656	-0.17	0.656
CMD * Mn Comp Size Slope (unitless)	<b>0.71</b>	<b>0.032</b>	<b>-0.69</b>	<b>0.041</b>
<b>Subject Characteristics</b>				
Gender (0: Male, 1: Female)	-0.35	0.361	0.43	0.244
Age (Yrs)	0.24	0.527	-0.10	0.796
Smoking Status (0: Never, 1: Former or Current)	0.09	0.825	-0.35	0.361
Pre Serum Fe ( $\mu\text{g/dl}$ )	-0.42	0.265	0.30	0.433
Post Serum Fe ( $\mu\text{g/dl}$ )	-0.55	0.123	-.03	0.949
Difference Serum Fe ( $\mu\text{g/dl}$ )	-0.32	0.406	-0.28	-.460

**Table 4.8** Blood Mn analytical quality assessment measures.

Subject Group	Batches	Samples	MDL				SRM Recovery	
	#	#	Avg $\mu\text{g/L}$	Range $\mu\text{g/L}$	# <MDL	% <MDL	Avg %	Range %
Exposed	9	176	2.09	(0.85-4.01)	2	1	116	(104-140)
Unexposed	2	84	1.74	(1.61-1.87)	1	1	111	(99-122)

\*Average of all SRM recoveries, no SRM analyzed in these batches.

**Figure 4.1** Results of three individuals' paired exposed and unexposed EBC Mn concentrations. A) Participant #6, "early" maximum EBC Mn concentration when exposed; B) Participant #13, "late" maximum EBC Mn concentration when exposed; C) Participant #13, no significant peak. (Sample concentrations that were <MDL were replaced with  $\frac{1}{2}$  the MDL. Data shown not normalized.)

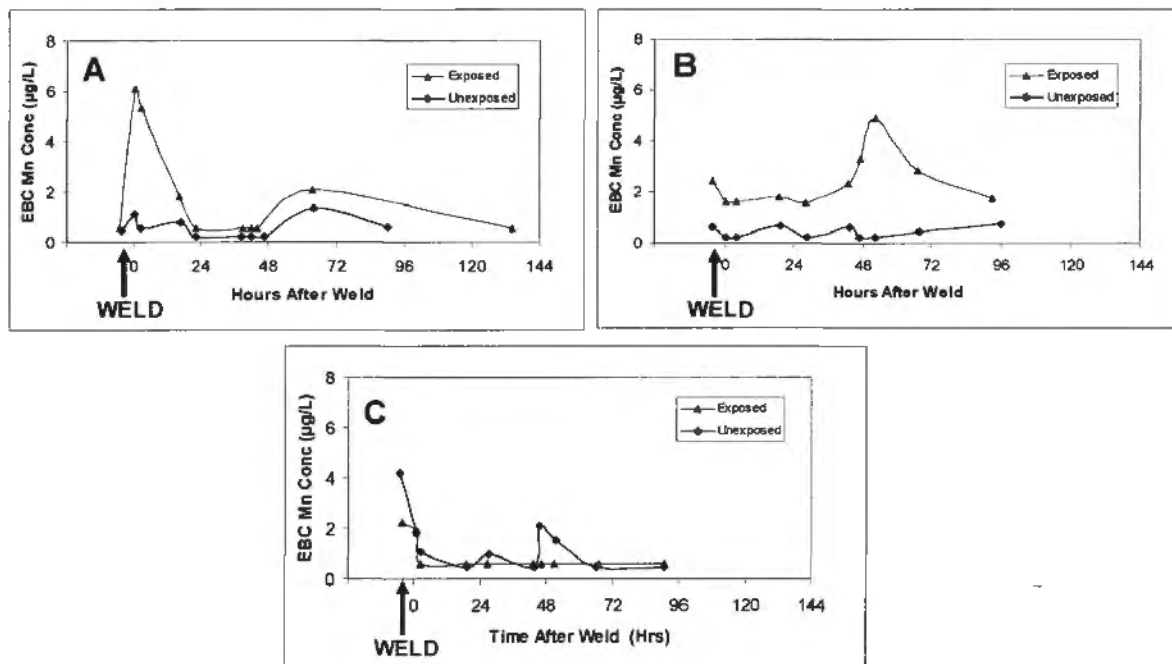


**Figure 4.2** Scatterplots of EBC Mn concentrations in the exposed and unexposed group. (The line represents the median concentration.)

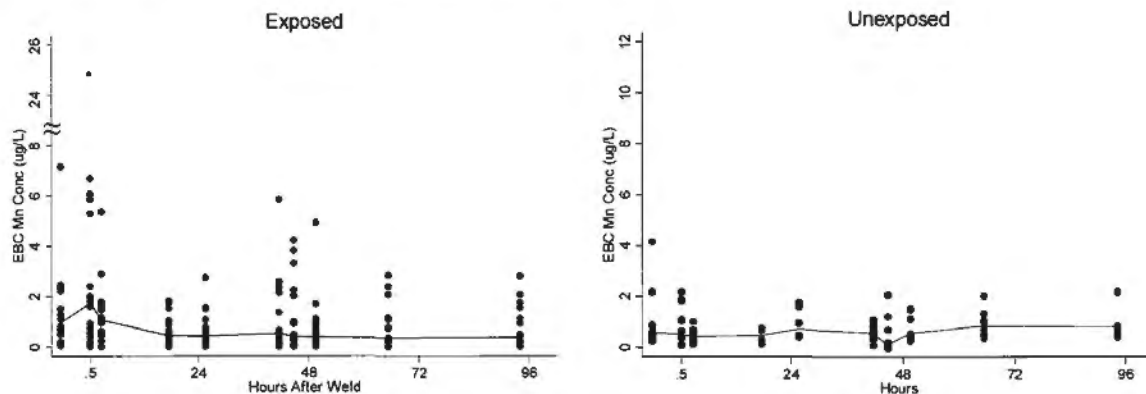


**Figure 4.3** Results of three individuals' paired exposed and unexposed blood Mn concentrations. A) Participant #6, no peak after normalizing; B) Participant #13, no peak after normalizing; C) Participant #15, significant peak after normalizing. (Data shown not normalized.)

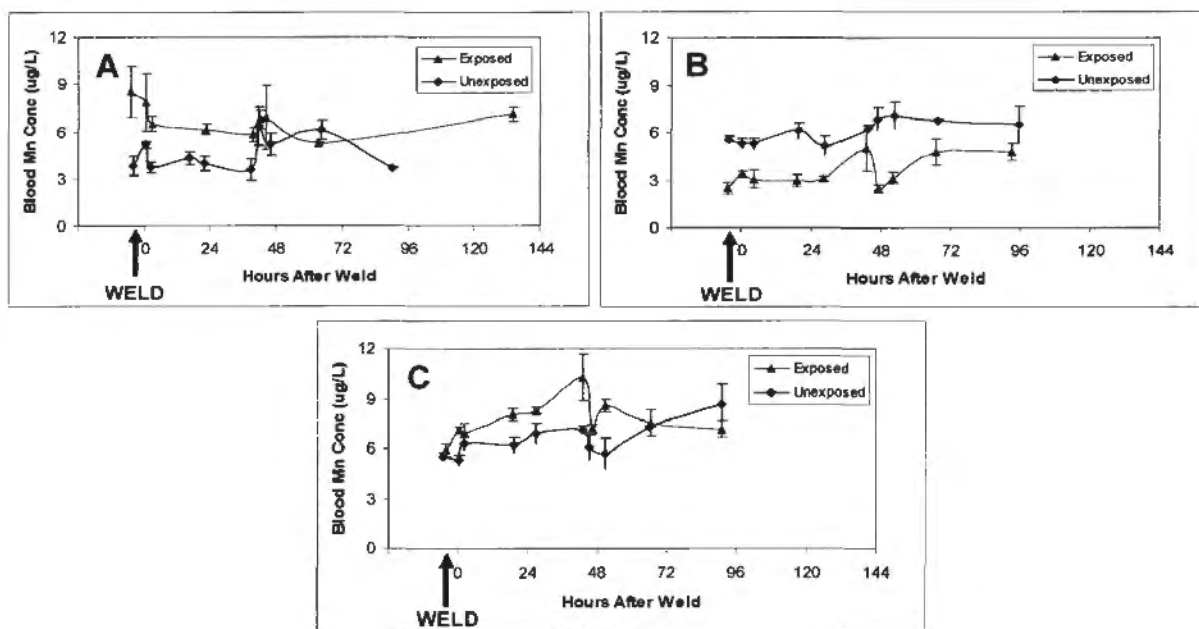
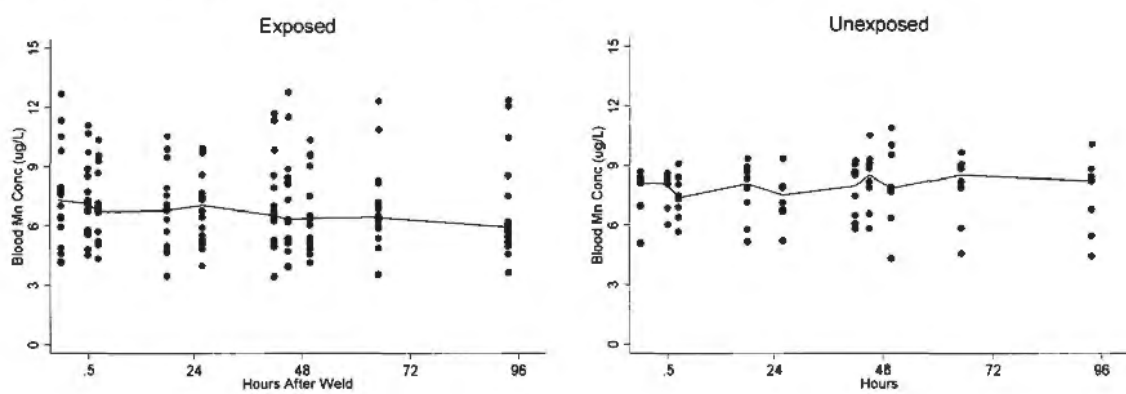


**Figure 4.4** Scatterplots of blood Mn concentrations in the exposed and unexposed group. The line represents the median concentration.



# 5

## Conclusion

Current debate continues over the amount and duration of Mn inhalation exposure that is required to cause neurotoxicity. In 1955, Rodier reported from observation of Mn miners that manganism could develop within just months of exposure (5). The Mn concentrations in the mines were greater than  $100 \text{ mg/m}^3$ , an enormous exposure level that is not typically reported today among even the highest exposures. This might have implied that manganism and neurotoxic effects only occur under gross exposure conditions. Unfortunately, more recent research refutes this. Though the diagnosis of manganism is currently investigation, several research groups have reported evidence of Mn neurotoxicity, and potentially Mn-induced Parkinson's disease in the past 50 years in workers exposed within several different occupations, but especially among Mn miners (96). Park et al. conducted a risk assessment of welders that worked on the San Francisco Bay Bridge between 2003 and 2004, and estimate that neurological impairment of both motor and cognitive function, defined as performance on neurological tests less than the 5<sup>th</sup> percentile of normal performance, is associated with 2 years of exposure to just 0.045-0.068  $\text{mg/m}^3$  (53). These exposures are orders of magnitude less than the mining exposures Rodier reported. Evidence reported by Mergler et al. also indicates that even lower levels of exposure may be associated with neurotoxicity, as they measured neurological deficits in the general population from environmental exposures (15). These



findings suggest that the OSHA upper threshold permissible exposure limit of 5 mg/m<sup>3</sup> (as a ceiling) for Mn in fume, and an 8-hour time weighted average of 1 mg/m<sup>3</sup> for Mn<sub>3</sub>O<sub>4</sub> are unlikely to be protective limits.

In 1994, the EPA stated in a risk assessment that it was unable to determine if introduction of MMT (a compound that contains Mn) into US fuel would result in a health risk for the public (97). In the mean time, the EPA is waiting for further research on Mn exposure and toxicity to make an informed decision. Collection of stationary particle samples is much easier than collecting personal measures. However, stationary particle sampling does not directly measure the movement and activity patterns of individuals, which significantly alters personal exposure. Measuring personal inhalation exposures in human populations is a much better estimate of personal exposure, but it is expensive and is a burdensome task for both researchers and subjects. In contrast, collection and analysis of biomarkers of internal dose is typically a less expensive and time-saving measurement that assesses exposure at the individual level. Exposure assessment is necessary in order to establish exposure form, level, and duration in relation to the biomarker of internal dose.

In this exposure assessment study of welding fume, two novel measures of inhalation exposure were developed and characterized: a measure of the primary particle size distribution (measured as the primary particle count median diameter), and a measure of the Mn composition by particle size (measured as Mn composition-size slope), (Chapter 2). In addition, a method for the collection of exhaled breath condensate (EBC), a relatively new media used for biomarkers of metal exposure, was modified for this study and characterized for analysis of metal content as a biomarker of exposure

(Chapter 3.) These measures were applied along with well-established measures of total metal exposure and blood-Mn to a longitudinal study of acute inhalation exposure to welding fume in recreational or beginner welders (Chapter 4).

In this study, there was no indication of uptake of Mn measured in blood due to the welding fume exposure. This suggests that the pulmonary system is capable of managing and clearing elevated Mn exposures ( $8\text{--}1800\text{ }\mu\text{g}/\text{m}^3$ ) that occur over a short duration ( $1\frac{1}{2}$  -  $5\frac{1}{2}$  hours). As these Mn exposure concentrations are not trivial, this indicates that blood Mn is not a useful biomarker of recent exposure. Park et al. estimate that Mn in blood increases by  $1\text{ }\mu\text{g}/\text{L}$  for each increase of  $1\text{ mg}/\text{m}^3$  in exposure multiplied by the months of exposure (53). The incorporation of duration indicates that Mn bioaccumulates in blood following elevated exposure for extended periods.

While no uptake of Mn was measured in blood from the acute inhalation exposure in this study, uptake within the body is inferred by the finding of EBC Mn clearance measured in EBC Mn. It is possible that Mn was either cleared before entering circulatory system or that the amount of Mn that reached circulatory system from the pulmonary system was less than the detection limit of the measure of blood Mn. This indicates that EBC Mn is a more sensitive marker of acute inhalation exposure than blood Mn, which could make it useful in a wide range of exposure scenarios.

A significant peak of EBC Mn was measured in 9 of 17 subjects. No measure of exposure was associated with the presence of an EBC Mn peak, and in fact some subjects who did not have a significant EBC Mn peak had the highest Mn exposure levels. Subject characteristics of age or gender were also not related to the presence of an EBC Mn peak. The only measure that was associated with the presence of an EBC Mn peak

was a lower post-welding serum Fe concentration. This finding indicates that decreased iron status may increase the clearance of Mn from the respiratory system, and supports findings that iron status alters Mn absorption and clearance (9;34). This fits with the current understanding that both DMT1 and transferrin, which are two carriers of Mn in the circulatory system, both transport Fe under normal, healthy conditions (4;6).

While Mn exposure was not found to be related to the presence of an EBC Mn peak, among subjects who had a peak, both the maximum concentration of EBC Mn and the timing of the maximum concentration were related to the form of Mn in the exposure, but not to the total Mn concentration. Both the primary particle size distribution and the Mn composition by particle size were associated with the concentration and timing of the maximum EBC concentration. This fits with emerging evidence from toxicity studies of nanoparticles that the primary particle size may be related to the resulting translocation and clearance of particles (66;67). However, our findings suggest that a larger primary particle CMD was associated with faster clearance while research of rat inhalation by Pauluhn et al. indicates that smaller primary particles are associated with faster clearance (67). Primary particle CMD estimates in this study had a fairly narrow range of 3-14 nm. Further research will be needed to learn if a wider range of CMD's, as would occur across other sources of Mn exposure would result in an even greater observed difference in EBC Mn and to discern and confirm differences between the results obtained in this human exposure assessment study and animal toxicological studies.

This investigation of uptake and clearance of Mn in biomarkers following Mn inhalation exposure was intended to facilitate the planning and interpretation of biomarker collection in epidemiological studies. Findings in this research indicate that

there is great variability in the elimination of EBC Mn that could significantly alter the interpretation of the relationship between exposure and health effects. However, there is indication that measures of EBC metals could facilitate our understanding of acute exposures. Until further research has confirmed the parameters that alter the time course of clearance and the degree of influence these parameters have on EBC Mn concentrations, conclusions of EBC Mn as a biomarker of internal dose should be made cautiously.

As technology enables more sophisticated measures of exposures that incorporate both chemical and physical characteristics, it is becoming clear that having more refined measures improves our understanding of the resulting health outcomes. Growing evidence indicates that future regulations generally need to incorporate chemical composition simultaneously with physical composition measures of a much smaller size range than either the respirable fraction of particles (OSHA: particles with a median aerodynamic diameter  $4\text{ }\mu\text{m}$ ) or  $\text{PM}_{2.5}$  (EPA: particles with an aerodynamic diameter  $<2.5\text{ }\mu\text{m}$ ) or the in order to protect the health of workers and the public.

## Reference List

- (1) US Department of Labor. Occupational Employment Statistics. 51-4121: Welders, Cutters, Solderers, and Brazers. Bureau of Labor Statistics . 5-4-2009. 11-14-0009.  
Ref Type: Electronic Citation
- (2) Antonini JM. Health effects of welding. Crit Rev Toxicol 2003; 33(1):61-103.
- (3) Antonini JM, Santamaria AB, Jenkins NT, Albini E, Lucchini R. Fate of manganese associated with the inhalation of welding fumes: Potential neurological effects. Neurotoxicology 2005; 27.
- (4) Dobson AW, Erikson KM, Aschner M. Manganese neurotoxicity. Ann N Y Acad Sci 2004; 1012:115-128.
- (5) RODIER J. Manganese poisoning in Moroccan miners. Br J Ind Med 1955; 12(1):21-35.
- (6) Roth JA, Garrick MD. Iron interactions and other biological reactions mediating the physiological and toxic actions of manganese. Biochem Pharmacol 2003; 66(1):1-13.

- (7) International Programme on Chemical Safety WHO. Manganese. Environmental Health Criteria 17. 1981.
- Ref Type: Report
- (8) Scientific Committee on Food ECH&CPD-G. Opinion of the Scientific Committee on Food on the Tolerable Upper Intake Level of Manganese. SCF/CS/NUT/UPPLEV/21 Final. 11-28-2000.
- Ref Type: Report
- (9) Aschner M, Erikson KM, Dorman DC. Manganese dosimetry: species differences and implications for neurotoxicity. *Crit Rev Toxicol* 2005; 35(1):1-32.
- (10) Stepens A, Logina I, Liguts V et al. A Parkinsonian Syndrome in Methcathinone Users and the Role of Manganese. *N Engl J Med* 2008; 358(10):1009-1017.
- (11) Costello S, Cockburn M, Bronstein J, Zhang X, Ritz B. Parkinson's Disease and Residential Exposure to Maneb and Paraquat From Agricultural Applications in the Central Valley of California. *Am J Epidemiol* 2009; 169(8):919-926.
- (12) Ferraz HB, Bertolucci F, Pereira JS, Lima JGC, Andrade F. Chronic exposure to the fungicide maneb may produce symptoms and signs of CNS manganese intoxication. *Neurology* 1988; 38(4):550.

- (13) Sopata J. MMT Use. Richman JD, editor. 10-20-2009.  
Ref Type: Personal Communication
- (14) Pellizzari ED, Clayton CA, Rodes CE et al. Particulate matter and manganese exposures in Indianapolis, Indiana. *J Expo Anal Environ Epidemiol* 2001; 11(6):423-440.
- (15) Mergler D, Baldwin M, Belanger S et al. Manganese neurotoxicity, a continuum of dysfunction: results from a community based study. *Neurotoxicology* 1999; 20(2-3):327-342.
- (16) Crossgrove J, Zheng W. Manganese toxicity upon overexposure. *NMR Biomed* 2004; 17(8):544-553.
- (17) Aschner M, Vrana KE, Zheng W. Manganese uptake and distribution in the central nervous system (CNS). *Neurotoxicology* 1999; 20(2-3):173-180.
- (18) Normandin L, Hazell AS. Manganese neurotoxicity: an update of pathophysiologic mechanisms. *Metab Brain Dis* 2002; 17(4):375-387.
- (19) Sinczuk-Walczak H, Jakubowski M, Matczak W. Neurological and neurophysiological examinations of workers occupationally exposed to manganese. *Int J Occup Med Environ Health* 2001; 14(4):329-337.

- (20) Clewell HJ, Lawrence GA, Calne DB, Crump KS. Determination of an occupational exposure guideline for manganese using the benchmark method. *Risk Anal* 2003; 23(5):1031-1046.
  
- (21) Bast-Pettersen R, Ellingsen DG, Hetland SM, Thomassen Y. Neuropsychological function in manganese alloy plant workers. *Int Arch Occup Environ Health* 2004; 77(4):277-287.
  
- (22) Chia SE, Foo SC, Gan SL, Jeyaratnam J, Tian CS. Neurobehavioral functions among workers exposed to manganese ore. *Scand J Work Environ Health* 1993; 19(4):264-270.
  
- (23) Iregren A. Psychological test performance in foundry workers exposed to low levels of manganese. *Neurotoxicol Teratol* 1990; 12(6):673-675.
  
- (24) Roels H, Lauwerys R, Buchet JP et al. Epidemiological survey among workers exposed to manganese: effects on lung, central nervous system, and some biological indices. *Am J Ind Med* 1987; 11(3):307-327.
  
- (25) Mergler D, Huel G, Bowler R et al. Nervous system dysfunction among workers with long-term exposure to manganese. *Environ Res* 1994; 64(2):151-180.



- (26) Lucchini R, Apostoli P, Perrone C et al. Long-term exposure to "low levels" of manganese oxides and neurofunctional changes in ferroalloy workers. *Neurotoxicology* 1999; 20(2-3):287-297.
- (27) Myers JE, Thompson ML, Ramushu S et al. The nervous system effects of occupational exposure on workers in a South African manganese smelter. *Neurotoxicology* 2003; 24(6):885-894.
- (28) Iregren A. Manganese neurotoxicity in industrial exposures: proof of effects, critical exposure level, and sensitive tests. *Neurotoxicology* 1999; 20(2-3):315-323.
- (29) Myers JE, teWaterNaude J, Fourie M et al. Nervous system effects of occupational manganese exposure on South African manganese mineworkers. *Neurotoxicology* 2003; 24(4-5):649-656.
- (30) Lucchini R, Selis L, Folli D et al. Neurobehavioral effects of manganese in workers from a ferroalloy plant after temporary cessation of exposure. *Scand J Work Environ Health* 1995; 21(2):143-149.
- (31) Jonderko G, Kujawska A, Langauer-Lewowicka H. Problems of chronic manganese poisoning on the basis of investigations of workers at a manganese alloy foundry. *Int Arch Arbeitsmed* 1971; 28(3):250-264.

- (32) Olanow CW. Manganese-induced parkinsonism and Parkinson's disease. *Ann N Y Acad Sci* 2004; 1012:209-223.
- (33) Crossgrove JS, Allen DD, Bukaveckas BL, Rhineheimer SS, Yokel RA. Manganese distribution across the blood-brain barrier. I. Evidence for carrier-mediated influx of manganese citrate as well as manganese and manganese transferrin. *Neurotoxicology* 2003; 24(1):3-13.
- (34) Heilig E, Molina R, Donaghey T, Brain JD, Wessling-Resnick M. Pharmacokinetics of pulmonary manganese absorption: evidence for increased susceptibility to manganese loading in iron-deficient rats. *Am J Physiol Lung Cell Mol Physiol* 2005; 288(5):L887-L893.
- (35) Ellingsen DG, Haug E, Ulvik RJ, Thomassen Y. Iron status in manganese alloy production workers. *J Appl Toxicol* 2003; 23(4):239-247.
- (36) Burns-Nass LE, Meade BJ, Munson AE. Toxic Responses of the Immune System. In: Klaassen CD, editor. *Casarett & Doull's Toxicology: The Basic Science of Poisons*. New York: McGraw-Hill, 2001: 419-470.
- (37) COTZIAS GC, PAPAVALIOU PS, MILLER ST. MANGANESE IN MELANIN. *Nature* 1964; 201:1228-1229.

- (38) Dorman DC, Struve MF, Wong BA. Brain manganese concentrations in rats following manganese tetroxide inhalation are unaffected by dietary manganese intake. *Neurotoxicology* 2002; 23(2):185-195.
- (39) Goldoni M, Catalani S, De Palma G et al. Exhaled breath condensate as a suitable matrix to assess lung dose and effects in workers exposed to cobalt and tungsten. *Environ Health Perspect* 2004; 112(13):1293-1298.
- (40) Caglieri A, Goldoni M, Acampa O et al. The effect of inhaled chromium on different exhaled breath condensate biomarkers among chrome-plating workers. *Environ Health Perspect* 2006; 114(4):542-546.
- (41) Mutti A, Corradi M, Goldoni M, Vettori MV, Bernard A, Apostoli P. Exhaled metallic elements and serum pneumoproteins in asymptomatic smokers and patients with COPD or asthma. *Chest* 2006; 129(5):1288-1297.
- (42) Horvath I, Hunt J, Barnes PJ et al. Exhaled breath condensate: methodological recommendations and unresolved questions. *Eur Respir J* 2005; 26(3):523-548.
- (43) Jackson AS, Sandrini A, Campbell C, Chow S, Thomas PS, Yates DH. Comparison of Biomarkers in Exhaled Breath Condensate and Broncho-Alveolar Lavage. *Am J Respir Crit Care Med* 2006.

- (44) Corradi M, Pignatti P, Manini P et al. Comparison between exhaled and sputum oxidative stress biomarkers in chronic airway inflammation. *Eur Respir J* 2004; 24(6):1011-1017.
- (45) Broding HC, Michalke B, Goen T, Drexler H. Comparison between exhaled breath condensate analysis as a marker for cobalt and tungsten exposure and biomonitoring in workers of a hard metal alloy processing plant. *Int Arch Occup Environ Health* 2009; 82(5):565-573.
- (46) Goldoni M, Caglieri A, Corradi M et al. Chromium in exhaled breath condensate and pulmonary tissue of non-small cell lung cancer patients. *Int Arch Occup Environ Health* 2008; 81(4):487-493.
- (47) Dodig S, Vlastic Z, Cepelak I, Zrinski TR, Turkalj M, Nogalo B. Magnesium and calcium in exhaled breath condensate of children with asthma and gastroesophageal reflux disease. *J Clin Lab Anal* 2009; 23(1):34-39.
- (48) Roels H, Lauwerys R, Genet P et al. Relationship between external and internal parameters of exposure to manganese in workers from a manganese oxide and salt producing plant. *Am J Ind Med* 1987; 11(3):297-305.
- (49) Jarvisalo J, Olkinuora M, Kiilunen M et al. Urinary and blood manganese in occupationally nonexposed populations and in manual metal arc welders of mild steel. *Int Arch Occup Environ Health* 1992; 63(7):495-501.

- (50) Bader M, Dietz MC, Ihrig A, Triebig G. Biomonitoring of manganese in blood, urine and axillary hair following low-dose exposure during the manufacture of dry cell batteries. *Int Arch Occup Environ Health* 1999; 72(8):521-527.
- (51) Apostoli P, Lucchini R, Alessio L. Are current biomarkers suitable for the assessment of manganese exposure in individual workers? *Am J Ind Med* 2000; 37(3):283-290.
- (52) Myers JE, Thompson ML, Naik I et al. The utility of biological monitoring for manganese in ferroalloy smelter workers in South Africa. *Neurotoxicology* 2003; 24(6):875-883.
- (53) Park RM, Bowler RM, Roels HA. Exposure-response relationship and risk assessment for cognitive deficits in early welding-induced manganism. *J Occup Environ Med* 2009; 51(10):1125-1136.
- (54) Finley JW, Johnson PE, Johnson LK. Sex affects manganese absorption and retention by humans from a diet adequate in manganese. *Am J Clin Nutr* 1994; 60(6):949-955.
- (55) Dorman DC, McManus BE, Marshall MW, James RA, Struve MF. Old age and gender influence the pharmacokinetics of inhaled manganese sulfate and manganese phosphate in rats. *Toxicol Appl Pharmacol* 2004; 197(2):113-124.

- (56) Roels H, Meiers G, Delos M et al. Influence of the route of administration and the chemical form ( $\text{MnCl}_2$ ,  $\text{MnO}_2$ ) on the absorption and cerebral distribution of manganese in rats. *Arch Toxicol* 1997; 71(4):223-230.
- (57) Drown DB, Oberg SG, Sharma RP. Pulmonary clearance of soluble and insoluble forms of manganese. *J Toxicol Environ Health* 1986; 17(2-3):201-212.
- (58) Vitarella D, Wong BA, Moss OR, Dorman DC. Pharmacokinetics of inhaled manganese phosphate in male Sprague-Dawley rats following subacute (14-day) exposure. *Toxicol Appl Pharmacol* 2000; 163(3):279-285.
- (59) Dorman DC, Struve MF, James RA, Marshall MW, Parkinson CU, Wong BA. Influence of particle solubility on the delivery of inhaled manganese to the rat brain: manganese sulfate and manganese tetroxide pharmacokinetics following repeated (14-day) exposure. *Toxicol Appl Pharmacol* 2001; 170(2):79-87.
- (60) Reaney SH, Bench G, Smith DR. Brain Accumulation and Toxicity of Mn(II) and Mn(III) Exposures. *Toxicol Sci* 2006.
- (61) Hinds WC. Respiratory Deposition. *Aerosol Technology*. New York: John Wiley & Sons, Inc., 1999: 233-259.
- (62) Jenkins NT, Eagar TW. Chemical Analysis of Welding Fume Particles. *Welding Journal* 2005;(Welding Research Supplement):87-s-93-s.

- (63) Minni E, Gustafsson TE, Koponen M, Kalliomaki PL. A study of the chemical structure of particles in the welding fumes of mild and stainless steel. *J Aerosol Sci* 1984; 15(1):57-68.
- (64) Voitkevich VG. Investigation of heterogeneity of welding fume particle composition by the method of X-ray photoelectron spectroscopy. *Soudage dans le monde [Welding in the world]* 1988; 26:108-111.
- (65) Oberdorster G, Oberdorster E, Oberdorster J. Nanotoxicology: an emerging discipline evolving from studies of ultrafine particles. *Environ Health Perspect* 2005; 113(7):823-839.
- (66) Oberdorster G. Significance of particle parameters in the evaluation of exposure-dose-response relationships of inhaled particles. *Inhal Toxicol* 1996; 8 Suppl:73-89.
- (67) Pauluhn J. Pulmonary Toxicity and Fate of Agglomerated 10 and 40 nm Aluminum Oxyhydroxides following 4-Week Inhalation Exposure of Rats: Toxic Effects are Determined by Agglomerated, not Primary Particle Size. *Toxicol Sci* 2009; 109(1):152-167.
- (68) Minni E, Hofmann S, Sivonen SJ. An AES study of particles in welding fumes of mild and stainless steel. *Surface and interface analysis* 1990; 16(1-12):563-564.

- (69) Gross DS, Galli ME, Silva PJ, Wood SH, Liu DY, Prather KA. Single Particle Characterization of Automobile and Diesel Truck Emissions in the Caldecott Tunnel. *Aerosol Science and Technology* 2000; 32(2):152-163.
- (70) Antonini JM, Stone S, Roberts JR et al. Effect of short-term stainless steel welding fume inhalation exposure on lung inflammation, injury, and defense responses in rats. *Toxicol Appl Pharmacol* 2007; 223(3):234-245.
- (71) Antonini JM, Roberts JR, Stone S, Chen BT, Schwegler-Berry D, Frazer DG. Short-Term Inhalation Exposure to Mild Steel Welding Fume had no Effect on Lung Inflammation and Injury but did Alter Defense Responses to Bacteria in Rats. *Inhal Toxicol* 2008;1.
- (72) Farrants G, Schuler B, Karlsen J, Reith A, Langard S. Characterization of the morphological properties of welding fume particles by transmission electron microscopy and digital image analysis. *Am Ind Hyg Assoc J* 1989; 50(9):473-479.
- (73) Berlinger B, Ellingsen DG, Naray M, Zaray G, Thomassen Y. A study of the bio-accessibility of welding fumes. *J Environ Monit* 2008; 10(12):1448-1453.
- (74) Egerton RF. *Electron Energy Loss Spectroscopy in the Electron Microscope*. 2nd ed. New York: Plenum Press, 1996.



- (75) Moore KT, Elbert DC, Veblen DR. Energy-filtered transmission electron microscopy (EFTEM) of intergrown pyroxenes. *American Mineralogist* 2001; 86(7-8):814-825.
- (76) Hinds WC. Microscopy Measurement of Particle Size. *Aerosol Technology*. New York: John Wiley & Sons, Inc, 1999: 402-427.
- (77) Gessner C, Kuhn H, Seyfarth HJ et al. Factors influencing breath condensate volume. *Pneumologie* 2001; 55(9):414-419.
- (78) Liu J, Thomas PS. Relationship between exhaled breath condensate volume and measurements of lung volumes. *Respiration* 2007; 74(2):142-145.
- (79) Effros RM, Dunning MB, III, Biller J, Shaker R. The promise and perils of exhaled breath condensates. *Am J Physiol Lung Cell Mol Physiol* 2004; 287(6):L1073-L1080.
- (80) McCafferty JB, Bradshaw TA, Tate S, Greening AP, Innes JA. Effects of breathing pattern and inspired air conditions on breath condensate volume, pH, nitrite, and protein concentrations. *Thorax* 2004; 59(8):694-698.
- (81) Goldoni M, Caglieri A, Andreoli R et al. Influence of condensation temperature on selected exhaled breath parameters. *BMC Pulm Med* 2005; 5:10.

- (82) Parsons PJ, Reilly AA, Esernio-Jenssen D. Screening children exposed to lead: an assessment of the capillary blood lead fingerstick test. Clin Chem 1997; 43(2):302-311.
- (83) US Environmental Protection Agency. Hazardous Waste Test Methods: Chapter 3. SW-846, Revision 6, 3-1-3-28. 2009. 2007.  
Ref Type: Report
- (84) Agilent Technologies. Inductively Coupled Plasma Mass Spectrometry: A Primer. Agilent Technologies, 2005.
- (85) Vlasic Z, Dodig S, Cepelak I et al. Iron and ferritin concentrations in exhaled breath condensate of children with asthma. J Asthma 2009; 46(1):81-85.
- (86) Goyer RA, Clarkson TW. Toxic Effects of Metals. In: Klaassen CD, Watkins III JB, editors. Casarett & Doull's Essentials of Toxicology. New York: McGraw-Hill, 2003: 348-359.
- (87) Ellingsen DG, Konstantinov R, Bast-Pettersen R et al. A neurobehavioral study of current and former welders exposed to manganese. Neurotoxicology 2008; 29(1):48-59.

- (88) Smyth LT, Ruhf RC, Whitman NE, Dugan T. Clinical manganism and exposure to manganese in the production and processing of ferromanganese alloy. *J Occup Med* 1973; 15(2):101-109.
- (89) Kim Y, Kim KS, Yang JS et al. Increase in signal intensities on T1-weighted magnetic resonance images in asymptomatic manganese-exposed workers. *Neurotoxicology* 1999; 20(6):901-907.
- (90) Dietz MC, Ihrig A, Wrazidlo W, Bader M, Jansen O, Triebig G. Results of magnetic resonance imaging in long-term manganese dioxide-exposed workers. *Environ Res* 2001; 85(1):37-40.
- (91) Yuan H, He S, He M, Niu Q, Wang L, Wang S. A comprehensive study on neurobehavior, neurotransmitters and lymphocyte subsets alteration of Chinese manganese welding workers. *Life Sci* 2005.
- (92) Normandin L, Ann BL, Salehi F et al. Manganese distribution in the brain and neurobehavioral changes following inhalation exposure of rats to three chemical forms of manganese. *Neurotoxicology* 2004; 25(3):433-441.
- (93) Cowan DM, Fan Q, Zou Y et al. Manganese exposure among smelting workers: blood manganese-iron ratio as a novel tool for manganese exposure assessment. *Biomarkers* 2009; 14(1):3-16.

- (94) Finley JW. Manganese absorption and retention by young women is associated with serum ferritin concentration. *Am J Clin Nutr* 1999; 70(1):37-43.
- (95) Crossgrove JS, Yokel RA. Manganese distribution across the blood-brain barrier III. The divalent metal transporter-1 is not the major mechanism mediating brain manganese uptake. *Neurotoxicology* 2004; 25(3):451-460.
- (96) Pal PK, Samii A, Calne DB. Manganese neurotoxicity: a review of clinical features, imaging and pathology. *Neurotoxicology* 1999; 20(2-3):227-238.
- (97) US Environmental Protection Agency. Comments on the Gasoline Additive MMT (methylcyclopentadienyl manganese tricarbonyl). Kortum D, editor. Environmental Protection Agency . 12-29-2005. 1-11-0006.  
Ref Type: Electronic Citation
- (98) Parsons PJ, Slavin W. A rapid Zeeman graphite furnace atomic absorption spectrometric method for the determination of lead in blood. *Spectrochimica Acta Part B: Atomic Spectroscopy* 1993; 48(6-7):925-939.
- (99) De Boer JL, Ritsema R, Piso S, Van SH, Van Den BW. Practical and quality-control aspects of multi-element analysis with quadrupole ICP-MS with special attention to urine and whole blood. *Anal Bioanal Chem* 2004; 379(5-6):872-880.

- (100) Palmer CD, Lewis J, Geraghty CM, Barbosa J, Parsons PJ. Determination of lead, cadmium and mercury in blood for assessment of environmental exposure: A comparison between inductively coupled plasma-mass spectrometry and atomic absorption spectrometry. *Spectrochimica Acta Part B: Atomic Spectroscopy* 2006; 61(8):980-990.
- (101) White MA, Sabbioni E. Trace element reference values in tissues from inhabitants of the European Union. X. A study of 13 elements in blood and urine of a United Kingdom population. *Sci Total Environ* 1998; 216(3):253-270.
- (102) Elaine Hasty. Blood Microwave Digest. CEM Corporation, Matthews, NC . 11-17-2008.

Ref Type: Internet Communication

# **APPENDIX**

# **Appendix I**

## **Total Metal Content of Welding Fume Particle Samples (Additional Metals)**

### **A. Introduction**

The samples collected on Teflon filters discussed in Chapter 2 and Chapter 4 were analyzed for other metals in addition to those presented previously. The corresponding samples analyzed for total metals content in Chapter 2 (for comparison with samples analyzed via microscopy) were 25 mm Teflon particle filters collected in the dual sampling PMASS. The samples discussed in Chapter 4 (for estimation of each subject's personal exposure to total metals) were the 37 mm Teflon particle filters.

### **B. Methods**

The following metals were analyzed in each set of particle samples: magnesium (Mg), aluminum (Al), vanadium (V), chromium (Cr), manganese (Mn), iron (Fe), nickel (Ni), copper (Cu), zinc (Zn), and cadmium (Cd). However, among these only Al, V, Mn, Fe, and Zn had standard reference material recoveries that were consistently within 40% of the expected value, so only data from these metals is shown here. (The data for Mn and Fe is repeated from Chapters 2 and 4.)

For a description of the sample preparation and analysis of the particles, see Chapter 2 (section 2.2F "Measurement of Total Metal Content"). For these metals, the reaction gas applied in the analysis of each metal was Helium for Al, V, Mn, and Zn. Hydrogen was used as the reaction gas only for Fe. The internal standard used for Al, V, Mn, and Fe was scandium (Sc). For Zn the internal standard was germanium (Ge).

### C. Results

The 25 mm Teflon particle samples were prepared by microwave digestion in 3 batches and analyzed in 2 batches. The 37 mm Teflon particle samples were also prepared by microwave digestion in 3 batches and analyzed in two batches.

For estimates of exposure with the 37mm Teflon particle samples, multiple samples were collected from subjects to reduce sample overload. The exposure concentration reported for 37 mm Teflon particle samples is the time-weighted average of the duration of measurement on each particle sample during a subject's exposure. For every 10 samples at least 2 standard reference material samples (SRM) were analyzed (NIST material 2709 "San Joaquin soil" or NIST material 1648a "Urban Particulate Matter"; National Institute of Standards, Rockville, MD). At least one blank was obtained within each welding session, resulting in collection of >10% blanks. The method detection limit (MDL) is calculated as 3 \* standard deviation of the field blank concentration. SRM Recoveries and MDL's are presented in Table A1.1. Applying the MDL's resulted in 4 samples <MDL for Al and 2 samples <MDL for V.

**Table A1.1** Quality assurance measures for total metals analysis.

<b>Metal</b>	<b>SRM Recovery Range (%)</b>	<b>MDL Range (<math>\mu\text{g}/\text{m}^3</math>)</b>
Al	95-99	0.73-2.5
V	102-106	0.0015-0.0069
Mn	100-111	0.18-0.62
Fe	95-102	2.5-17
Zn	104-140	0.14-0.30



**Table A1.2** Total metals concentrations ( $\mu\text{g}/\text{m}^3$ ) of 25 mm Teflon particle samples. (ID's correspond to ID's listed in Chapter 2.)

Sample	Total Particle	Al	V	Mn	Fe	Zn
<b>Similar Weld Conditions</b>						
1	1250	<MDL	0.010	126	475	1.0
2	8470	1.8	0.058	359	1981	13.5
3	18700	20.5	0.202	1619	8816	75.3
4	9110	6.1	0.206	681	4242	3.8
5	9500	3.3	0.153	576	2994	14.3
<b>Average</b>	9410	7.9	0.126	672	3701	21.6
<b>Std Dev</b>	6200	8.6	0.088	570	3175	30.6
<b>Varied Weld Conditions</b>						
6	648	30.0	<MDL	5	187	14.5
7	639	3.7	0.013	30	148	1.8
8	503	60.5	<MDL	4	113	0.3
9	9250	5.2	0.034	808	4111	7.3
10	534	1.4	0.070	31	119	9.8
<b>Average:</b>	2320	20.2	0.039	176	936	6.7
<b>Std Dev</b>	3880	25.3	0.029	354	1775	5.8

**Table A1.3** Total metals exposures ( $\mu\text{g}/\text{m}^3$ ) from 37 mm Teflon particle samples. (ID's correspond to ID's listed in Chapter 4.)

Participant	Total Particle	Al*	V	Mn	Fe	Zn
1	1540	10.8	0.018	8	766	3.6
2	1920	207.2	0.024	15	634	0.8
3	1330	14.2	0.032	20	354	1.9
4	965	2.8	0.071	30	335	7.6
5	5100	343.6	0.042	37	2120	114.4
6	1080	3.0	0.084	39	374	12.2
7	1400	5.3	0.057	56	540	8.3
8B	1470	<MDL	0.015	116	711	1.2
9	2210	<MDL	0.021	172	1050	1.0
10	3200	<MDL	0.027	258	1440	1.8
11	3050	2.8	0.032	264	1550	5.7
12	3180	1.7	0.037	282	1570	4.3
13	5210	4.5	0.057	398	2430	16.3
14	8500	7.9	0.091	623	3850	28.9
15	9330	8.1	0.191	799	4180	3.8
16	9940	8.0	0.202	823	4410	4.4
17	10500	14.2	0.214	1010	4500	4.6
8A	25600	19.3	0.219	1810	14000	40.6
<b>Average</b>	<b>5300</b>	<b>43.6</b>	<b>0.080</b>	<b>375</b>	<b>2488</b>	<b>14.5</b>
<b>Std Dev</b>	<b>6030</b>	<b>97.7</b>	<b>0.073</b>	<b>477</b>	<b>3221.4</b>	<b>27.1</b>

## APPENDIX II

### Quality Control Experiments for Analysis of Blood Manganese

A series of experiments were conducted to address issues of quality control for analysis of Mn in blood. The experiments were designed to address the following issues: 1) Mn background levels in phlebotomy supplies, 2) storage of blood for Mn analysis, 3) Mn sample preparation, and 4) measures of Mn in blood from capillary collection vs. venipuncture.

#### A. Phlebotomy Supply Background Manganese

##### *Experiment Introduction & Method*

In order to determine if blood Mn concentrations may be contaminated by Mn present in the supplies that sample blood contacts that is not due to Mn naturally present in the blood, the background Mn levels were investigated. Three methods to test background Mn concentrations were tested.

**Method 1:** Phlebotomy supplies were immersed in 2% nitric acid overnight.

**Method 2:** According to Parsons et al., samples were immersed in 2% acetic acid (glacial, Fisher Biotech, Wembley, Western Australia) for 10 minutes. The solution was then diluted 1:10 in a 2% nitric acid (optima grade, Fisher Chemical, Columbia, MD) solution and analyzed (98).

**Method 3:** A pooled blood sample was collected and mixed in a 50 ml acid-washed centrifuge tube. Three aliquots were removed and placed directly into three separate 0.7 ml blood collection tube (used for capillary collection. Three additional aliquots were drawn through a butterfly and into three separate 2 ml blood collection tubes. These samples, in addition to 3 aliquots taken directly from the pool were then prepared in a 1:50 dilution in a 1% nitric acid and 0.01% triton x100 solution (electrophoresis grade, Fisher Scientific, Fairlawn, NJ ) and analyzed within 24 hours.

### *Results*

In the first method, the needles were nearly completely digested in the solution. These samples were not analyzed because it was clear that this method was too vigorous in determining leach levels in the supplies.

The results of the leachate from the second method are shown in Table A2.1. A description of the phlebotomy supplies described in the table follows.

#### **Description of phlebotomy supplies analyzed:**

- Blood collection tube (2 ml): BD Vacutainer, K2 EDTA tube, pink top, 2 ml
- Needle (22 G): BD Vacutainer, Eclipse, 22 G
- Needle (21 G): BD Vacutainer Eclipse, 21 G
- Butterfly: BD Vacutainer SafetyLok, 23 G
- Blood collection tube (0.7 ml): BD Vacutainer, K2 EDTA tube, pink top, 0.7 ml
- Lancet: Safe-T-Pro Accu-Chek Lancet

Results of the third method are shown in Table A2.2. In Table A2.2, the “pre-mimic” samples were taken directly from the blood pool, and “post-mimic” samples were drawn into blood containers used for either capillary collection or venipuncture to mimic either type of blood collection. A t-test of the pre- and post-mimic samples indicates that

there was no significant difference compared to a fresh blood pool (p-value for venipuncture mimic: 0.87, p value for capillary collection mimic: 0.66).

**Table A2.1** Background Mn concentrations ( $\mu\text{g/L}$ ) of phlebotomy supplies.

Item	Mn		
	Conc	Average	Std Dev
Venipuncture Supplies			
Blood Collection Tube (2 ml)	0.55	0.92	0.28
	1.00		
	0.91		
	1.21		
Needle (22 G)	0.17	0.14	0.10
	0.21		
	0.03		
Needle (21 G)	0.15	0.11	0.06
	0.14		
	0.05		
Butterfly	0.04	0.09	0.04
	0.11		
	0.12		
Capillary Collection Supplies			
Blood Collection Tube (0.7 ml)	0.39	0.34	0.06
	0.35		
	0.28		
Lancet	1.89	4.31	3.86
	2.29		
	8.76		

**Table A2.2** Blood Mn concentrations ( $\mu\text{g/L}$ ) of a fresh blood pool “pre-mimic” vs. Mn concentrations following collection into blood containers “post-mimic”.

Condition	Mn Conc (n=3)			
	Venipuncture		Capillary Collection	
	Average	Std Dev	Average	Std Dev
Pre-Mimic	6.14	0.19	6.54	0.61
Post-Mimic	6.26	0.97	6.04	1.58

## *Discussion & Conclusion*

According to the results of method two for Mn background estimation in phlebotomy supplies, the Mn concentrations appear relatively low for all items except the capillary lancet and the 2 ml blood collection container. As capillary blood was not used in further research, so the high lancet background level was not an issue for the study samples. For the venipuncture blood collection tube, there was no known trace element blood collection container for a 2 ml sample available at the time of the study, so there was no apparent improved alternative. However, given the results of the background check from method three, in which an attempt was made to mimic a blood draw from a pool of blood, there was no significant change in the blood Mn concentrations when analyzed within 24 hours. This indicates that Mn contamination due to phlebotomy supplies is not significant when samples are analyzed within 24 hours.

## **B. Blood Manganese Storage Tests**

### *Introduction & Methods*

Multiple storage tests were conducted in order to determine the duration of storage time that blood Mn concentrations remain stable prior to analysis when stored under varying conditions.

**Blood Storage Test 1:** From a well-mixed pool of blood, blood was withdrawn with a butterfly into 2 ml blood collection containers. Each blood collection container of blood represents a unique sample (two aliquots analyzed from each sample), and 3 aliquots of the sample were analyzed at each time point. Samples were stored at -20°C until preparation. Blood was diluted 1:50 in 1% nitric acid and 0.01% Triton X100 in acid-washed tubes and then analyzed.

**Blood Storage Test 4:** From a well-mixed pooled blood sample, samples were pipetted out and diluted 1:50 in 0.5% nitric acid (optima) and 0.05% triton x100) in acid-washed tubes. Digested samples were stored at -20°C until analysis.

**Blood Storage Test 7:** The same method as Blood Storage Test 4 was applied. (These samples were analyzed within a shorter time period than Blood Storage Test 4.)

**Blood Collection to Processing Storage Test:** The same method as Blood Storage Test 4 was applied, except that 3 individuals' blood was analyzed separately (not pooled), and the duration between collection and sample preparation prior to analysis was intentionally varied. Blood samples were stored at -4°C in blood collection tubes prior to sample preparation.

### *Results*

The Mn concentration results of Blood Storage Test 1 are shown in Table A2.3 and Figure A2.1. Blood Mn concentrations increased significantly over a 31 day period when blood was stored in the blood collection container. A linear regression of the slope is: 0.14 Mn µg/L per day ( $p < 0.005$ ).

The resulting Mn concentrations of Blood Storage Test 4 are shown in Table A2.4 and Figure A2.2 below. Blood Mn concentrations had a negative linear regression of slope of -0.016 µg/L per day over a 122 day period that was not significant ( $p = 0.12$ ). However, between days 1 and 8, the slope of -0.73 µg/L per day was significant ( $p < 0.005$ ).

The Mn concentrations of Blood Storage Test 7 (Table A2.5 and Fig A2.3) decreased significantly within a 9-day period of storage, with a slope of -0.35 µg/L per day ( $p < 0.005$ ).

The Mn concentrations of the collection to processing storage test were found to increase significantly within a 16 hour period (selected because all samples were processed within this time period in the study. The slope of increase was: 0.18  $\mu\text{g/L}$  per hour for Participant A, 0.15  $\mu\text{g/L}$  per hour for Participant B, and 0.26  $\mu\text{g/L}$  per hour for Participant C.

**Table A2.3** Blood Mn Storage Test 1 results ( $\mu\text{g/L}$ ). (n=2 for each day analyzed)

# of Days Stored	Avg Conc	Std Dev Conc
1	6.26	0.97
7	7.41	0.60
16	8.66	0.09
31	10.65	0.47

**Table A2.4** Blood Mn Storage Test 4 results ( $\mu\text{g/L}$ ). Blood stored as digest in centrifuge tubes. (n=4 for each day analyzed)

# of Days Stored	Avg Conc	Std Dev Conc
1	10.0	0.7
8	4.9	0.7
31	5.3	1.4
69	4.7	1.9
122	5.7	1.1



**Table A2.5** Blood Mn Storage Test #7 ( $\mu\text{g/L}$ ) results. Blood stored as digest in centrifuge tubes. (n=5 for each day analyzed)

Days Stored	Avg Conc	Std Dev Conc
0	7.8	1.4
1	5.5	0.8
2	5.7	0.6
3	7.0	0.3
4	6.1	0.7
5	5.3	0.3
6	2.0	0.8
7	4.8	0.4
8	4.2	1.3
9	4.6	0.6

**Figure A2.1** Blood Mn Storage Test #1 results. Blood stored in blood collection tubes.

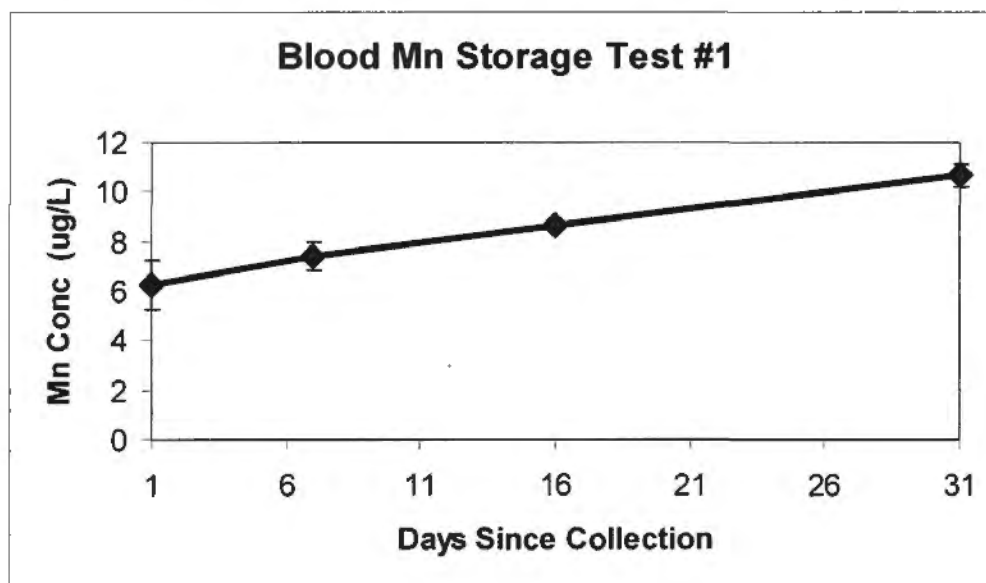


**Figure A2.2** Blood Mn Storage Test #4 results. Blood stored digested in centrifuge tubes.

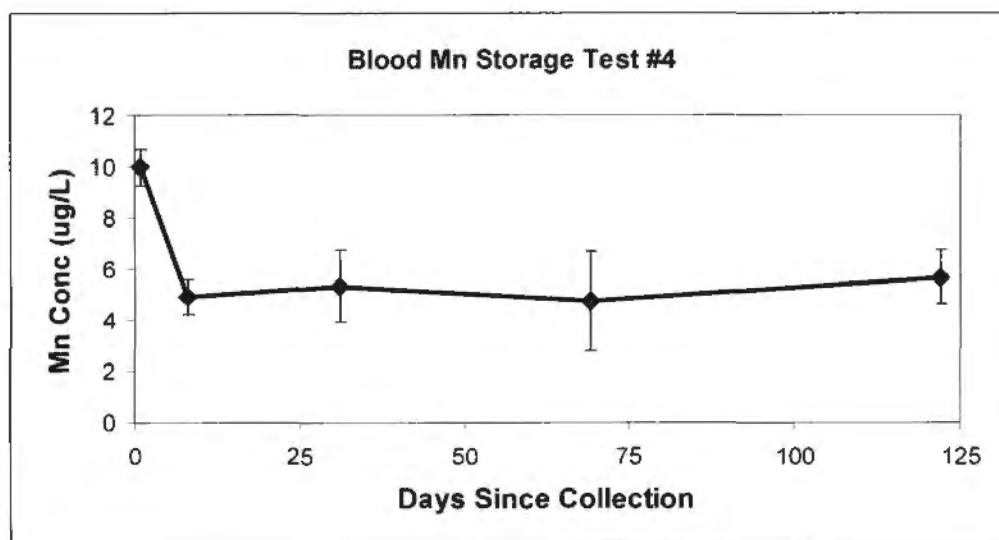


**Figure A2.3** Blood Mn Storage Test #7. (Blood stored digested in centrifuge tubes.)

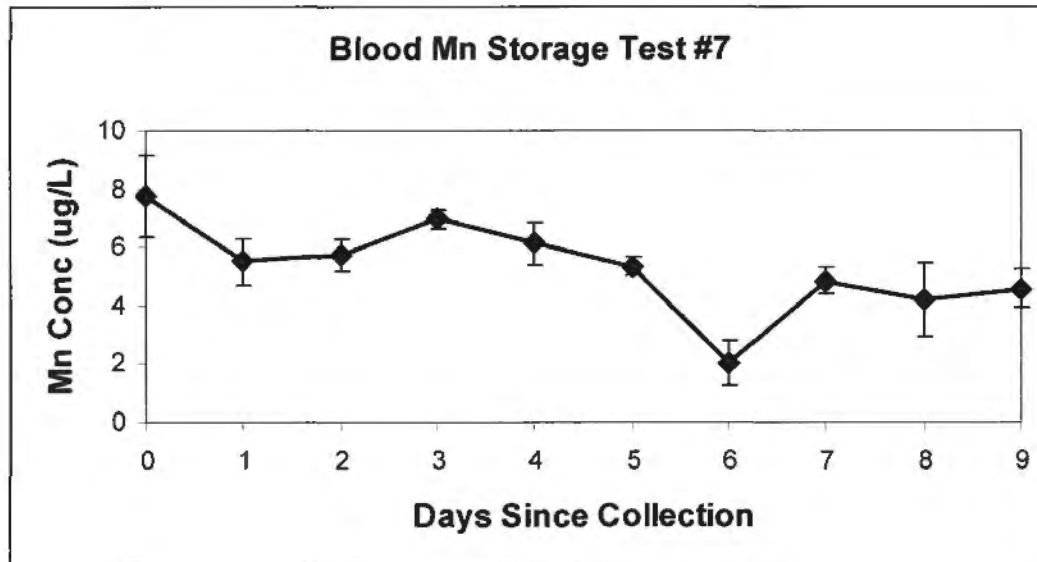
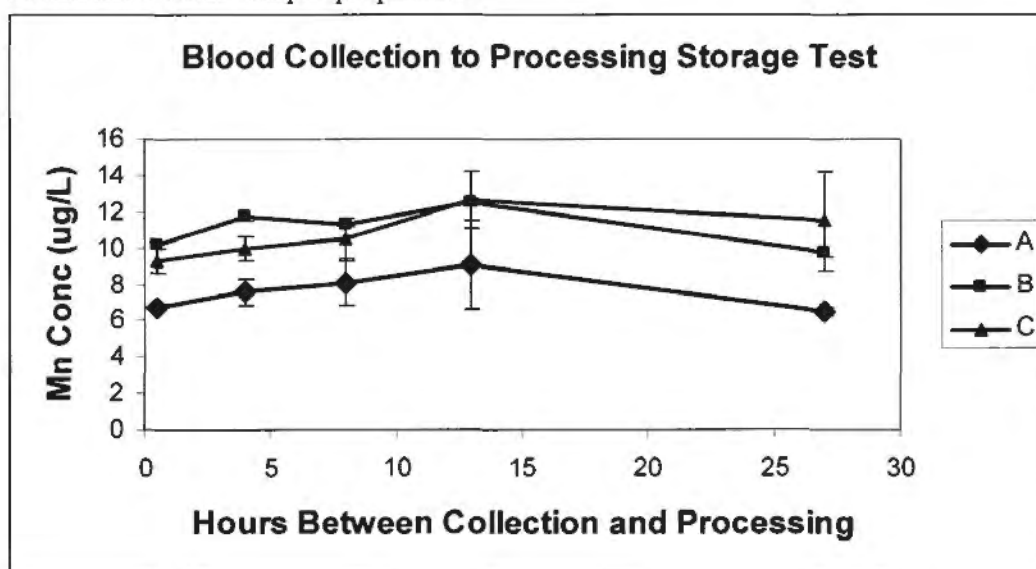


**Table A2.6** Blood Mn collection to processing storage test results ( $\mu\text{g/L}$ ). Blood stored in blood collection containers until sample preparation. (n=3 for each hour analyzed)

Hours Until Processed	Participant A		Participant B		Participant C	
	Avg Conc	Std Dev Conc	Avg Conc	Std Dev Conc	Avg Conc	Std Dev Conc
0.5	6.8	0.1	10.2	0.2	9.3	0.7
4	7.6	0.7	11.8	0.2	10.0	0.7
8	8.1	1.2	11.3	0.1	10.5	1.1
13	9.0	2.5	12.5	0.2	12.6	1.6
27	6.5	0.2	9.7	0.2	11.5	2.7

**Figure A2.4** Blood Collection to Processing Mn Storage Test results. Blood stored in blood containers until sample preparation.



### Discussion & Conclusion

The storage tests revealed several different issues with changing Mn concentrations depending on how the samples were stored and processed. Blood Mn Storage Test 1 showed that there was a significant increase in Mn concentrations when the samples were stored for 31 days in the blood collection containers at  $-20^{\circ}\text{C}$  ( $0.14 \mu\text{g/L}$  per day,  $p < 0.005$ ). Blood Storage Test 4 demonstrated that when the blood samples

were processed on the same day as collection and stored as digested sample in acid-washed centrifuge tubes at  $-20^{\circ}\text{C}$ , there was not significant over a 122 day period, but after 8 days the decline was significant ( $-0.73\text{ }\mu\text{g/L}$  per day,  $p<0.005$ ). Blood Storage Test 7 was conducted in the same way as Blood Storage Test 4, but was a more rigorous focus on a 9 day period of storage, where the decline in Mn concentration was measured as  $-0.35\text{ }\mu\text{g/L}$  per day ( $p<0.005$ ). The Blood Collection to Processing Storage Test demonstrated that there was a measureable increase in Mn concentrations for blood stored at  $-4^{\circ}\text{C}$  in the blood collection containers prior to processing, (an average of  $0.2\text{ }\mu\text{g/L}$  per hour).

Based on the findings of these tests, a decision was made to process blood as quickly as possible on the day of collection, and to store the samples as digested blood at  $-20^{\circ}\text{C}$ . Each subject's blood was analyzed in a single batch as quickly as possible following their 5-7 period of participation (within 9 days for all samples in the exposure assessment study).

### **C. Blood Preparation Method for Mn Analysis**

#### *Experiment Introduction & Method*

To investigate if a simple benchtop method of adding acid to blood is as effective in digesting the blood for Mn analysis as more vigorous methods, five different methods of sample preparation were examined. Three aliquots of standard reference material (SRM) blood and 3 aliquots of a pooled sample of human blood were compared to each method. A pooled blood sample was collected the day before sample preparation. The SRM ("Serorm Trace Elements in Whole Blood L-1", Lot MR4206, Sero AS,

Billingstad, Norway), is freeze-dried blood, was reconstituted the day before sample preparation.

#### *Blood Preparation Methods*

**Simple Benchtop Method:** Based on the methods of Palmer et al. and de Boer et al, a diluent made of: 0.5% nitric acid (optima), 0.05% triton x100, and 51.02 ppb ISTD (for final ISTD conc of 50 ppb) was prepared in ultrapure water (99;100). A 1:50 dilution of the blood was made by adding 100 µl of blood in 4.9 ml of diluent in a 15 ml centrifuge tube. The prepared sample was vortexed, sonicated for 5 minutes at room temp.

**Centrifuged Benchtop Method:** The sample was prepared the same way as in the simple benchtop method, but was centrifuged for 10 minutes at 2000 X G prior to analysis.

**Freeze-thaw Method:** According to the method of White et al, containers holding blood samples were dipped in liquid nitrogen until the blood was frozen and then it was allowed to thaw (repeated 3 times) (101). The blood was sonicated for 15 minutes at 40°C. Then it was stored at -20°C overnight. The sample was then prepared following the simple benchtop method.

**Microwave Digest A Method:** Based on the recommendation of CEM Sr Applications Chemist, Elaine Hasty, a volume of 0.25 ml blood, 0.3 ml nitric acid (optima), and 0.3 ml of ultrapure water were combined in 7 ml Teflon digest vessel (102). The solution was allowed to react for 10 min at room temperature before digesting in a closed vessel microwave ("Mars Express", CEM Corp, Matthews, NC). The sample was microwave digested a first time, allowed to cool, and then 0.25 ml of 30% hydrogen

peroxide was added to the mixture. The solution was allowed to react for 10 minutes at room temperature, and then microwave digested a second time according to the same microwave protocol. The final digest was diluted 1:10 with ultrapure water, for a final acid concentration of 2.73% (0.5 ml digest solution filled to 5ml) with 50 ppb ISTD.

Microwave Digest Program :

- Ramp to temperature.
- Stage 1.
- Power: 300 W, 100%
- Pressure Limit: 350
- Hold Temperature: 130°C
- Hold Time: 10 minutes
- Vessel: capped 7 ml Savilex Teflon vessels inside HP500 Teflon vessels, with 10 ml of water.

**Microwave Digest B Method (102):** A volume of 0.25 ml of blood, 0.6 ml of nitric acid (optima), and 0.25 ml of ultrapure water were combined in 7 ml Teflon digest vessel. The solution was allowed to react for 10 min at room temperature, and then microwave digested according to same program as in Microwave 1 method. The digest was diluted 1:20 with ultrapure water, for final acid concentration of 2.72% (0.25 ml digest solution filled to 5 ml) with 50 ppb conc.

*Results*

The results of preparing the SRM and pooled blood samples for Mn analysis are shown in Table A2.7.

**Table A2.7** Blood Mn concentration ( $\mu\text{g/L}$ ) of sample digested using 5 different methods.

Method	SRM			Pooled Blood	
	Recovery (%)	Avg Conc	Std Dev Conc	Avg Conc	Std Dev Conc
	n=3 (n=2)*	n=3 (n=2)*	n=3 (n=2)*	n=3 (n=2)*	N=3 (n=2)*
1. Simple Benchtop	123 (93)	13 (9.9)	5.4 (0.2)	24.2 (9.8)	24.9 (0.2)
2. Centrifuge Benchtop	99	10.5	0.7	8.9	0.6
3. Freeze-Thaw	133	14.1	2.9	11.1	0.6
4. Microwave A	156 (109)	16.5 (11.6)	8.6 (1.6)	11.2	1.8
5. Microwave B	212 (112)	22.5 (11.9)	18.3 (0.7)	11.5	1.0

\*Three aliquots were prepared for each method. In some cases one of three aliquot concentrations was found to be an outlier, in this case results of all three aliquots are shown as well as the results with the outlier dropped.

### *Discussion & Conclusion*

Among the three aliquots analyzed for each method, in the methods of simple benchtop, and both microwave method A and B there was one aliquot that appeared to be an outlier. Outliers did not appear to be present in either the centrifuge benchtop method or the freeze-thaw method. Whether or not outliers are considered (dropped) from the comparison, the method that resulted best recoveries of Mn compared to the standard reference material was the centrifuge benchtop method. If outliers are not considered in the other methods, the centrifuge benchtop method also had the lowest variability among SRM samples and pooled blood. Based on these results blood samples were analyzed according to the centrifuge benchtop method.

### **D. Capillary vs. Venous Blood**

#### *Experiment Introduction & Method*

In most studies of blood Mn, venipuncture was performed. However, since only a small volume of blood would be needed for our analysis ( $\sim 200 \mu\text{l}$ ), we explored the use of using capillary blood rather than venous blood. Measurements of Mn concentration in

capillary blood vs. venous blood were compared by collecting a single capillary and venous sample from five people, the duplicate measurements were collected at the same time. Samples were then prepared using the simple benchtop method, and analyzed for Mn content within 24 hours of collection.

### *Results*

For each blood sample collected, 2 aliquots were prepared. However, for one subject it was not possible to obtain enough capillary blood for 2 samples. Results are shown in Table A2.8. An un-paired t-test indicates the mean Mn concentrations from capillary vs. venous blood are not different ( $p=0.52$ ). There was no trend of capillary blood having higher or lower Mn concentrations

**Table A2.8** Capillary vs. venous blood Mn concentration ( $\mu\text{g/L}$ ).

Subject	Capillary Blood			Venous Blood			Capillary Conc/ Venous Conc
	#1	#2	Avg	#1	#2	Avg	
1	20.1	25.8	23.0	12.9	8.5	10.7	<b>2.2</b>
2	13.2	--	13.2	13.3	12.7	13.0	<b>1.0</b>
3	13.6	13.4	13.5	13.8	10.8	12.3	<b>1.1</b>
4	8.2	9.9	9.1	9.6	12.9	11.2	<b>0.81</b>
5	13.0	15.0	14.0	16.7	17.2	16.9	<b>0.83</b>

### *Discussion & Conclusion*

There was no significant difference in Mn concentrations obtained from capillary vs. venous blood. We decided to collect blood via venipuncture for 2 reasons. 1) There was general concern that following welding in the exposure assessment study, it would be more likely for Mn on the dermis of hands to contaminate blood samples than Mn on the dermis of the forearm. 2) Both the phlebotomist and subjects preferred venipuncture over capillary collection, as it is more comfortable to subjects and takes less effort from the phlebotomist.



## **APPENDIX III**

### **Estimation of Lung Clearance of Mn from EBC Mn**

#### **A. Introduction**

Manganese in EBC represents Mn that has been eliminated, or cleared, from the respiratory system through exhaled breath. As there are other physiological routes of elimination from the respiratory system, such as mucocilliary clearance or uptake into the circulatory system, EBC does not represent the total clearance from the respiratory system (Figure A3.1). As such, measurements of EBC Mn represent a fraction of Mn that has already left the lung, but the measure of interest in toxicokinetics is rate of the Mn being eliminated from the lung. The elimination of Mn from the lung is the lung Mn clearance rate.

#### **B. Method**

Measures over time of EBC Mn represent the time course of the Mn that has left the lung. The moment to moment concentration of EBC Mn represents the rate of change in lung Mn concentration. In mathematical terms, this means that EBC Mn concentrations are the derivative of measures of lung Mn. Therefore, to estimate the lung clearance from EBC Mn, the integral of the EBC Mn peak data is calculated. As such, a peak level in EBC Mn represents the time of maximum acceleration of Mn clearance from the lung. As an example of the estimation of lung clearance from EBC Mn, the EBC Mn results from Participant #11 are selected and shown below (Figures A3.2 &

A3.3, Table A3.1). For simplicity, and due to a small number of data points for each sample, it is assumed that the clearance rate follows a single compartment model and first order kinetics, and that EBC Mn is the first derivative of lung Mn. For this estimation, basic calculations and trendlines to determine model coefficients were obtained using Excel software.

To determine the elimination rate constant ( $k_e$ ) using first order kinetics, the following equation applies:  $C/C_0 = e^{-k_e t}$  (where  $C$ =Mn concentration,  $C_0$ = initial Mn concentration in lungs, and where  $-k_e$  is the elimination rate constant,  $t$ =time after exposure).  $C_0$  is assumed to be the sum of  $dC \cdot dt$ . In Figure A3.3 an exponential trendline was fit to the regression of  $C_0 - dC$  vs time in order to obtain the term:  $e^{-k_e t}$ . In this example,  $k_e = 0.0014 \text{ hr}^{-1}$ . The first order half life of clearance,  $t_{1/2}$ , is obtained with the following equation:  $t_{1/2} = \ln(1/2)/k_e$ . In this example,  $t_{1/2} = 495$  hours.

**Figure A3.1** Schematic model of EBC Mn measure of lung clearance.

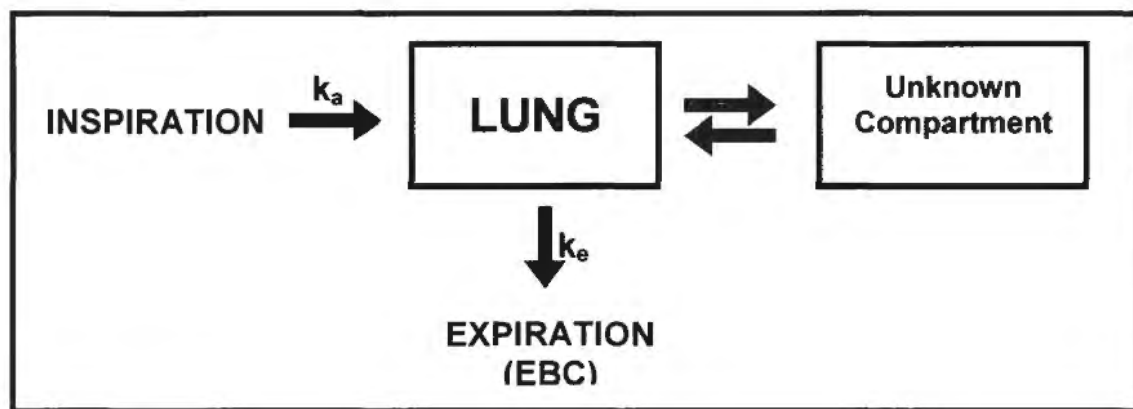


**Figure A3.2** EBC Mn concentration ( $\mu\text{g/L}$ ) following welding exposure for a single subject.

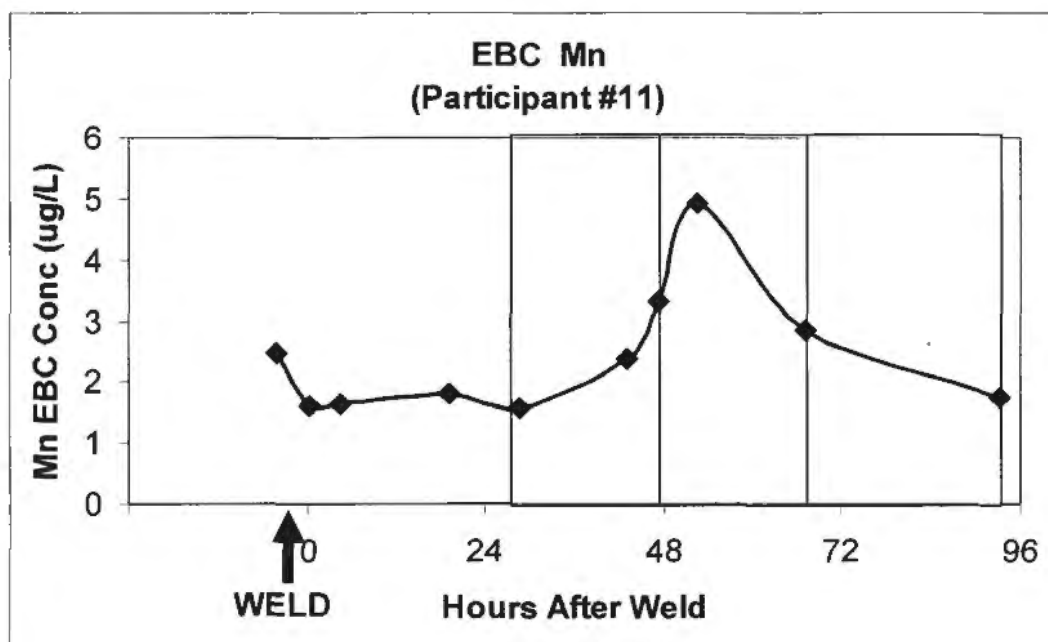


**Figure A3.3** Estimated lung clearance from EBC Mn concentration of a single subject.

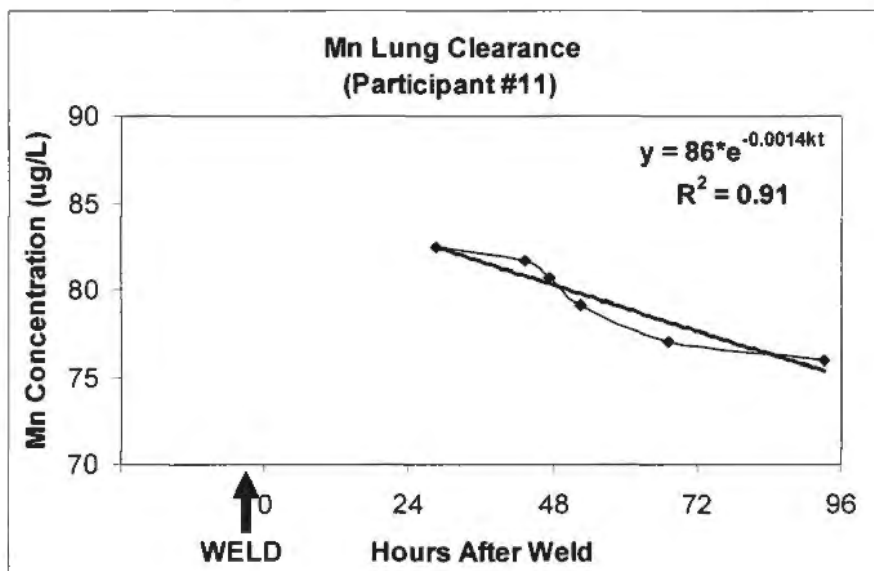


**Table A3.1** Values used to determine lung clearance from EBC Mn elimination in Participant #11.

<input type="checkbox"/>	Increase in EBC Mn peak
<input type="checkbox"/>	EBC Mn peak
<input type="checkbox"/>	Decrease in EBC Mn peak

Visit #	Time After Exposure	EBC Mn	Chg EBC Mn	Chg EBC Mn * Chg Hr	Lung Clearance Mn Conc
	t	C	dC	(dC*dt)	C <sub>0</sub> -(dC)
	(hrs)	(µg/L)	(µg/L)	(µg/L)*hr	(µg/L)
1	-4.1	2.47			
2	0.5	1.62			
3	4.5	1.65			
4	19.2	1.81			
5	28.5	1.58			82.5
6	43.2	2.36	0.78	11.5	81.7
7	47.3	3.32	0.95	3.9	80.7
8	52.5	4.91	1.59	8.3	79.1
9	67.2	2.84	2.07	30.5	77.0
10	93.1	1.75	1.09	28.2	76.0
			C <sub>0</sub> :	82.5	

### C. Results

Several of the EBC Mn peaks occurred immediately following the exposure, and there are only two points representing the peak. Estimates of lung clearance reported here are for EBC Mn results where the peak had at least three points (n=5) (Table A3.2). The average elimination rate constant is 0.21 hr<sup>-1</sup> (SD 0.45 hr<sup>-1</sup>) and the average half life of clearance is 204 hrs (SD 180 hrs).

**Table A3.2** First order elimination constant and half life of clearance for EBC Mn peaks that contained >2 points.

ID	Estimated Initial Lung Mn Conc (C <sub>0</sub> )	Elimination Constant (k <sub>e</sub> )	Half Time (t <sub>1/2</sub> )	Points in Peak	Immediate Peak?
	(ug/L)	(hr <sup>-1</sup> )	(hr)	(#)	
4	61.9	1.039	0.67	3	Yes
6	57.8	0.0046	151	4	Yes
3	98.2	0.0041	169	4	No
11	82.5	0.0014	495	6	No
14	52.6	0.0034	204	4	No
<b>Average</b>	<b>70.6</b>	<b>0.209</b>	<b>204</b>		
<b>Std Dev</b>	<b>19.1</b>	<b>0.464</b>	<b>180</b>		

#### D. Discussion & Conclusion

One subject's EBC Mn results are much different than the other (Participant #4). If results from Participant #4 are excluded, the elimination rate constant is: 0.003 hr<sup>-1</sup> (SD 0.001) and the half time is: 250 hrs (SD 160 hrs), or 10.5 days. In addition, there is less certainty that the full height of the EBC Mn peak was reached if the peak was the first point measured after welding. If results where the peak occurred immediately after the exposure are exclude (Participant #4 and #6), for the 3 subject results the average elimination rate constant is 0.003 hr<sup>-1</sup> and the average half life of clearance is 290 hrs.

## **JULIE RICHMAN**

1200 Saint Paul St. Apt. 3M  
Baltimore, MD 21202  
[jrichman@jhsph.edu](mailto:jrichman@jhsph.edu)  
(443) 604-7259

### **RESEARCH INTERESTS**

Exposure Assessment, Environmental Epidemiology, Biomarkers of Exposure and Dose,  
Indoor and Outdoor Aerosol Sampling, Chemical Pollutant Characterization

### **EDUCATION**

**2004-current PhD Candidate, Division of Environmental Health Engineering**  
*Johns Hopkins Bloomberg School of Public Health; Baltimore, MD*  
Advisor: Alison S. Geyh, PhD

**2005 Risk Sciences and Public Policy Certificate**  
*Johns Hopkins Bloomberg School of Public Health; Baltimore, MD*

**2002-2003 MHS, Division of Environmental Health Engineering, Industrial Hygiene**  
*Johns Hopkins Bloomberg School of Public Health; Baltimore, MD*  
Advisor: Patrick N. Breyse, PhD  
Thesis: "Noise Exposure in the Liquid Packaging Department of a Large Liquid Detergent Manufacturer"

**1994-1999 BA, Chemistry and International Studies**  
*University of Oregon, Robert D. Clark Honors College; Eugene, OR*  
Advisor: Frances Cogan, PhD  
Thesis: "Poisoned Lives: The Impact of Escalating Pesticide Use on Mexican Farmworkers"  
Awarded Distinction for Undergraduate Thesis

### **PROFESSIONAL EXPERIENCE**

**2006 Teaching Assistant**  
*Johns Hopkins Bloomberg School of Public Health; Baltimore, MD*  
Courses: Industrial Hygiene Laboratory, Principles of Environmental Health

- Developed course curriculum
- Wrote and reviewed exams and homework assignments

- 2004**      **Interim Industrial Hygienist**  
*DuPont at Chambers Works; Deepwater, NJ*
- Designed exposure assessment strategies of chemical workers
  - Reviewed exposure assessment sampling results to prioritize health and safety focus
  - Established and prioritized recommendations for occupational health and safety controls
- 2003**      **Safety, Health & Environment Intern**  
*Unilever Home & Personal Care; Baltimore, MD*
- Assessed noise exposure utilizing sound level monitoring and noise dosimetry instruments
  - Investigated scope of product sewage waste and use of analytical methods for monitoring
  - Assisted in general management of safety and health measurement, analysis and awareness
- 2000-2002**      **Research Assistant, Laboratory of Dr. Linda McCauley**  
*Oregon Health & Science University, Center for Occupational and Environmental Toxicology; Portland, OR*
- Extracted pesticide residues and metabolites from biological and environmental samples
  - Analyzed samples with gas chromatography and mass spectroscopy
  - Created field kits for environmental sampling and collected field samples from households
  - Interviewed Spanish-speaking migrant farmworkers about work and household practices

## **WORK EXPERIENCE**

- 1999-2000**      **National Rapid Response Corps Member, AmeriCorps**  
*Louisiana Capital American Red Cross, Disaster Services; Baton Rouge, LA*
- Provided immediate disaster assistance locally and nationally
  - Trained volunteers, youth and adults in emergency response and disaster preparedness
  - Updated database of volunteer and client information
- Fall 1998**      **Biological Study & Conservation Intern**  
*Jatun Sacha Foundation, Ecuador*
- Designed and developed plant test ground for investigation of medicinal plant propagation
  - Prepared Spanish language botanical and biochemical report of native plants for public use

- 1996-1998**      **Chemistry Technician, Laboratory of Dr. Catherine Page**  
*University of Oregon, Department of Chemistry; Eugene, OR*
- Produced Inorganic/Organic multi-layer thin films using sol-gel techniques
  - Synthesized and purified organic compounds for use in thin films
  - Examined samples extensively via X-ray diffraction, ellipsometry, and NMR

- 1997-1998**      **Waste Management Assistant**  
*University of Oregon, Office of Environmental Health and Safety; Eugene, OR*
- Categorized hazardous waste for suitable disposal
  - Investigated laboratories for proper inventory and storage of chemicals

## **HONORS & GRANTS**

- 2008**              National Institute of Environmental Health Sciences Training Grant
- 2007**              Awarded 1<sup>st</sup> Place in the Student Poster Session and 2<sup>nd</sup> Place Overall in Poster Session at the American Industrial Hygiene Conference and Expo
- 2002-2003 & 2004-2007 & 2009**      National Institute of Occupational Safety and Health Education and Research Center Training Grant
- 2007**              3M Industrial Hygiene Scholarship Award
- 2006**              National Institute of Occupational Safety and Health Pilot Study Grant
- 2006**              David Leslie Swift Fund in Environmental Health Engineering Award

## **PRESENTATIONS & POSTERS**

**Richman JD, Geyh AS (2009).** “Assessment of Pulmonary Exposure to Manganese: Uptake of Metals in Inhaled Welding Fumes Into the Pulmonary System”, to be presented at the International Society of Exposure Science 2009 Conference; November 2009, Minneapolis, MN.

**Richman JD, Livi KJT, Spannhake EW, Macri KK, Torrey CM, Geyh As (2009).** “Assessment of Pumonary Exposure to Manganese: Uptake of Inhaled Welding Fumes into the Pulmonary System” poster at the 17<sup>th</sup> Annual Scientific Workshop, sponsored by the NIEHS Training Program in Environmental Health Sciences & the NIEHS in Urban



Environmental Health at the Johns Hopkins Bloomberg School of Public Health;  
February 2009, Baltimore, MD.

**Richman JD**, Livi KJT, Spannhake EW, Macri KK, Torrey CM, Geyh AS (2008). "Assessment of Pulmonary Exposure to Manganese: Uptake of Metals from Inhaled Welding Fumes into the Circulatory System," presented at the International Society for Environmental Epidemiology & International Society of Exposure Analysis 2008 Joint Annual Conference; October 16, Pasadena, CA.

**Richman JD**, Stanberry MS, Mihalic JN, Guilarte TR, McGlothlan JL, Huang H, Mori S, Eftim SE, and Geyh AS (2007). "*In vivo* Monitoring by MRI Imaging of the Accumulation of Welding Fume Associated Manganese Within the Central Nervous System Using a Murine Model" poster at the American Industrial Hygiene Conference and Expo; May 2007, Philadelphia, PA.

**Richman JD**, Livi KJ, Fairbrother H, Mihalic JN, Geyh AS (2007). "Characterization of Manganese in Welding Fumes Utilizing Transmission Electron Microscopy," poster at the Institute of Nanobiotechnology Poster Fair at Johns Hopkins University; April 2007, Baltimore, MD.

## **PROFESSIONAL ACTIVITIES**

JHSPH Environmental Health Sciences Student Organization, Secretary: 2007  
JHSPH Student Assembly, Divisional Representative: 2006  
American Conference of Governmental Industrial Hygienists, Member  
American Industrial Hygiene Association, Member  
International Society of Exposure Science, Member